INFORMATION TO USERS

This material was produced from a microfilm copy of the original document. While the most advanced technological means to photograph and reproduce this document have been used, the quality is heavily dependent upon the quality of the original submitted.

The following explanation of techniques is provided to help you understand markings or patterns which may appear on this reproduction.

1. The sign or "target" for pages apparently lacking from the document photographed is "Missing Page(s)". If it was possible to obtain the missing page(s) or section, they are spliced into the film along with adjacent pages. This may have necessitated cutting thru an image and duplicating adjacent pages to insure you complete continuity.

2. When an image on the film is obliterated with a large round black mark, it is an indication that the photographer suspected that the copy may have moved during exposure and thus cause a blurred image. You will find a good image of the page in the adjacent frame.

3. When a map, drawing or chart, etc., was part of the material being photographed the photographer followed a definite method in "sectioning" the material. It is customary to begin photoing at the upper left hand corner of a large sheet and to continue photoing from left to right in equal sections with a small overlap. If necessary, sectioning is continued again — beginning below the first row and continuing on until complete.

4. The majority of users indicate that the textual content is of greatest value, however, a somewhat higher quality reproduction could be made from "photographs" if essential to the understanding of the dissertation. Silver prints of "photographs" may be ordered at additional charge by writing the Order Department, giving the catalog number, title, author and specific pages you wish reproduced.

5. PLEASE NOTE: Some pages may have indistinct print. Filmed as received.

University Microfilms International
300 North Zeeb Road
Ann Arbor, Michigan 48106 USA
St John's Road, Tyler's Green
High Wycombe, Bucks, England HP10 8HR

78-4201

WYDRZYNSKI, Thomas John, 1947-
THE ROLE OF MANGANESE IN PHOTO-
SYNTHETIC OXYGEN EVOLUTION.

University of Illinois at
Urbana-Champaign, Ph.D., 1977
Biophysics, general

University Microfilms International, Ann Arbor, Michigan 48106

THE ROLE OF MANGANESE IN PHOTOSYNTHETIC OXYGEN EVOLUTION

BY

THOMAS JOHN WYDRZYNSKI

A.B., University of Missouri (St. Louis), 1969

THESIS

Submitted in partial fulfillment of the requirements
for the degree of Doctor of Philosophy in Biology
in the Graduate College of the
University of Illinois at Urbana-Champaign, 1977

Urbana, Illinois

UNIVERSITY OF ILLINOIS AT URBANA-CHAMPAIGN

THE GRADUATE COLLEGE

June, 1977

WE HEREBY RECOMMEND THAT THE THESIS BY

THOMAS JOHN WYDRZYNSKI

ENTITLED THE ROLE OF MANGANESE IN PHOTOSYNTHETIC OXYGEN EVOLUTION

BE ACCEPTED IN PARTIAL FULFILLMENT OF THE REQUIREMENTS FOR THE DEGREE OF DOCTOR OF PHILOSOPHY

Director of Thesis Research

Head of Department

Committee on Final Examination†

Chairman

† Required for doctor's degree but not for master's

O 517

In memory of my father,
who gave me all that he
could not - would not - have.

To suffer woes which hope thinks infinite,
To forgive wrongs darker than death or night,
To defy power which seems omnipotent,
Neither to change nor falter nor repent,
This is to be good, great and joyous, beautiful
and free;
This is a lone life -
JOY, EMPIRE and VICTORY!

Shelley
from 'Prometheus Unbound'

ACKNOWLEDGMENTS

During the course of my thesis research I have received unlimited help and advice from many people. I owe deep gratitude to Dr. Govindjee for his guidance and help in my thesis research and, in particular, for his persistent enthusiasm and excitement for photosynthesis in which I hope I reflect in some way. Likewise, I also owe deep gratitude to Dr. Paul Schmidt for introducing me to NMR methods, for his interest and help in this research. I wish to thank Dr. H. S. Gutowsky for many fruitful discussions, for his encouragement and support.

Much of the NMR measurements and analysis of the data could not have been accomplished without the expert collaboration of Dr. Nick Zumbulyadis and Dr. Steve Marks. To them I am grateful for teaching me the many fine points of NMR theory and for their good friendship. I thank Dr. Ray Finney for the design and construction of the NMR probe used in the light experiments, Dr. Philip Hopke for the manganese determinations by neutron activation analysis and Dr. Steve Ulrich for help in the use of the facilities of the Molecular Spectroscopy Laboratory.

I also owe my thanks to the many members of the Photosynthesis Laboratory, both past and present, whom I had the good fortune to meet during my stay in Urbana for their friendship

and support, in particular to Mr. Daniel Wong and Ms. Rita Khanna.

Finally, I wish to thank the Department of Botany, the Department of Physiology and Biophysics, the National Science Foundation (BMS 73-06735 and PCM 76-11657) and the National Institutes of Health (PHS GM 7283-1 604) for financial support and assistance.

TABLE OF CONTENTS

LIST OF TABLES

LIST OF FIGURES

LIST OF ABBREVIATIONS

General Symbols

A	plastoquinone pool
α	miss parameter
ADRY	reagents which accelerate the deactivation reactions in the oxygen evolving mechanism
B(R)	secondary electron acceptor of System II
β	double hit parameter
CCCP	carbonyl cyanide m-chlorophenylhydrazone
Chl	chlorophyll
DCMU	3-(3,4-dichlorophenyl)-1,1-dimethyl urea
DCPIP	2,6-dichlorophenol indophenol
DLE	delayed light emission
EDTA	ethylenediamine tetraacetic acid
EPR	electron paramagnetic resonance
FeCy	potassium ferricyanide
HEPES	N-2-hydroxyethylpiperazine-N'-2-ethanesulfonic acid
$NADP^+$	nicotinamide adenine dinucleotide phosphate
NMR	nuclear magnetic resonance
P_{680}	reaction center chlorophyll of System II
Q	"primary" electron acceptor of System II
R	endogenous reductant in chloroplast membranes
S_n	intermediate associated with the oxygen evolving mechanism; n refers to the state of the intermediate where n = 0,1,2,3,4
T	temperature

T-A	TRIS-acetone washed chloroplast membranes
TPB	sodium tetraphenylboron
TRIS	tris(hydroxymethyl)aminomethane
Y_n	oxygen yield after the n'th light flash
Z	first electron donor to P_{680}

NMR Symbols

B	constant in Bloembergen-Morgan equation containing the value of the resultant electronic spin and the zero field splitting parameters
$\bar{H}_o$	external applied magnetic field
$\bar{H}_1$	rf magnetic field, applied orthogonal to $\bar{H}_o$
$\bar{M}$	net magnetization of a spin system
$\bar{M}_o$	equilibrium magnetization
ν	frequency (Hz)
p	mole fraction of ligand nuclei bound
PRR	proton relaxation rates
q	number of ligand nuclei bound
rf	radio frequency radiation
$1/T_1$	longitudinal or spin-lattice relaxation rate, corrected with the buffer medium rate
$1/T_2$	transverse or spin-spin relaxation rate, corrected with the buffer medium rate
$1/T_{1,2(D)}$	diamagnetic contribution to the relaxation rates
$1/T_{1,2(free)}$	relaxation rates at the unbound site
$1/T_{1,2(M)}$	relaxation rates at the bound site
$1/T_{1,2(obs)}$	observed relaxation rates

$1/T_{1,2(OS)}$	non-site specific or outer sphere relaxation rates
$1/T_{1,2(P)}$	paramagnetic contribution to the relaxation rates
$1/T_{1,2(T-A)}$	relaxation rates of TRIS-acetone washed chloroplast membranes
$1/T_{1,2(corr)}$	$\left(1/T_{1,2(obs)} - 1/T_{1,2(T-A)}\right)$
τ_C	dipolar correlation time
τ_D	diffusional correlation time
τ_M	chemical exchange lifetime
τ_R	rotational correlation time
τ_S	electron spin relaxation time
τ_V	correlation time for the modulation of zero field splitting
ω_I	nuclear Larmor frequency
ω_S	electronic larmor frequency

CHAPTER I

OXYGEN EVOLUTION IN PHOTOSYNTHESIS

1 Historical Considerations

1.1 Substrate for Oxygen Evolution

Very little is known about the actual chemistry involved in oxygen evolution, although it is almost universally accepted that water is the substrate. Water decomposition during photosynthesis was discussed as early as 1864 by Berthelot [see Metzner (1)] and later by Wurmser (2) and others; the idea, however, did not receive general recognition until the time of Van Niel's formulation of photosynthesis in 1930's [for review of early literature see Rabinowitch (3)]. Based on a comparative biochemical study of bacterial and higher plant photosynthesis, Van Niel proposed that light catalyzes a separation of oxidizing and reducing entities. He generalized photosynthesis as follows:

$$CO_2 + 2H_2A \xrightarrow[Chl]{h\nu} [CH_2O] + H_2O + 2A \qquad (1)$$

H_2A represented some substrate which is oxidized in the light. In bacteria, for example, H_2A could be H_2S, isopropanol or even H_2, while in higher plants H_2A would be water.

The first experimental evidence to support the water decomposition hypothesis was obtained by Hill and Scarisbrick

(4). They showed that in dry leaf powders, incapable of CO_2 reduction, oxygen could be produced in the light upon the addition of an electron acceptor such as ferrioxalate. This was the first clear demonstration that O_2 evolution and CO_2 reduction could be separated functionally.

The strongest argument for water decomposition later came from the ^{18}O labeling experiments of Ruben, Randle, Kamen and Hyde (5). They showed that the proportion of ^{18}O in the oxygen produced by a suspension of Chlorella cells is equal to its proportion in water and independent of its concentration in carbonate. This was recently confirmed by Stemler and Radmer (6) who demonstrated that bicarbonate is not the substrate for oxygen within the first few minutes of illumination.

Recently, the concept of water decomposition has been challenged by Metzner (1), who prefers to describe a bicarbonate complex as the substrate for oxygen. In the early theories of photosynthesis by Willstätter and Stoll (see reference 3) the primary photochemical process was depicted as an hydroxyl-hydrogen exchange reaction in a carbonic acid-chlorophyll complex. The complex was assumed to release oxygen and to produce formaldehyde as an intermediate. No evidence could be obtained for the involvement of formaldehyde in photosynthesis and the theories were considered obsolete after the work of Ruben et al. and Hill. The idea

of a chlorophyll-carbonic acid complex, however, was later resurrected in 1960 by Warburg and Krippahl (7) to explain their discovery that the Hill reaction was actually dependent on the presence of bicarbonate. Warburg termed the complex "photolyte" and considered it the direct precursor to O_2 upon excitation of chlorophyll by a single quantum:

$$\underset{\text{(photolyte)}}{\text{Chl} - H_2CO_3} \xrightarrow{h\nu} \text{Chl} + H_2CO + O_2 \qquad (2)$$

Metzner (1) argues for the photolyte hypothesis by critizing the evidence for water decomposition. He dismisses Van Niel's argument since green plants--in contrast to photosynthetic bacteria--require two photosystems to transfer electrons to CO_2. The bacterial photosystem is incapable of O_2 evolution and, in that sense, more similar to System I of green plants rather than the oxygen generating System II. Metzner stresses the point, as did Warburg (8), that the Hill reaction does require the presence of bicarbonate ions. And, again using Warburg's arguments, he criticizes the results of Ruben et al. on grounds of rapid isotope exchange in H_2O-CO_2 mixtures.

It is true that a direct comparison of bacterial and green plant photosynthesis can no longer be made owing to the much greater complexities of the green plant system. But Govindjee and co-workers (9-11) have shown that the major

site of action of bicarbonate in the Hill reaction is on the reducing side of System II (at the level of the primary and secondary electron acceptors) and not at the O_2 evolving step. In his criticism of Ruben et al. Metzner ignores the recent data of Stemler and Radmer showing that HCO_3^- is not the substrate for O_2 even at short times.

At present there is no evidence for a chlorophyll-bicarbonate complex, although there may be a requirement of bicarbonate for the activity of the System II reaction centers (12). Bicarbonate may be acting as an allosteric effector in this case; but in all likelihood it is not the direct precursor for O_2 in photosynthesis.

1.2 Early Theories on Oxygen Evolution

1.2.1 Photolysis of Water

The first suggestions for a chemical mechanism for O_2 evolution were a direct photolysis of water mediated by chlorophyll (3). In Van Niel's oxidation reduction formulation, the primary photoact may be represented as:

$$PX \xrightarrow{h\nu} [P^+] + [X^-] \qquad (3)$$

where $[P^+]$ and $[X^-]$ represent the primary oxidation and reduction products, respectively, $[P^+]$ leading to the oxidation of water. From an energetic standpoint Rabinowitch argued that the energy in one quantum of visible light (particularly

in the red which excites photosynthesis) is insufficient for this reaction,unless the energy of association of the products $[P^+]$ and $[X^-]$ with their acceptors is much greater than that for water--an unlikely situation. An oxidizing potential of $E_o' \geq 0.8$ eV is needed to oxidize water and no single redox couple with such a high oxidizing potential has been shown in plants. Various chemical models (13-16) have been shown to yield sufficiently high potentials to break down water, but only at the expense of a greater energy input. A direct photolysis of water seems unlikely in photosynthesis.

1.2.2 Peroxide Intermediates

With the advent of the cooperation of 8 quanta for overall photosynthesis (i.e., transfer of electrons from water to $NADP^+$) (17) sufficient energy was available to account for water oxidation. However, the reaction would have to be mediated by some strong oxidant formed in the light. Rabinowitch (3) postulated such an intermediate based on energetic arguments and called it Z:

$$A + ZH \xrightarrow{h\nu} Z + AH \qquad (4a)$$

$$Z + H_2O \longrightarrow \{OH\} + ZH \qquad (4b)$$

where {OH} leads to the release of O_2.

The search for the mechanism of O_2 evolution has since centered around trying to explain how the primary oxidant, Z,

leads to water oxidation. The most plausible types of reactions yielding the release of O_2 involve peroxide intermediates. For example, hydrogen peroxide can be readily dismuted to O_2 by the catalase reaction and photosynthesis could be represented as follows:

$$2A + 2ZH \xrightarrow{h\nu} 2AH + 2Z \qquad (5a)$$

$$2Z + 2H_2O \longrightarrow H_2O_2 + 2ZH \qquad (5b)$$

$$H_2O_2 \xrightarrow{\text{catalase}} 1/2\, O_2 + H_2O \qquad (5c)$$

Alternatively, a low molecular weight organic peroxide could be invoked to replace H_2O_2.

The involvement of H_2O_2 in O_2 evolution, however, was quickly eliminated as a possibility. If H_2O_2 were formed as an intermediate in photosynthesis, it would add 40% more to the energy requirement of the overall process (3). Even though in early investigations it was found that catalase activity (which would be required to break down H_2O_2) paralleled photosynthesis in response to various inhibitors, other conditions were soon found (e.g., aging or temperature shock) where the two activities responded differently. Finally, Gaffron was able to obtain a strain of Scenedesmus where catalase activity could be completely inhibited with KCN, but photosynthesis could still take place (see reference 3).

Willstätter and Stoll utilized small organic peroxide intermediates in their early theories of photosynthesis. The

function of organic peroxides as precursors to free O_2 can be fitted into photosynthetic schemes, but the search for such intermediate has failed to come up with any plausible candidates. From an energetic standpoint organic peroxides have the same disadvantages as H_2O_2, unless the peroxide formation is readily reversible.

1.2.3 Reversal of Oxidase Reactions

Another possibility that has been given considerable attention in the literature is to view O_2 evolution as the reversal of an oxidase reaction, without the formation of free peroxide intermediates:

$$4HZ + O_2 \underset{\text{photosynthesis}}{\overset{\text{oxidase}}{\rightleftharpoons}} 4Z + 2H_2O \qquad (6)$$

In this case Z would be some organic complex, most likely containing a transition metal. In the light peroxidic bonds would form which upon hydration would yield O_2. The advantage of such a system is that the peroxidic bonds could be stabilized with the resonance structures of organic complexes or transition metal oxidation states.

Dorough and Calvin in 1951 (18) suggested that O_2 might be liberated upon the light-induced formation of carotenoid epoxides or furans. However, using ^{18}O labled water, they were able to show only a small increase in the incorporation of ^{18}O in the carotenoid fraction in light-grown cells over

dark-adapted cells. Since that time carotenoid-less mutants have been isolated which are capable of O_2 evolution (19).

More recently Mauzerall and Chivvis (20) have suggested that O_2 evolution may result from a light induced formation of a dioxolium ion. Such an ion could form between the methyl ester carbonyl oxygen and the carbonyl oxygen in the cyclopentanone ring in chlorophyll a. However, bacteriochlorophyll a possesses the same structural features as chlorophyll a, yet bacteria do not evolve O_2.

The failure to identify peroxidic type intermediates during photosynthesis does not imply that they do not exist or take part in O_2 evolution. Other models for O_2 evolution involving manganese (to be discussed in Chapter IV) also employ peroxidic type intermediates. The mechanism of oxidase reactions are still unknown, although considerable effort is being made to understand these reactions (21). From a chemical standpoint, the reversal of an oxidase reaction may be the most plausible approach to the mechanism of O_2 evolution at this time.

2 Involvement of Manganese

2.1 Electron Flow in Photosynthesis

To facilitate discussion in later sections the major aspects of the electron transport chain in photosynthesis are briefly presented here. Details are given in reference

22. Figure 1 shows an abbreviated version of the photosynthetic electron transport chain. The transfer of electrons from water to $NADP^+$ requires the cooperation of two light reactions connected in series. The light reactions are mediated by two specialized chlorophyll species, designated as P_{680} and P_{700} according to one of their characteristic absorption bands. P_{680} along with its antenna pigments has been termed (Pigment) System II and is associated with O_2 evolution while P_{700} along with its antenna pigments is called (Pigment) System I and is responsible for $NADP^+$ reduction. Upon photoactivation P_{680} and P_{700} become oxidized giving up an electron to their respective primary electron acceptor, Q or X. Chlorophyll cations, thus produced, are unstable as such and readily become reduced by neighboring electron donors. P_{680}^+ is reduced back to its original state by an electron from an unknown intermediate labeled Z, which itself is reduced by another intermediate S. The S intermediate has been postulated from O_2 flash yield kinetics and is believed to be associated with the chloroplast manganese.

The reduced primary acceptor of System II, Q^-, eventually transfers its electrons to System I to restore P_{700}. The transfer of electrons from Q^- to System I is mediated by a two electron carrier B(R), the pool of photoquinone molecules, or A pool, cytochrome f and the primary electron

Figure 1. Electron Flow in Photosynthesis. P_{680} and P_{700} are the reaction center chlorophylls for System II and System I, respectively. Z is the first electron donor to P_{680}, S is the intermediate associated with O_2 evolution and Q is the primary electron acceptor. Electron flow between System II and System I is mediated by several plastoquinone molecules (10 per P_{680}) or A pool. In System I, PC (plastocyanin) is generally accepted to be the primary electron donor, X is the primary electron acceptor, Fd is ferridoxin and $NADP^+$ is nicotinamide adenine dinucleotide phosphate. The location of cytochrome f is not fully clear but it is often suggested to be between the A pool and PC.

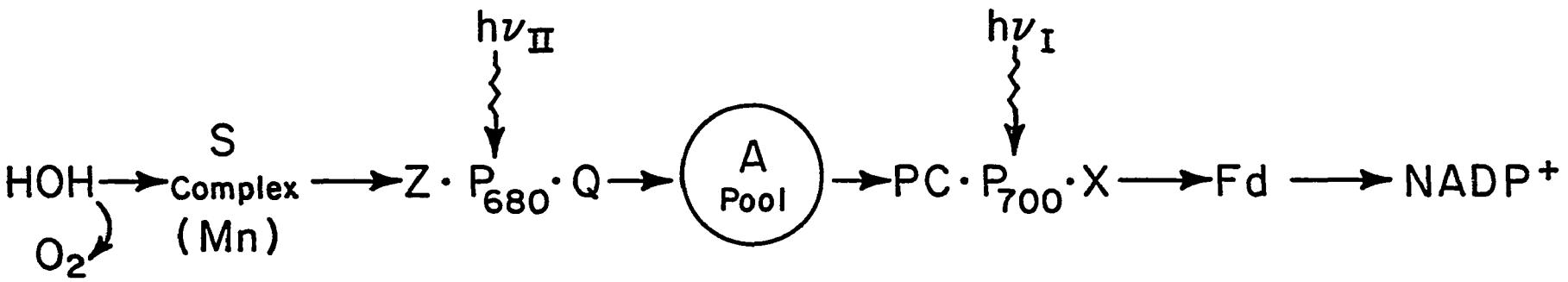

Electron Flow in Photosynthesis

donor to P_{700}, plastocyanin (PC). The reduced primary acceptor of System I, X^-, then leads to the reduction of $NADP^+$ via several other intermediates, ferridoxin (Fd) being one of them. The electron transfer from H_2O to $NADP^+$ is coupled to energy conserving steps resulting in the formation of ATP. Reduced $NADP^+$ ($NADPH_2$) and ATP are then utilized in the Calvin-Benson-Bassham Cycle for the fixation of CO_2 into carbohydrate.

2.2 Manganese Requirement in Photosynthesis

The involvement of manganese in photosynthesis was first realized in the deficiency studies of Pirson (23). He observed a considerable decrease in photosynthetic activity in Mn-deficient Ankistrodesmus, but no significant changes in respiration rates or in the total chlorophyll content. Similar results were later found for other green algae, blue-green algae and chloroplasts from a number of higher plants, indicating that Mn deficiency affects all O_2 evolving organisms.

It was found that Mn was specifically required for the O_2 evolving mechanism itself. Kessler et al. (24) observed the Mn deficiency had no affect upon the photoreduction of CO_2 after H_2 adaptation in Ankistrodesmus, but did result in the suppression of the luminescence (which is associated with System II reactions (25)) in aerobically grown cells. Spencer and Possingham (26) found than FMN catalyzed but not pyocyanin

catalyzed photophosphorylation was decreased by Mn deficiency. In the first but not the second system O_2 is produced. Hoch and Martin (27) later showed no effect of Mn deficiency on the photoreduction of $NADP^+$ in the presence of DCPIP-ascorbate (a System I reaction) in Scenedesmus. This was confirmed by Cheniae and Martin (28). Thus, the site of Mn in photosynthesis was shown to be in the O_2 evolving System II.

The amount of Mn contained in various photosynthetic organisms varied considerably. Early determinations showed a 40-fold spread in Mn abundance from 14 to 600 chlorophylls per g-atom of Mn (29). The more recent data suggest a value of 50-100 chlorophylls per g-atom of "bound" Mn. Cheniae and Martin (30) determined the effect of Mn depletion (obtained by short term growth of Scenedesmus on Mn free medium) on flash yields of O_2. They found that the relative O_2 flash yields were linearly related to the abundance of chloroplast Mn over a 20-fold range, and that 5-8 Mn per System II trap (or per P_{680}) were required for maximal efficiency of O_2 evolution. The earlier discrepancies in Mn content probably arose from varying amounts of "inactive" Mn which may be lost or retained during sample preparation.

2.3 Site of Manganese in System II

It was discovered that chloroplasts subjected to various treatments such as TRIS extraction (31), hydroxylamine

extraction (32) or temperature shock (33,34) loose all ability to evolve O_2 but are still capable of System II sensitized electron flow from artificial electron donors. Since each of these procedures results in the release of bound manganese, as demonstrated by the appearance of an aqueous Mn(II) EPR signal (35), they provide a good way to study the site of Mn in System II.

Using the TRIS extraction procedure, Cheniae and Martin (32) quantitated the loss of O_2 activity with the amount of Mn extracted. They showed that ~90% loss of O_2 activity is correlated with the loss of about 2/3 of the Mn and that the O_2 activity was linear with Mn content of this larger Mn pool. The smaller Mn pool could be removed only after exhaustive treatment, but it did not appear to be involved in O_2 evolution. However, a role of this small Mn pool in O_2 evolution cannot be excluded at this time.

These results were confirmed by NH_2OH (36) and temperature shock (34) extraction procedures. However, the amount of Mn released by these procedures, particularly for TRIS washing, was found to vary by other investigators, even though O_2 activity was always completely inhibited. Reports range from as little as 30% (37,38) to 66% Mn release (32). Blankenship and Sauer (39) quantitated the release of Mn from the membrane by the measurement of the aqueous Mn(II) EPR signal. They found that 60% of the total chloroplast Mn was

indeed correlated with the loss of O_2 activity, confirming the two pool concept. However, the Mn could not be readily washed away from the chloroplast, leading them to conclude that the Mn associated with O_2 evolution was located to the inside of the membrane. After TRIS treatment the Mn was apparently released into the inside space of the chloroplast vesicle; the diffusion of Mn to the outside was slow, $t_{1/2}$ ~2.5 hr. Apparently, depending on the source of plant material and method of preparation, the diffusion of Mn across the membrane can vary, explaining the variations that other investigators have observed.

Recently, Takahashi and Asada (40) have estimated the binding constants for the two fractions of manganese from Scatchard plots using NaCN extraction procedure. For the loosely bound Mn, $K_L = 1.2 \times 10^4 M^{-1}$ and for the tightly bound Mn, $K_T = 1.9 \times 10^5 M^{-1}$.

The large loosely bound Mn pool needed for O_2 evolution is not associated with Q or P_{680} in System II. Perturbation of this Mn fraction by TRIS washing does not decrease the amplitude of the 150 μs component of P_{680} absorption change (41) nor the X-320 absorption change related to Q (42).

Using fast time response EPR techniques, Sauer and co-workers (43-47) have found a rapidly formed flash-induced EPR transient with a rise time of ~100 μs. They ascribe this transient to Z^+, the oxidized form of the first electron

donor to P_{680}. In normal chloroplasts this transient decays very rapidly - $t_{1/2}$=400-900 μs (Sig. II_{vf}), while in TRIS washed or heat treated chloroplasts the decay is ~1000 times slower (Sig. II_f). As O_2 evolution is inactivated by heat treatment, there is a proportional decrease in Sig. II_{vf} amplitude and a parallel increase in Sig. II_f amplitude. To explain this result they propose that the paramagnetic interaction of native bound Mn efficiently relaxes the Z^+ free radical (giving rise to Sig. II_{vf}). Upon release of bound Mn by TRIS washing or heat treatment, paramagnetic interactions are eliminated and the decay of the Z^+ free radical slows down (giving rise to Sig. II_f). Thus, they conclude that Mn is near Z and that Mn must be acting between Z and the O_2 evolving step.

The function of the smaller, tighter bound Mn pool is unknown. The removal of virtually all Mn (≤1 Mn/4000 chlorophylls) still does not affect electron flow from artificial donors NH_2OH (32) or diphenylcarbazide (48) through System II to System I. One possible role of this pool of Mn may be in a lamellar bound superoxide dismutase activity (49); however, there is still controversy over whether this activity is due to a manganese enzyme or to a copper-zinc enzyme (50,51).

2.4 Biochemical Studies

Most workers believe that the chloroplast Mn is bound to an easily denatured protein, although to date there is no

convincing evidence for it. That proteins are involved in O_2 evolution is suggested by inhibitory studies using antibodies (52), protein chemical modifiers (53) and trypsin digestion (54). Upon extraction of chloroplasts with organic solvents bound Mn is retained in the protein phase (28,55,56). But none of these Mn-proteins could be re-incorporated back into chloroplast membranes to reconstitute the O_2 evolving mechanism. The one possible exception is a Mn-containing low molecular weight polypeptide isolated from Phormidium luridum by Tel-Or and Avron (57). The readdition of this polypeptide to washed algal spheroplasts can apparently restore O_2 evolving capacity. The current view is that the O_2 evolving system and associated Mn is located to the inside of the chloroplast thylakoid vesicle (39,58,59), making a biochemical identification of Mn-proteins and reconstitution studies difficult.

Under some conditions of TRIS-induced inactivation of O_2 evolution in chloroplasts, the inactivated O_2 evolving center can be reactivated with lipophilic reducing reagents (i.e., $DCPIPH_2$ or hydroquinone) (60). This reactivation is unique to TRIS treatment and cannot be observed in chloroplasts inactivated by temperature shock or NH_2OH extraction. The reactivation of TRIS-treated chloroplasts results in the disappearance of aqueous Mn(II) EPR signal, apparently as a consequence of the rebinding of Mn to the membrane (61). There is also a consequent conversion of Sig. II_f to Sig. II_{vf}

(43). These results further support the assignment of Mn to reactions very close to the O_2 evolving mechanism.

As originally observed by Pirson (23) Mn deficiency in Scenedesmus cells can be relieved by simply adding Mn(II) salts to the growth medium. In 15-30 min O_2 evolution is restored. The reactivation of O_2 activity does not depend upon the synthesis of either protein or chlorophyll, as inhibition of protein synthesis by cyclohexamide has no effect on reactivation (29). The reactivation does, however, require light (29). The photoactivation of O_2 evolution by the incorporation of Mn has been demonstrated in blue green algae and higher plants under various conditions (Mn deficiency (62), NH_2OH extraction (63) and dark-grown plants (64)). The first step in reactivation of O_2 activity is the accumulation of cellular Mn (65). The actual photoactivation step involves the light-induced incorporation of Mn into the membrane. This photoactivation is strictly a System II reaction and appears to be a multiquantum process (at least two photoreactions are involved, possibly three (66)). Since photoactivation is inhibited by reductants such as hydroquinone, it has been suggested that the photoactivation process first involves the photooxidation of Mn(II) to a higher oxidation state before binding occurs. The bound Mn must then be activated by another light quantum before O_2 evolution can begin.

3 Kinetic Analysis of Oxygen Evolution

3.1 Early Experiments

3.1.1 Intermediates in Oxygen Evolution

Because of the fragility of the O_2 evolving mechanism and the requirement for a intact membrane, the biochemical approach has provided very little information about the chemistry of O_2 evolution, other than that manganese is somehow involved in it. An entirely different approach is a kinetic one, in which the dynamic relationship between the input of light energy and the output of O_2 is studied. This approach has led to the current model for O_2 evolution.

The first studies of O_2 evolution in flashing light were the classic experiments of Emerson and Arnold (67). They subjected Chlorella cells to repetitive brief (10^{-5} s) saturating flashes of light so that only photochemical conversions would take place and measured the average O_2 produced per flash. When the dark period between the flashes was chosen to be optimum, the amount of O_2 per flash reached a maximal value of about 1 O_2 per 2500 chlorophyll molecules. The flash yield decreased to half maximum value if the dark times separating the flashes were shortened to ~10 ms at 20°C. Emerson and Arnold concluded that several hundred chlorophylls (in a unit) cooperate together to collect light energy and to photochemically form a "long lived" intermediate which

promotes the production of O_2. They assumed that the intermediate was an "enzyme" present at low concentrations and represented the rate-limiting step in photosynthesis. It became clear later that the rate limiting step in the electron transport chain is the reoxidation of plastoquinone (~20 ms) (68).

The dependence of the flash yield upon the dark time between flashes, however, proved to be more complex than the simple first order kinetics assumed by Emerson and Arnold (see discussion of Tamiya's work in reference 3, pp. 1470-1472). Later it was found that flashes longer than 10^{-5} s, but shorter than the dark half time of 10 ms, produced considerably higher yields than expected (69). This led to the idea that at least two intermediates were involved. Accordingly, light would excite an intermediate E (or photocenter):

$$E \xrightarrow{h\nu} E^* \qquad (7)$$

which would be rapidly discharged by another intermediate U (or enzyme) at the same concentration as E:

$$E^* + U \longrightarrow E + U^* \qquad (8)$$

The U intermediate would then facilitate O_2 evolution. The large yields in long flashes could be accounted by multiple turnover of the photocenter.

3.1.2 Light Activation Requirement

The first measurements of O_2 production by a single brief flash were made by Allen and Frank (70). They observed that after a single flash (<1 ms) no O_2 could be detected in anaerobic Scenedesmus. But O_2 could be observed when (1) a weak background light was given in the dark period preceeding the flash, (2) two brief flashes were given with a spacing of 1 s or (3) long flashes (~25 ms) were used.

Wittingham and Brown (71) confirmed and extended these measurements to the alga Ankistrodesmus. Flashes ≤5 ms yielded no observable O_2 while longer 35 ms flashes did (1 O_2/800 Chl). With a 100 μs flash preceding a long flash, the yield of O_2 produced was twice as great as that of the long flash alone (1 O_2/400 Chl). However, the maximum enhancement of the O_2 yield occurred only when a certain dark time was interposed between the flashes. The yield increased to a maximum at 0.7 s dark time and then slowly declined at longer dark times. Whittingham and Brown interpreted their results to mean that the first single flash was required to light activate some catalyst needed for O_2 evolution and that it must stabilize in the dark before it could be used to catalyze O_2 evolution upon the next flash. To account for these results, Equations 7 and 8 can be expanded as follows (29):

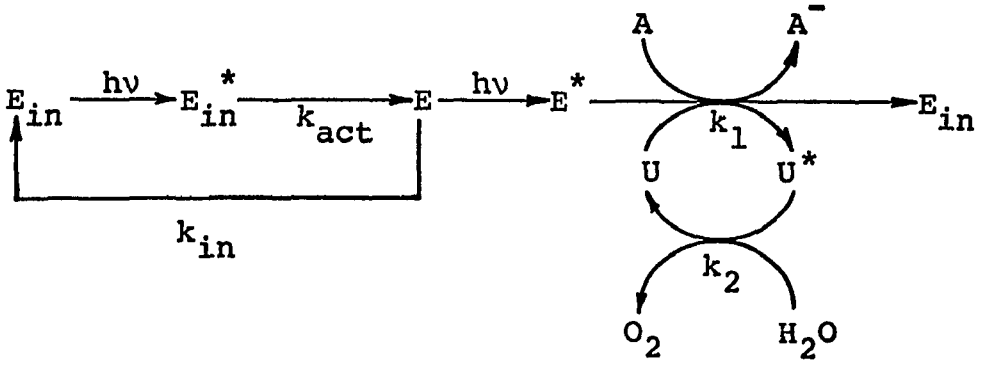

(9)

As defined before, E is the active form of the photocenter, E_{in} a dark inactivated form, E_{in}^* and E^* light induced excited states, k_{act} the rate constant for dark stabilization of E_{in}^* to E, k_{in} the rate constant for dark inactivation, k_1 the rate constant for the formation of U^* from U (the oxygen evolving enzyme), k_2 the rate constant for the actual O_2 evolving step and A some intermediate reduced during the process (which eventually leads to the reduction of CO_2 or a Hill oxidant). Thus, according to this scheme light is first required to activate E_{in} to E which requires a finite dark time for stabilization. The active photocenter, E, can thus be converted by another light quantum into an excited intermediate E^* which promotes the evolution of O_2 via the enzyme U in the dark. As a consequence A is reduced as U is oxidized. The light activated capacity to evolve O_2 is lost in the dark after sufficient time if not driven forward by another incoming quantum.

3.1.3 Concept of Charge Accumulation

Whittingham and Bishop (72) and later Gingras and Lemasson (73) assumed that the light activation process was

the "preparation of System II for O_2 evolution by System I;" however, Joliot (74) clearly demonstrated that the activation step (formation of E) was sensitized solely by System II. He measured the initial time course of O_2 evolution in weak 650 nm light (which excites primarily System II) or 695 nm light (which excites primarily System 1), adjusted in intensity so as to give equal rates of O_2 evolution, with and without a preilluminating flash. The kinetics were identical under all conditions. The initial rate of O_2 evolution had a precise action spectrum of System II. The results, therefore, indicated that the activation process ($E_{in} \xrightarrow{h\nu} E_{in}^*$) is mediated by System II.

Joliot (74) also looked at the O_2 yield as a function of the time of illumination (0.01-0.25 s) in weak light and compared the results between dark-adapted samples and samples given a brief preflash (10^{-4} s) two seconds before the illumination period. The initial slope for the curve measured with an activating preflash gives the dark rate at which the photochemically active photocenter (E^*) is deactivated in the dark i.e, it measures the following reaction from Equation 9:

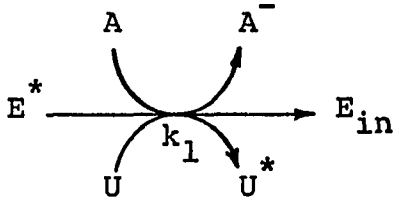

The interesting result was that in the curve obtained with no activating preflash, the O_2 yield showed an initial lag

and then increased with a slope identical to the slope of the curve obtained with one preflash. Since the initial slope of the curve with no preflash gives the rate of the dark reaction in the activation step i.e., $E_{in} \xrightarrow{k_{act}} E$, Joliot concluded that $k_{act} = k_1$ and that the two steps must involve a reaction with the same intermediate, i.e., with A.

Since the reaction of E^* with A is a reduction of A, then the reaction of E_{in}^* with A must also lead to a reduction of A. This led Kok and Cheniae to suggest that there must be some reaction partner M (later designated as S) which is photooxidized twice, once to M^+ during the activation process and a second time to M^{++} during the O_2 evolving step. Here, then, was a proposal for a charge accumulation mechanism as part of O_2 evolution in photosynthesis.

3.2 Model for Oxygen Evolution

3.2.1 Basic Features of the Model

To summarize then the early work, the classic experiments in flashing light by Emerson and Arnold and as extended by Kok (69) established that O_2 evolution was not a direct breakdown (photolysis) of water, but rather occurred through a dark reaction via an intermediate created in the light. The work of Allen and Frank and that of Wittingham and Brown demonstrated that a light activation step was required before O_2 could be produced. Joliot showed that this light activation step was

mediated by System II and that it utilized the same photochemical apparatus by which O_2 itself was made. This led to the idea of charge accumulation on the oxidizing side of System II.

When the O_2 yield of a dark-adapted sample is measured as a function of a series of brief saturating flashes, a unique oscillatory pattern is obtained. Typical results are shown in Figure 2. Very little (or no) O_2 is evolved after the 1st and 2nd flashes. Maximum O_2 is produced after the 3rd flash and peaks on the 7th, 11th, etc. flashes, following a periodicity of four. The O_2 oscillations eventually damp out after the third or fourth cycle. Based on this unique pattern and other kinetic data several hypotheses were advanced to explain the O_2 evolving mechanism (75,76). However, the model as proposed by Kok and co-workers (77-79) appears at present to be the minimal hypothesis to account for all the available data. The model is shown in Figure 3.

In this model the various so-called S states are assumed to differ from each other by the number of accumulated oxidizing equivalents. The model entails the following basic features: (1) the S_1 state is stable in the dark; (2) although each step is a one quantum process, there is a small probability of double hits (β) (i.e., some of the O_2 centers advance two states during a flash) and of misses (α) (i.e., some of the O_2 centers do not advance during a flash); (3) the S_2

Figure 2. O_2 Yield Measured as a Function of Number of Saturating Light Flashes. Closed circles are the measured O_2 yield normalized to the steady state value. Open circles refer to the calculated flash yield based on the Kok et al. model (77). $[S_0]_0$ and $[S_1]_0$ refer to the concentration of S_0 and S_1 in darkness, α to a miss parameter and β to a double hit parameter. For details see text. (After Forbush et al. (78).)

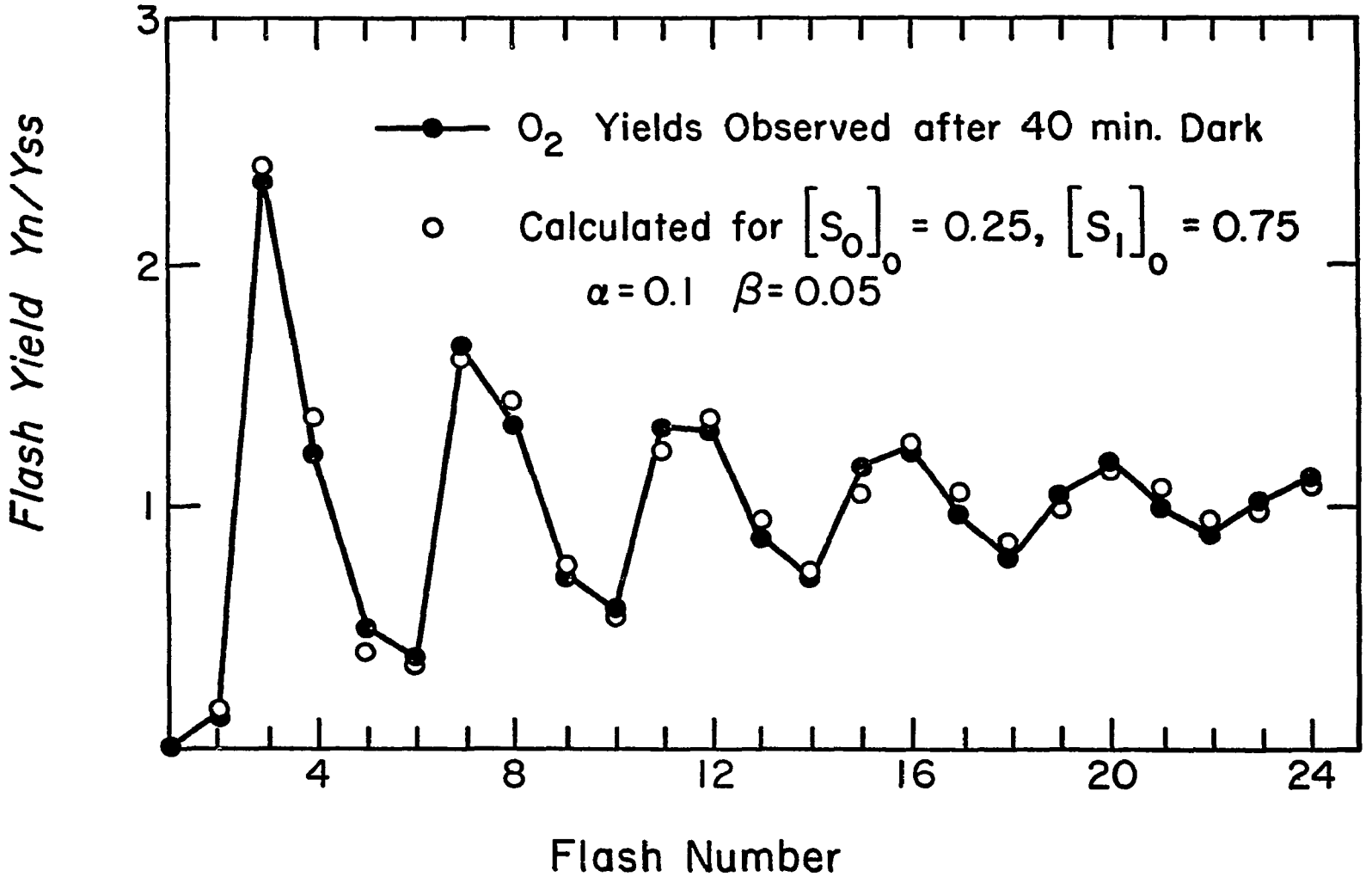
Flash Yield Yn/Yss
3
2
1
4
8
12
16
20
24
Flash Number
O2 Yields Observed after 40 min. Dark
Calculated for [S0]0 = 0.25, [S1]0 = 0.75
α = 0.1 β = 0.05

Figure 3. Current Model for O_2 Evolution. S refers to the O_2 evolving intermediate. There are four possible states (designated by the subscripts) differing from each other presumably by an additional oxidizing equivalent. The S_n' refers to a light activated state which relaxes to the succeeding S_{n+1} state in the dark. The dashed arrows represent dark deactivation of the higher S_3 and S_2 states. The S_4 state is transitory reacting immediately with water to produce O_2 and the original S_0 state. For details see text.

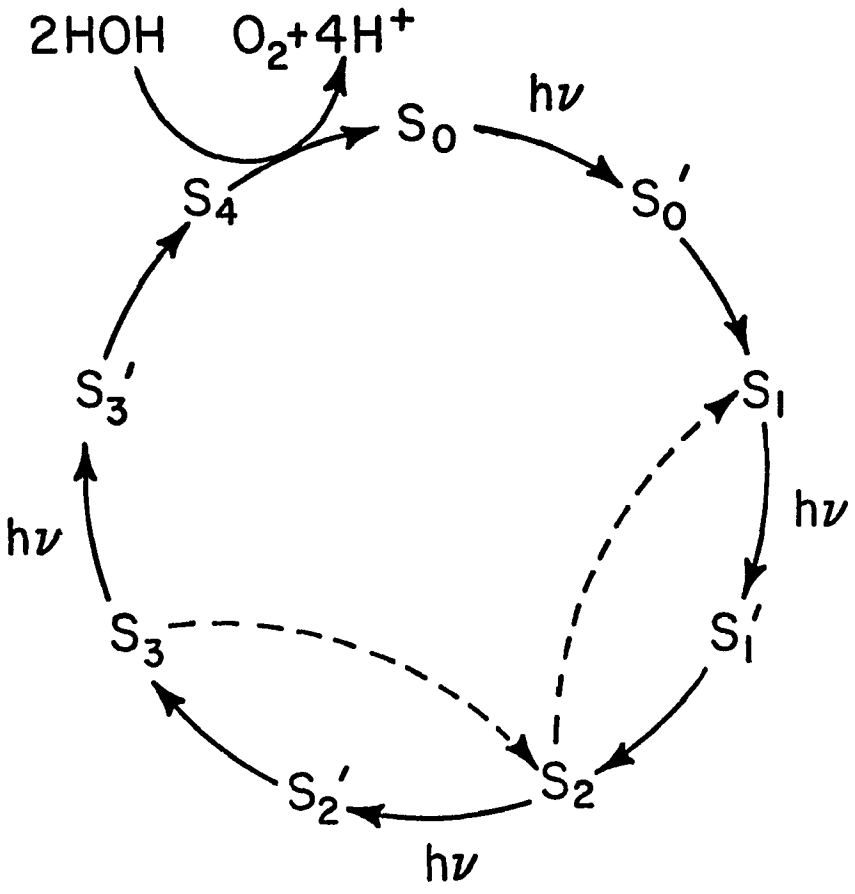

Model for Oxygen Evolution in Green Plants

and S_3 states deactivate during the dark; (4) after light activation there is a finite relaxation time before the state can be activated by another quantum ($S_n' \rightarrow S_{n+1}$) and (5) the $S_4 \rightarrow S_0$ transition corresponding with the release of O_2 is an instantaneous dark reaction (occurring in ≤1 ms). The following sections discuss in some detail these features of the model.

3.2.2 Stability of the S_1 State

In order to explain why the O_2 yield is maximal after the 3rd flash and not the 4th flash (as would be expected if all of the oxidized states deactivated to the S_0 state in the dark), Kok *et al.* (77) had to postulate that the S_1 was stable in the dark. One of the arguments used to support this assumption was that the S_1/S_0 ratio can be varied by appropriate preillumination. According to the model, during steady state all four states are equally distributed (*i.e.*, 1:1:1:1 ratio). Assuming that only the S_2 and S_3 deactivate completely in the dark, then after a long enough dark period the distribution of S states would be $3S_1:1S_0$. If one preflash is given and a sufficient dark time is allowed for S_2 and S_3 to deactivate, then all centers will be in the S_1 state, if indeed S_1 is stable in the dark. Likewise, if three preflashes are given and a sufficient dark time allowed, then most centers will be in the S_0 state.

The O_2 yield after a particular flash (Y_n) can be expressed in terms of the concentrations of the S states and the α and β factors (78). Although the exact α and β may be unknown, they are relatively small and the Y_3/Y_4 ratio can be assumed to be proportional to the S_1/S_0 ratio. Forbush et al. (78) did the preillumination experiments described above on chloroplasts and calculated the Y_3/Y_4 ratios. With no preillumination Y_3/Y_4 was 1.58, while with one and three preflashes the Y_3/Y_4 ratios were 2.37 and 1.33, respectively. In the first case there appears to be more S_1 than in the no preflashed sample while in the second case there is less S_1. They conclude that the S_1/S_0 ratio can be varied and that S_1 must be stable in the dark (at least during the dark times they used, i.e., 10 min).

Bouges-Bocquet (see Joliot and Kok (79)) using the same approach but with much longer dark times (60 min) between the pre-illuminating flashes and the determination of the flash yields, observed that the Y_3/Y_4 ratio was quite close to the ratio in the no preflash condition. This was interpreted to mean that the S_0 and S_1 equilibrate after long dark periods (longer than it takes for S_2 and S_3 deactivation) to the ideal dark distribution of $3S_1:1S_0$.

3.2.3 Double Hits and Misses

Joliot et al. (80) observed that the oscillations in saturating flashes of light after a continuous preillumination

period were <5% of the oscillations with no preillumination. Since the preillumination period causes an equilibration of the S state distribution, this result suggested that each step in the mechanism has the same quantum efficiency. Kok et al. (77) had found a linear relationship between the initial quantum efficiency of the rate of O_2 evolution in weak light and the maximum O_2 flash yield, indicating that the final O_2 evolving step was a one quantum process. Thus, these results taken together suggested that all steps in the O_2 evolving mechanism are a one quantum process. It was also assumed that the O_2 evolving centers act independently of each other since inhibition of up to 90% of O_2 evolution by UV irradiation, DCMU addition or Mn deficiency did not alter the relative O_2 flash yields for the first five saturating flashes given to dark-adapted samples.

To account for the damping of the O_2 oscillations Forbush et al. (78), therefore, had to assume that the system was perturbed in some other way so as to mix up the states. In algae the oscillatory pattern damps off at about the 11th flash while in isolated chloroplasts at about the 20th flash. Two mechanisms were proposed by Forbush et al. (78) as the major perturbations to the system--double hits and misses. Double hits would tend to advance while misses would tend to retard the stepwise conversion of the states in flashing light. The extent of double hits will necessarily depend on the relaxation time of the $S_n' \xrightarrow{k_n} S_{n+1}$ transition. As will be discussed

later, the half times of relaxation (k_n) are of the order of 200-600 μs so that the probability of double hits decreases as the flash duration decreases from several μs to sub μs range. Weiss and Sauer (81) showed no double hits in the first few activation steps using very brief 40 ns laser flashes, as did Joliot et al. (82) with 2 μs xenon flashes spaced 320 ms apart. In the 10 μs flashes used by most workers the percent double hits remains negligible.

The most significant factor perturbing the system is, therefore, the percent misses. Misses can be explained either as the failure of charge separation to take place at the reaction center or as an annihilation of the charge separation, for example, by a back reaction (i.e., if the reaction center is represented as $ZP_{680}Q$, then the back reaction is given as the recombination of charges on the primary electron acceptor and donor: $ZP_{680}{}^{+}Q^{-} \longrightarrow ZP^{*}_{680}Q \longrightarrow ZP_{680}Q + h\nu$).

The number of misses remains constant even if the flash intensity is increased far above the saturation level. In order to explain the damping, the misses, as well as double hits, must occur randomly in all reaction centers. Misses are calculated to be 10-11% for isolated chloroplasts and ~20% for intact cells. It is not known yet whether misses are the same or have different probabilities for the four steps.

3.2.4 Deactivation

Since no O_2 is evolved on the first and very little on the second flash, it was assumed that S_2 and S_3 states completely deactivate in the dark.

Joliot et al. (82) observed that deactivation is faster in algae than in chloroplasts. Also in algae the deactivation of S_3 is about 5x faster than the deactivation of S_2, while in chloroplasts the rates of deactivation for both states are about the same. However, in both algae and chloroplasts the S_2 deactivation closely approximates first order kinetics, whereas S_3 deactivation does not. On the other hand, in the analysis by Forbush et al. (78) on chloroplasts all of the decay curves showed second order kinetics.

Forbush et al. (78) observed a transient increase in S_2 state at short dark times. From this they suggested that the deactivation process was a one step mechanism, i.e., $S_3 \rightarrow S_2 \rightarrow S_1$. Based on Y_3/Y_4 ratios Joliot et al. (82) concluded that a two step mechanism was also involved, i.e., $S_3 \rightarrow S_1$ and $S_2 \rightarrow S_0$. If there is strictly a one step deactivation, then in completely dark-adapted systems the S_0/S_1 ratio would be 1:3 while for a two step mechanism the S_0/S_1 ratio would be 1:1. The observed Y_3/Y_4 in dark-adapted algae had intermediate values, suggesting that both types of mechanisms were probably involved in the total deactivation process.

3.2.5 Reaction Center Turnover

After light activation, each S state undergoes a finite dark relaxation time before it can be activated by another incoming quantum. This relaxation time is now ascribed to the recovery of the reaction center back to its original state which is limited by the reoxidation of Q^- (see e.g., reference 83).

Forbush et al. (78) determined the half time for the $S_1' \rightarrow S_2$ transition to be ~200 μs and for the $S_2' \rightarrow S_3$ transition to be ~400 μs. Bouges-Bacquet (84) made a detailed study of the relaxation times for all of the S states and came up with somewhat different results. Both the $S_0' \rightarrow S_1$ and $S_1' \rightarrow S_2$ transitions showed non-exponential kinetics with half times of ~400 μs. The non-exponential behavior of the kinetics for these transitions did not change when non-saturating flashes were used, suggesting that this was an inherent property of the O_2 evolving centers in these states. The $S_2' \rightarrow S_3$ transition, on the other hand, showed sigmoidal kinetics with an initial lag of ~100 μs. Bouget-Bocquet suggested that perhaps two first order reactions were involved in this transition mediated by another transitory state (S_2''). But a direct measure of this state would be necessary to include it in the scheme for O_2 evolution. The $S_3' \rightarrow S_0$ transition showed exponential kinetics and proceeded much slower than the other relaxation steps. The halftime was 1.2 ms. This transition involves the S_4 state which immediately reacts

with water, i.e.,

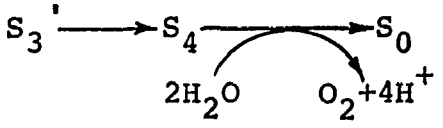

3.3 Significance of the Model for Oxygen Evolution

In the scientific approach one takes all of the experimental findings available at the time and builds a hypothesis--a model--which will attempt to explain all that is known, or else gives reasons for discrepant observations. A good hypothesis will suggest new experiments to test the validity of the ideas. There is now appearing in the literature experimental data which cannot be readily explained by the current model of O_2 evolution. This model is a kinetic one and up to this time has no real basis in the actual chemistry of the reaction. Several of the assumptions in the model will thus either need a strong justification in order to retain them or else be revised to account for the newer observations. It is the purpose of this section to go over some of these newer data which do not fit in with the current model.

3.3.1 Energetics

The first problem to be considered is that of energetics. To oxidize water a potential > +0.8v is required. The accumulation of charge by successive photoactivations could satisfy this energy requirement, but requires an increasing energy

input at each step. It is much easier to remove an electron from a neutral species rather than from a positively charged species. Thus as positive charges accumulate they must be stabilized in some way and the activation energy must be reduced (or equalized) for succeeding steps.

Van Gorkom and Donze (85) have proposed that one possible way to stabilize the charge is through the creation of an electrical field gradient. They describe the System II reaction center as MZPQ where P is the reaction center chlorophyll, Z and Q have their usual meanings and M is the charge accumulating species. As charge accumulates after successive photoreactions an electric field is created across the center (which is pictured more or less as a linear rigid structure of MZPQ). The electric field will not affect the rate of forward reactions (i.e., transfer of an electron to the A pool) presumably because the activation energy is unaffected. In their definition of the S state the positive charge can be distributed anywhere over the three possible oxidized species, e.g., for the S_3 state the following equilibrium could exist:

$$M^{+}Z^{+}P^{+} \rightleftharpoons M^{2+}ZP^{+} \rightleftharpoons M^{2+}Z^{+}P \rightleftharpoons M^{3+}ZP \qquad (10)$$

Since the electrons can be channeled to the A pool, an energetically downhill reaction, the equilibrium shifts towards the more highly oxidized form of M, i.e., $M^{3+}ZP$. This

prepares P to give up another electron by the next photoreaction. As a consequence the energy is stored in the form of an electric field across the reaction center. When the M^{4+} state is reached it will rapidly oxidize water.

The model is based on the assumption that the reaction center is a linear array of MZPQ oriented orthogonal to the thylakoid membrane. Work done in several laboratories does suggest that Q is toward the outside of the thylakoid membrane and the O_2 evolving site is toward the inside (see review by Trebst (86)). Recently, Mathis et al. (87) and Jursinic and Govindjee (83) have proposed the existence of another intermediate between Z and M based on luminescence studies. Thus, the reaction center would be MZ_1Z_2PQ.

The other major assumption in the above model is that an electric field gradient is created across the reaction center. From electrochromic shifts in the carotenoid absorption band Witt and co-workers (88) have shown that an electric potential is created very rapidly (<20 ns) across the membrane. According to Joliot and Delosme (89) the potential created in the very fast time region represents only a small fraction of the total potential that is created in longer times. However, it appears that potential gradient is probably not involved in the initial stabilization of charge. Recently Jursinic et al. (90) have shown that the dissipation of the potential gradient with ionophores has no effect on the fast microsecond

component of DLE. This component is believed to arise from recombination of P_{680}^{+} and Q^{-} and is in competition with transfer of an electron from Z to P_{680}^{+}. This does not exclude, however, the possibility of the involvement of a potential gradient in the final stabilization of charge on M (or S) at longer times.

3.3.2 Stability of the S_1 State

One of the most unsatisfying assumptions in Kok's model is the stability of the S_1 state in the dark. Why should one oxidizing equivalent be stable? Doschek and Kok (91) tried to circumvent this assumption by explaining the peak in the O_2 yield on the third flash as a double transition occurring after the first flash, i.e., all centers would start out in S_0 and advance two steps after the first flash. However, such a transition could not be sequential (i.e., $S_0 \rightarrow S_1 \rightarrow S_2$) since O_2 is produced on the third flash even in short flashes (82) while the turnover time is >100 μs. This idea is also inconsistent with the equal quantum yields for each of the four steps.

As discussed earlier the best evidence for the stability of S_1 is that the S_1/S_0 ratio can be varied by appropriate flash preillumintion and that during long dark periods the S_1/S_0 ratio tends to approach a constant value (~3), independent of preillumination. Bouges-Bocquet (84) also showed that the S_1/S_0 ratio can be changed chemically. In the

presence of 0.1 M FeCy after 5 min in the dark the S_1/S_0 ratio increased. Since the average percent misses did not appear to be affected by FeCy, this result was explained as chemical oxidation of S_0 to S_1. With DCPIP-ascorbate (0.1 mM) the S_1/S_0 ratio decreased, indicating a chemical reduction of S_1 to S_0. These results suggest an equilibration of S_1 and S_0 that can be affected by redox reagents.

Kok et al. (92) have recently estimated the midpoint redox potential for the various S transitions and calculated the S_0/S_1 couple to be more oxidized than +0.5v. Therefore, they would not expect weak redox reagents such as FeCy and DCPIP-ascorbate to affect the S state directly. They suggest instead that only O_2 is capable of direct oxidation of the S states. Accordingly, an equilibrium between S_0 and S_1 is established by the oxidizing potential of O_2 and a pool of some endogenous reductant R, i.e.,

$$S_0 \underset{R}{\overset{O_2}{\rightleftharpoons}} S_1 \qquad (11)$$

The effect of the redox reagents would be to alter the pool size of R and thereby indirectly affect the S_0/S_1 equilibrium.

Greenbaum and Mauzerall (93) disagree with the above interpretation. Under anaerobic conditions the O_2 yield was very low and no oscillations were observed in Chlorella cells. Ley et al. (94) obtained similar results with Anacystis. However, Greenbaum and Mauzerall do get normal oscillations when

the oxidant benzoquinone is added, as though the normal S_1/S_0 ratio was reestablished. In fact, the yield after the second flash was very high compared with aerobic conditions. Assuming double hits are primarily a technical problem, they suggested that the benzoquinone has sufficient oxidizing power to form some S_2.

However, Kok and Velthuys (95) point out that due to cell respiration, under anaerobic conditions the A pool is largely reduced. This causes the reaction center turnover to slow down, effectively increasing the number of misses; hence, very little O_2 and no oscillations are observed. The low O_2 yield could also be due to the fact that any O_2 which is produced is rapidly used in cell respiration before it can be detected by the electrode. When benzoquinone is added cell respiration is inhibited and the A pool becomes oxidized thus allowing for a normal O_2 flash yield pattern. Since S_2 does not deactivate in the presence of benzoquinone (even after 60 min) the yield after the 2nd flash will be higher.

Recently, Velthuys and Visser (96) suggested that all centers could start in the S_1 state. Babcock and Sauer (97, 98) showed that the EPR Signal II (in second time region) arose from some free radical that apparently forms from the S_2 and S_3 state but not the S_1 state. Since according to Bouges-Bocquet (84) DCPIP-ascorbate shifts the S_1/S_0 equilibrium to fewer S_0, then after one flash less centers will

be in S_2 in the sample containing the reductant than in samples without reductant. When they measured EPR Signal II after a flash, the magnitude did not change with the reductant, as though the S_1/S_0 equilibrium did not change. To account for the high O_2 yield after the fourth flash (which would arise from the initial S_0 state) in the usual flash pattern, they predicted a high miss parameter in the first flash, but gave no reason why this would occur.

Some insight into the question of why one oxidizing equivalent should be stabilized in the dark comes from the work of Bouges-Bocquet (99). She was able to determine the number of electrons transferred from System II to the acceptor pool A as a function of flash number by monitoring the extent of methyl viologen reduction in far red light after a flash sequence. The number of electrons coming from System II oscillated with a period of two and damped out simultaneously with O_2 oscillations. From these results she concluded that there was a component, termed B, on the reducing side of System II which transfers electrons two by two into the A pool. From flourescence measurements Velthuys and Amesz (100) independently arrived at the same conclusion and named this intermediate R. The unique aspect of this model is that electrons can only be transferred to the A pool by twos. If there is only one electron on B(R) it will not be transferred but stored on that intermediate. In this way a

charge separation can exist for long periods of time in the dark, the positive charge stabilized on the S intermediate and the electron on the B(R) intermediate.

3.3.3 Misses and Deactivation

In their original analysis, Forbush et al. (78) assumed that the percent misses was equal at each of the four steps and calculated an average value of ~11% for isolated chloroplasts. However, they did point out that this may not necessarily be the case, that one step may have more misses than another step. In Velthuys and Visser's interpretation (96) misses are greater during the first flash than on succeeding flashes. Recently, Delrieu (101) reanalyzed the O_2 flash yield pattern and obtained a better computer fit when misses were assumed to be high for the $S_2 \rightarrow S_3$ and $S_3 \rightarrow S_4$ transitions in the first cycle. After light activation the reaction center must relax to its uncharged state before it can undergo another photoreaction (i.e., $S_n \xrightarrow{h\nu} S_n' \longrightarrow S_{n+1}$). The reaction center turnover depends on the transfer of electrons from Q^- to A [or B(R)]. In the dark the rate constant, K_A, for the $Q \rightleftharpoons A$ equilibrium is very large favoring transfer of electrons to A. As long as Q^- remains reduced the center is closed and effectively causes a miss. Assuming this to be the situation, Delrieu calculated $\alpha = 0.548$ for $S_2 \rightarrow S_3$ transition and 0.20 for $S_3 \rightarrow S_4$ transition. These values seem unreasonably high for one step in a mechanism which has a high overall

efficiency. That something peculiar occurs in the $S_2' \rightarrow S_3$ transition, however, is supported by the sigmoidal kinetics of this reaction, which is not apparent in the other relaxation steps.

The failure of the reaction center to turnover because Q^- remains reduced represents one possible mechanism for misses. However, the recovery time of reduced Q^- occurs with $t_{1/2}$ ~600 μs (83) and for flashes given 1-2 s apart one would not expect this to limit the reaction center turnover, unless Q^- remains reduced in some centers for long periods of time for some reason.

The other possible mechanism to account for misses is a back reaction between P_{680}^+ and Q^-. Indeed, μs DLE oscillates with a period of four as though it is being modulated by the S states (83). However, the oscillations damp out much more quickly than the O_2 oscillations and the DLE yield is much too small to account for the high percentage of misses. The mechanism of misses still remains to be determined.

Deactivation is usually referred to the discharge of the higher S states. Lemasson and Barbieri (102) reported that S_3 decays at a faster rate after preillumination with 650 nm light than with 700 nm light. Since 650 nm light tends to reduce an appreciable fraction of the A pool between the two photosystems, these authors suggested that deactivation proceeds via the back reaction which depends on the extent of

reduction of the Q and A pools. However, they could find no effect of the redox state of the A pool on deactivation of S_2. As mentioned above the DLE yield at the long time range where deactivation occurs is too small to account for all of the loss of oxidizing equivalents.

Alternatively, deactivation could be due to a direct reduction of the positive hole by some electron donor other than water. To explain the second order kinetics, Forbush et al. (78) invoked the endogenous reductant, R, which is oxidized during deactivation. R could be cytochrome b559 which is closely associated with System II reaction center and is reduced in the light (103).

Renger (104) has discovered several reagents which speed up the rate of deactivation. Certain uncouplers, such as CCCP and variously substituted thiophenes, increase the rate of decay by as much as 100 fold. Renger called such reagents ADRY reagents for the acceleration of the deactivation reactions of the water splitting enzyme system Y (in Witt's group Y is used in place of S).

Several mechanisms for ADRY behavior were considered (105). Since all ADRY reagents contain a weak acidic amine group, one proposal was that ADRY reagents cause a breakdown of the proton gradient and thereby deactivate the higher S states. But NH_4Cl also breaks down the proton gradient, yet had no effect on the deactivation of the higher S states at

the same concentration. A possible direct reduction of S by ADRY reagents was considered unlikely for stochiometric reasons. Instead, the mechanism which was considered most likely was an induced cyclic electron flow catalyzed by the ADRY reagents, perhaps via a conformational change, which involved the S intermediate and some reduced intermediate after Q in the electron transport chain.

Many reagents have been found to exhibit ADRY behavior. Of particular interest is DCMU (106, 107). Bouges-Bocquet et al. (107) showed that high concentration of DCMU accelerates the deactivation of both S_2 and S_3 states in chloroplasts, but only the S_2 state in Chlorella. This apparently explained the discrepancy in the results between Duysens (108) who could demonstrate O_2 evolution by algae in the S_3 state in the presence of DCMU and Rosenberg et al. (109) who could not in chloroplasts. Etienne (110) was able to show later that even the S_3 state deactivates in Chlorella if the DCMU concentration is high enough.

In the model misses are presumed to be only of photochemical origin. If the percent misses increase then the quantum yields at steady state necessarily decrease. Lavorel (111) pointed out (what has been known for a long time) that in intact Chlorella cells the O_2 oscillation damps out faster than in isolated chloroplasts, although the quantum yield is higher, directly opposite of what is expected.

To explain this Lavorel proposed a model in which the O_2 evolving enzyme (E) is mobile with respect to the photocenter (P) allowing for a cooperation among photocenters--as opposed to Kok's et al (77) original assumption. In this model E can take on the usual possible states (n = 0,1,2,3,4), but can only advance to the next higher state when bound to the photocenter, i.e.,

$$E_n + P^+ \rightleftharpoons E_nP^+ \longrightarrow E_{n+1} + P \qquad (12)$$

Thus, when the number of enzyme units is greater than the number of photocenters ([E] > [P]), as might be assumed to be the situation in intact Chlorella cells, the percent misses appear large (many of the enzyme units are not activated) while the overall O_2 yield is high (all photocenters are active in O_2 evolution). On the other hand when the number of photocenters are greater than the number of enzyme units ([E] < [P]), as might be assumed for isolated chloroplasts, the percent misses are low (all enzyme units are activated) but the O_2 yield is low (not all photocenters are active in O_2 evolution). Since E is mobile with respect to P, then in this situation the probability of double hits increases as an enzyme can be activated by more than one photocenter during the flash. Since the lifetime of the active photocenter is short, the extent of double hits still remains small. Lavorel considers that E is mobile within the intrathylakoid space, but this seems unlikely

considering the failure to isolate such a complex and attempts to reconstitute the O_2 evolving system. It is more reasonable to assume that the O_2 evolving complex is restricted to the chloroplast membrane and mobile with respect to a limited number of photocenters. At this time there is no evidence to support Lavorel's hypothesis nor a good explanation for the relationship between the miss parameter and O_2 yield.

3.3.4 Release of Protons

In the Kok et al. (77) model it is assumed that four oxidizing equivalents accumulate in the light and in a concerted reaction oxidize water to O_2 and four protons. Thus, the protons are believed to be released simultaneously with the O_2 release. Initial measurements of proton release made by Fowler and Kok (59) revealed a period of four and were interpreted in terms of the model. However, the pattern of oscillations is also complicated by the proton release and uptake by the plastoquinone pool. The major discrepancy in the data with the model is the large proton release after the second flash. In their paper Fowler and Kok had to include the possibility of some proton release on the $S_2 \rightarrow S_3$ transition. More recent analysis of the proton yield flash pattern by Fowler (unpublished) and by Crofts (unpublished) indicate that the protons are released in the $S_0 \rightarrow S_1$ transition as well. The release of protons indicates the occurrence of the reaction with water and gives a clue to the chemistry of the

reaction--water must be reacting with the S intermediate before the final O_2 evolving step (i.e., $S_3 \rightarrow S_4 \rightarrow S_0$ transition).

3.4 Objective of Thesis Research

The Kok et al. (77) model still presents the minimal hypothesis to explain most of the observations on O_2 evolution. But the model is a kinetic one and until the chemistry of the reactions is known, it can only be considered as a working hypothesis. As pointed out in the preceeding section, there is an increasing number of experimental observations which cannot be readily explained by the model as it now stands. A new approach for a direct study of the S intermediate is needed to clarify the problems.

Manganese is known to be required for O_2 evolution and has been assumed by many to be part of the S intermediate. However, when we began our research there was no evidence to prove the involvement of manganese in this capacity. We first realized that the NMR relaxation rates of water protons can be used to monitor the native bound manganese in cloroplast membranes (112). The objective of our research, then, was to extend the NMR studies to determine what the role of manganese is in O_2 evolution. We have found that manganese does indeed participate in the intermediate states which lead to O_2 evolution, and that NMR methods provide direct experimental approach to the study of the "S" intermediate in the oxygen evolving mechanism.

CHAPTER II

PROTON RELAXATION THEORY

In the last several years pulsed NMR methods have proved to be a powerful tool in the study of complex biological macromolecules. Details of the theory, technique and applications, particularly for manganese-enzyme complexes, have appeared in several excellent reviews and monographs (113-118). In this chapter some of the basic NMR theory as we have applied it to the study of proton relaxation of chloroplast membranes is presented.

1 Basic Resonance Phenomenon

Nuclei with an odd charge number possess a net angular momentum or spin, $\bar{J}$. These nuclei, acting as spinning charges, give rise to a magnetic dipole moment, $\bar{\mu}_I$. The relationship between $\bar{\mu}_I$ and $\bar{J}$ is:

$$\bar{\mu}_I = \gamma_I \bar{J} \tag{13}$$

where, γ_I is the nuclear magnetogyric ratio. γ_I is an intrinsic property of the structure and is characteristic for each nucleus. The angular momentum is quantized such that

$$\bar{J} = \hbar[I\ (I + 1)]^{\frac{1}{2}} \tag{14}$$

where I is the nuclear spin quantum number.

In the absence of a magnetic field the individual nuclear magnetic dipoles will be randomly oriented and the net magnetization ($\bar{M}$)--defined as the vector sum of all magnetic dipoles in the spin system--will be zero. When an external field, $\bar{H}_o$, is applied, the nuclear magnetic dipoles tend to orient with the field and to precess about the axis of the field at a frequency given by the Larmor equation:

$$\omega_I = \gamma_I \bar{H}_o \qquad (\text{rad } s^{-1}) \tag{15}$$

where ω_I is the nuclear Larmor frequency. Since an individual nuclear dipole can take on (2I + 1) orientations in a magnetic field, then for spin 1/2 nuclei, such as protons, two orientations are possible--parallel and antiparallel with the field. At thermal equilibrium a Boltzmann distribution is established between the energy levels for these two orientations.

The spin distribution can be perturbed by the application of a magnetic field--in the case of the NMR experiment, by radio frequency (rf) radiation. The spin system interacts with rf fields at the Larmor frequency. When this condition is met, resonance is said to take place. Those nuclei in a higher energy level can give up energy to the rf field, while those in a lower energy level can absorb energy from the rf field. Since there are usually more nuclei in the lower energy level at room temperatures, there is a net

absorption of energy from the rf field in the NMR experiment.

2 Rotating Frame Analysis--Definition of $1/T_1$ and $1/T_2$

To visualize the pulsed NMR experiment it is helpful to consider a frame of reference which is rotating about the applied field. In Figure 4a, the individual nuclear dipoles are shown precessing around $\overline{H}_o$, which is defined along the z axis. Slightly more dipoles are oriented parallel with $\overline{H}_o$. To an observer positioned on the stationary y axis, the nuclear dipoles appear to be rotating around z at the Larmor frequency. As the frame also begins to rotate around z in the same direction as the dipoles, then to the observer (who is rotating along with the frame) the nuclear dipoles appear to be rotating slower than before. When the frame itself rotates at the Larmor frequency, the nuclear dipoles then appear stationary to the observer. This is depicted in Figure 4b, where the rotating frame is designated by the primed axes. The vector sum of the nuclear dipoles is the net magnetization, $\overline{M}$. Since more nuclei are aligned with $\overline{H}_o$ than against it, $\overline{M}$ lies parallel with the +z direction, as shown in Figure 4c.

It can be shown that the motion of $\overline{M}$ in the rotating (ROT) frame is:

$$(d\overline{M}/dt)_{ROT} = \gamma_I \, \overline{M} \times \overline{H}_{eff} \qquad (16)$$

where $\overline{H}_{eff}$ is the effective field and is the net sum of all

Figure 4. Definition of $1/T_1$ and $1/T_2$ Relaxation in the Rotating Frame. (a) Precession of nuclear spins ($I = 1/2$) about the applied field, $\bar{H}_o$. $\bar{H}_o$ is defined along the z-axis. (b) Spins appear stationary in the rotating frame (x', y', z'). (c) Net magnetization, $\bar{M}$, of the nuclear spins. (d) Application of an rf field, $\bar{H}_1$, in the rotating frame. (e) After rf is turned off, $\bar{M}$ relaxes back to equilibrium condition. The growth of $\bar{M}$ along the +z' axis is called longitudinal relaxation and is characterized by a time constant T_1 while the decay of $\bar{M}$ along the y axis is called the transverse relaxation characterized by a time constant T_2. (f) Contribution of the dephasing of the individual nuclear dipoles in the x'y' plane to $1/T_2$.

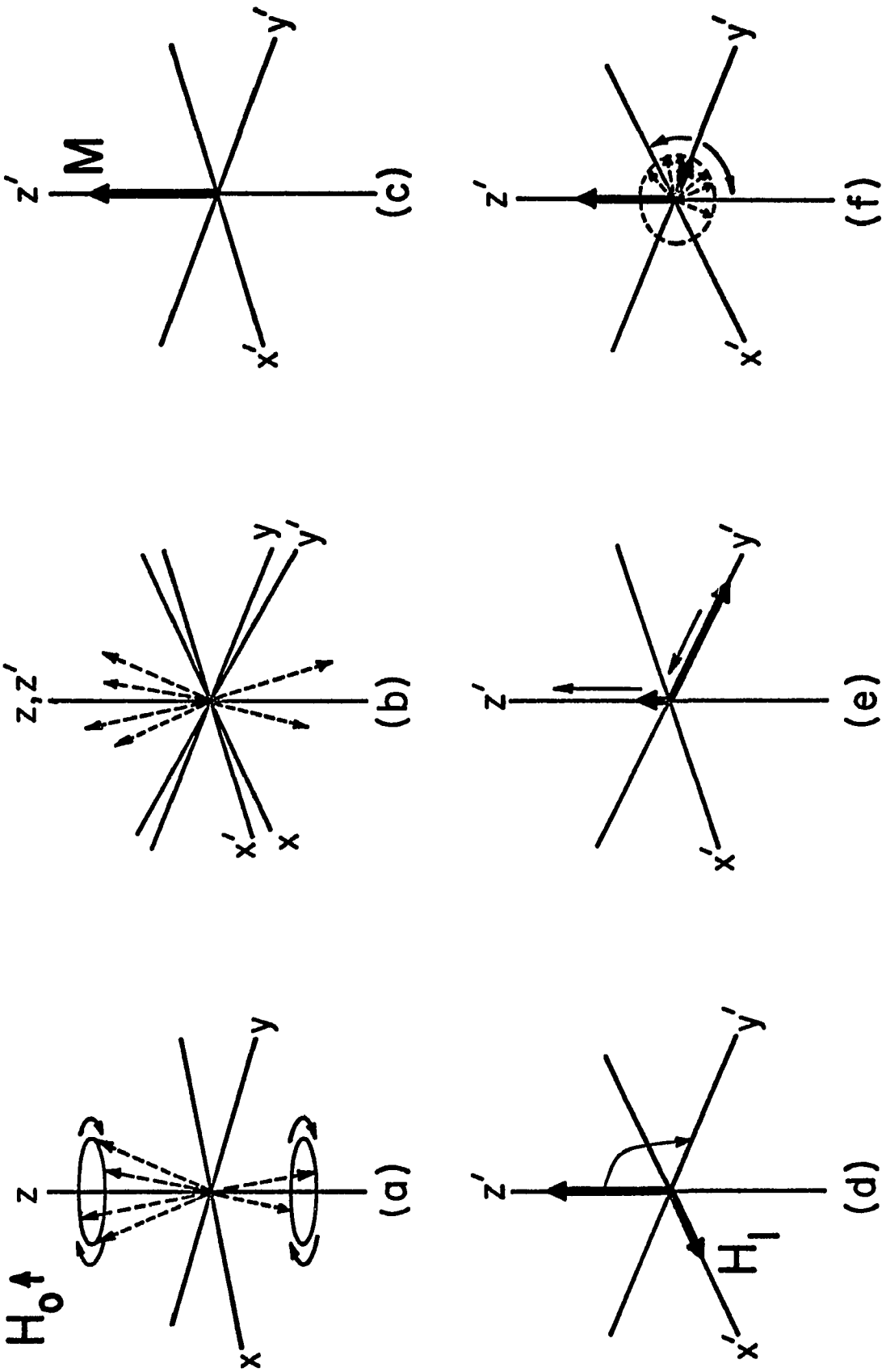
z'
M
y'
x'
(c)
z,z'
y,y'
x',x
(b)
z
y
x
H_0
(a)
z'
y'
x'
(f)
z'
y'
x'
(e)
z'
y'
x'
H_1
(d)

fields within the rotating frame. Included in $\bar{H}_{eff}$ is a "fictitious" field created by the effect of rotation. This "fictitious" field is given as ω/γ_I, where ω is the frequency of rotation. Thus, in the absence of an rf field:

$$\bar{H}_{eff} = \bar{H}_o - \omega/\gamma_I \tag{17}$$

When ω equals the Larmor frequency, ω_I then from Equation 15, $\bar{H}_{eff} = 0$. Hence, $\bar{M}$ does not change with time in a frame rotating at the Larmor frequency, as shown in Figure 4c.

If an rf field, $\bar{H}_1$, is introduced into the rotating frame so that its direction is along the x' axis, then $\bar{H}_{eff} = \bar{H}_1$. $\bar{H}_1$ is illustrated in Figure 4d where it also appears stationary since it is fluctuating at the Larmor frequency. However, $\bar{M}$ will now precess about $\bar{H}_1$ according to Equation 16. The extent that $\bar{M}$ moves about $\bar{H}_1$ depends on the length of time, t_p, $\bar{H}_1$ is applied. The angle, θ, through which $\bar{M}$ precesses is given as:

$$\theta = \gamma_I \bar{H}_1 t_p \tag{18}$$

Thus, the longer $\bar{H}_1$ is applied, the larger the angle $\bar{M}$ moves through.

In Figure 4d, $\bar{H}_1$ is left on long enough so that $\bar{M}$ tips to the y' axis. This is called a 90° pulse and under this condition the spin distribution has been equalized among the energy levels. If $\bar{H}_1$ is left on twice as long (a 180° pulse)

$\bar{M}$ rotates to the -z' direction, in which case the spin distribution has been inverted from the equilibrium condition.

After the rf pulse the spin population tends to return back to its original Boltzmann distribution. This is represented by the growth of $\bar{M}$ back along the +z' axis and is called the longtitudinal relaxation. It is described by a first order rate expression:

$$\bar{M}_{z'}(\tau) = \bar{M}_o[1 - 2\exp(-\tau/T_1)] \tag{19}$$

where $\bar{M}_{z'}(\tau)$ is the magnitude of the z' component of $\bar{M}$ at some time τ after the rf pulse, $\bar{M}_o$ is the maximum value of $\bar{M}$ at thermal equilibrium and T_1 is the time constant for longitudinal relaxation.

The decay of $\bar{M}$ along the y' axis ($\bar{M}_{y'}$) is defined as the transverse relaxation (Figure 4c) and is characterized by another first order time constant, T_2, i.e.,

$$\bar{M}_{y'}(\tau) = \bar{M}_o \exp(-\tau/T_2) \tag{20}$$

where $\bar{M}_{y'}(\tau)$ is the magnetization magnitude along the y' axis at some time $\tau \geq 0$.

During the rf pulse all of the individual nuclear dipoles are forced into phase. But after the rf pulse, they immediately begin to lose their phase coherency. This is represented in Figure 4f by the fanning out of the individual dipoles in the x'y' plane. As a result $\bar{M}_{y'}$ can decay faster

than the growth of $\bar{M}$ back along +z' direction and it will always be true that $1/T_2 \geq 1/T_1$.

The loss of phase coherency arises from the slightly different magnetic environments experienced by the individual nuclear dipoles. As a result the applied field inhomogeneities (inhom) will also contribute to the observed rate, $1/T_2^*$, i.e.,

$$1/T_2^* = 1/T_2 + 1/T_{2(\text{inhom})} \tag{21}$$

Thus, it is important that field inhomogeneity be made minimal or be corrected for in order to get the true $1/T_2$ of the spin system.

3 Pulse Methods for Measuring $1/T_1$ and $1/T_2$

3.1 Inversion Recovery Method for $1/T_1$

The most commonly used method for measuring $1/T_1$ is the 180°, τ, 90° pulse sequence. First an 180° pulse is applied to invert the equilibrium magnetization, $\bar{M}_o$ to along the -z' axis. Longitudinal relaxation now occurs, causing $\bar{M}$ to go from the value of $-\bar{M}_o$ through 0 to the equilibrium + $\bar{M}_o$. Technically, it is impossible to measure $\bar{M}$ along the z' axis since this is the direction of the applied field. The detector coils in the NMR spectrometer measure fields orthogonal to $\bar{H}_o$ along the y' axis. Thus, at a time τ after the 180° pulse, a 90° pulse is given to bring $\bar{M}$ to lie along the

-y' axis. A signal can now be measured by the detector coils, the initial height of which is proportional to the magnitude of $\bar{M}$ in the z' axis at time τ. If the system is now allowed to return to equilibrium by waiting at least $5xT_1$ a second 180°, τ, 90° pulse sequence can be repeated using a different τ value. From Equation 19, the slope of a plot of $\ln \frac{\bar{M}_{z'}(\tau)-\bar{M}_o}{2M_o}$ vs. τ gives $-1/T_1$.

3.2 Carr-Purcell-Meiboom-Gill Method for $1/T_2$

One might assume that since the detector coils are in the direction of y', then after a 90° pulse, the decay of the magnetization along y' should measure $1/T_2$. This signal is called the free induction decay, but as pointed out earlier in Section 2, it arises from a dephasing of the dipoles in the x'y' plane and contains contributions from both field inhomogeneities as well as the real $1/T_2$ (see Equation 21). A method for overcoming the inhomogeneity problem is to apply a 180° pulse at variable times, τ, after the initial 90° pulse, similar to the inversion recovery method for $1/T_1$. The 180° pulse inverts the direction of the dipoles to the -y' axis. The dipoles which fan out due to field inhomogeneities tend to refocus back along the -y' axis at a time, 2τ, after the 90° pulse, while the dephasing due to the real $1/T_2$ relaxation processes continues to decrease $\bar{M}$.

Although this pulse sequence corrects for reversible dephasing processes, it becomes limited by the effect of

molecular diffusion. The precise refocusing of the nuclear dipoles is dependent upon each nucleus remaining in a constant magnetic field during the time of the experiment (i.e., 2τ). If diffusion causes nuclei to move from one part of an inhomogeneous field to another, the advantage of the pulse sequence is defeated. A simple modification, however, can be made to overcome the effects of diffusion. Instead of following the initial 90° pulse with one 180° pulse, a whole series of 180° pulses are used until $1/T_2$ relaxation is complete, i.e., a 90°, τ, 180°, 2τ, 180°, 2τ, 180° . . . sequence. Thus, the sequence allows a continuous refocusing of the dipoles to eliminate field inhomogeneity errors; by making τ short all diffusional errors can, in principle, be made negligible.

There is still another problem in this method and that is the technical imperfection in the rf pulse. The accuracy of setting the pulse width is limited to about 5% by the inhomogeneity of $\overline{H}_1$ itself. For long $1/T_2$'s where long pulse trains are required (2,000 or more pulses) the cumulative error in pulse width can become quite serious. To overcome this the phase of $\overline{H}_1$ is shifted 90° after the initial 90° pulse, i.e., $\overline{H}_1$ is made to lie along the +y' axis on the second and succeeding 180° pulses. This allows the nuclear dipoles to flip about the y' axis after each 180° pulse rather than the x' axis. Since after each even numbered

pulse the nuclear dipole will be in the x'y' plane, any pulse width error present on the odd pulses are averaged out. For details, see Farrar and Becker, pp. 22-29 (117). From Equation 20 a plot of $\ln(\bar{M}_y'(\tau)/\bar{M}_o)$ vs. τ gives $-1/T_2$.

This pulse sequence is called the Carr-Purcell-Meiboom-Gill (CPMG) method and provides one of the best ways to measure $1/T_2$.

4 Magnetic Relaxation Processes

In general, any mechanism which gives rise to a fluctuating magnetic field at a nucleus is a possible relaxation mechanism. The important condition is that the interacting fields fluctuate at the Larmor frequency. In liquids and in particular for protons the major mechanism leading to relaxation involves dipole-dipole interactions. The frequency of the interacting dipolar fields is governed by molecular motions and is referred to as modulation. Each molecular motion is characterized by a correlation time, τ_c, which sets a time domain for random fluctuations (i.e., it correlates a given value of orientation or position at a particular instant with the value at some later time). Nuclei undergoing very rapid motions have a short τ_c since they quickly lose correlation (or memory) of their previous orientations, while nuclei undergoing slow motions have a long τ_c.

The other condition that governs the extent of magnetic interactions is the magnitude of the interacting fields. The

electronic magnetic dipole is about 1000x larger than the nuclear magnetic dipole. Thus, electron-nuclear dipolar interactions will always dominate over smaller nuclear-nuclear dipolar interactions and the introduction of a paramagnetic species (i.e., an ion with one or more unpaired electrons) will greatly enhance nuclear relaxation. The remaining part of this chapter deals with paramagnetic relaxation theory.

5 Proton Relaxation in Paramagnetic Systems

In water-paramagnetic ion systems the rate of the water proton relaxation is governed by the interaction with the paramagnetic species:

$$1/T_{1,2(P)} = 1/T_{1,2(obs)} - 1/T_{1,2(D)} \qquad (22)$$

where $1/T_{1,2(P)}$ is the paramagnetic contribution to longitudinal or transverse relaxation rates, $1/T_{1,2(obs)}$ is the observed rate and $1/T_{1,2(D)}$ represents the background diamagnetic contribution. The paramagnetic effect varies with the inverse 6th power of distance between the center of the paramagnetic ion and the relaxing nucleus; it is largest on nuclei directly bound to the paramagnetic ion and rapidly diminishes as the distance increases from the ion. In the presence of chemical exchange between bound and unbound sites and for Mn(II)-H_2O complexes where the chemical shift term is

negligible, (see reference 115, p. 211), the paramagnetic contribution is given as:

$$\frac{1}{T_{1,2(P)}} = \frac{pq}{T_{1,2(M)}+\tau_M} + \frac{1}{T_{1,2(OS)}} \qquad (23)$$

where the first term on the right hand side of this equation describes the paramagnetic interactions with nuclei bound in the first coordination sphere of the ion and $1/T_{1,2(OS)}$ represents paramagnetic interactions outside the first coordination sphere.

In Equation 23 p is the fraction of nuclei bound in the first coordination sphere and is given by the mole fraction of the paramagnetic ion with respect to the concentration of relaxing nuclei (e.g., [Mn]/55.5 for Mn-H_2O systems), q is the co-ordination number (i.e., $6 \geq q > 0$ for Mn (II)), $T_{1,2(M)}$ is the time constant for the relaxation rate of the bound nuclei and τ_M is the lifetime of a nucleus bound to the paramagnetic species.

When $\tau_M > T_{1,2(M)}$, chemical exchange dominates the first term on the right side in Equation 23 and the system is said to be slow (chemical) exchange limited. When $\tau_M < T_{1,2(M)}$, the paramagnetic effect on the bound nuclei dominates and the system is in the fast exchange region. The condition $\tau_M \simeq T_{1,2(M)}$ could also arise, in which case both paramagnetic and chemical exchange contributions govern the overall relaxation rates.

The electron-nuclear dipolar contributions to the relaxation of bound nuclei are expressed by the Solomon-Bloembergen equations (119-120). For magnetic interaction modulated in the range of the nuclear Larmor frequency, only the term in ω_I contributes and the equations reduce to:

$$\frac{1}{T_{1(M)}} = \frac{2}{15} \frac{S(S+1)\,\gamma_I^2\,g^2\,\beta^2}{r^6} \left[\frac{3\tau_C}{1+\omega_I^2\,\tau_C^2}\right] \quad . \tag{24}$$

and

$$\frac{1}{T_{2(M)}} = \frac{1}{15} \frac{S(S+1)\gamma_I^2\,g^2\,\beta^2}{r^6} \left[4\tau_C + \frac{3\tau_C}{1+\omega_I^2\,\tau_C^2}\right] \tag{25}$$

where r is the distance between the nucleus and the center of the paramagnetic ion, S is the total electron spin, γ_I is the nuclear magnetogyric ratio, g is the electron g factor, β is the Bohr magneton, ω_I is the nuclear Larmor frequency and τ_C is the overall correlation time for the electron nuclear dipole-dipole interaction. It has been found in many Mn(II) macromolecular systems that the hyperfine (contact) contribution is very small to both $1/T_{1(M)}$ and $1/T_{2(M)}$ (see reference 115, p. 205); therefore these terms were ignored in Equations 24 and 25.

The interaction between protons and paramagnetic ions in macromolecular systems may be modulated by several time dependent processes, the major ones being: (1) rate of

electronic relaxation of the paramagnetic ion ($1/\tau_S$), (2) rate of chemical exchange for nuclei between the bound and unbound sites ($1/\tau_M$), (3) rate of rotational motions of the paramagnetic ion complex ($1/\tau_R$), and (4) translational diffusion ($1/\tau_D$). The overall correlation time for nuclear relaxation is then given as:

$$1/\tau_C = 1/\tau_S + 1/\tau_M + 1/\tau_R + 1/\tau_D \qquad (26)$$

The fastest rate process dominates $1/\tau_C$. For aqueous Mn(II) solutions $1/\tau_R$ and $1/\tau_D$ govern the proton relaxation rate, while in Mn(II) macromolecular complexes these terms are usually negligible due to the slower tumbling motions of the macromolecules. In the analysis of relaxation mechanisms in such cases, one is usually concerned with $1/\tau_S$ and/or $1/\tau_M$. The contribution of $1/\tau_S$ and $1/\tau_M$ may be determined from the temperature and frequency dependence of the relaxation rates.

The temperature dependence of $1/\tau_M$ mechanisms show typical Arrhenius behavior with activation energies in the range of 5-15 kcal/mole. On the other hand, $1/\tau_S$ mechanisms show very little temperature dependence. Usually in Mn(II) systems the best approach to distinguish between $1/\tau_M$ and $1/\tau_S$ is through the frequency dependence of the relaxation rates. $1/\tau_M$ is frequency independent and when it governs $1/\tau_C$ in Equation 26, both $1/T_{1(M)}$ and $1/T_{2(M)}$ show very little frequency behavior (if anything, $1/T_{1(M)}$ will decrease with

increasing frequency--for the predicted theoretical curves from Equations 24 and 25 see reference 115, p. 199). On the other hand, $1/\tau_S$ may be frequency dependent since it is a function of the modulation of the zero field splitting by molecular collisions. The frequency dependence of τ_S is given by the Bloembergen-Morgan equation (121):

$$\frac{1}{\tau_S} = B \left[\frac{\tau_V}{1 + \omega_S^2 \tau_V^2} + \frac{4\tau_V}{1 + 4\omega_S^2 \tau_V^2} \right] \qquad (27)$$

where τ_V is the correlation time related to the rate at which the zero field splitting is modulated, ω_S is the electronic Larmor frequency ($\omega_S \simeq 658\ \omega_I$) and B is a constant containing the resultant interaction between the electron spin and zero-field splitting parameters. $1/\tau_S$ becomes frequency dependent when $\omega_S\tau_V >> 1$, $1/\tau_S$ then decreases with frequency. When $1/\tau_S$ dominates the nuclear relaxation rates, i.e., $1/\tau_C = 1/\tau_S$, $1/T_{1(M)}$ peaks when $\omega_I\tau_S \sim 1$ (Equation 24) while $1/T_{2(M)}$ increases with frequency (Equation 25) (see reference 115, p. 199).

In many Mn(II)-macromolecular systems, manganese is usually added at relatively high concentrations. The observed rates are large and the non-site specific or outer sphere interactions ($1/T_{1,2(OS)}$, Equation 23) are relatively small and usually neglected. However, in the analysis of the chloroplast system given in Chapter III it was necessary to include

$1/T_{1,2(OS)}$ contributions. Outer sphere mechanisms are difficult to analyze because they too will have a frequency dependence. Two limiting cases have been proposed to govern outer sphere relaxation: (1) electronic relaxation of the paramagnetic ion and (2) translational diffusion of the interacting nuclei (for details see, reference 115, pp. 190-191).

CHAPTER III

PROTON RELAXATION MEASUREMENTS OF CHLOROPLAST MEMBRANES

1 Experimental Methods

1.1 Preparation of Samples

Dwarf peas (Pisum sativum, var. Progress No. 9) were grown as follows. Seeds were soaked in aerated deionized water for 12 hr and planted in flats of vermiculite. At planting, each flat received 1 ℓ of Hoagland's solution (122) containing 9 μM $MnCl_2$; thereafter, the plants received only deionized water. The plants were grown under 16 hr light (23°C) / 8 hr dark (20°C) cycle. Light intensity during growth was 1.5×10^4 mW/cm^2 (ITT F72512/Cool White Fluorescence Lamps). Spinach and lettuce were purchased from the market and used in those experiments as indicated.

Chloroplast membrane fragments (hereafter called chloroplasts) were isolated from 12-16 day old pea plants (or market spinach or lettuce). Leaves were washed in deionized water (and deveined in the case of spinach and lettuce) and homogenized in a Waring blender for ~15 s in a medium consisting of 50 mM N-2-hydroxyethylpiperzine-N-2-ethanesulfonic acid (HEPES) buffer, adjusted to pH 7.5 with NaOH, 400 mM sucrose and 10 mM NaCl. During grinding 0.5% bovine serum albumin and 10 mM sodium ascorbate were included. The homogenate was filtered through 4 layers of cheesecloth and a nylon cloth

(10 μ mesh) and then centrifuged at 2,000 xg for 5 min. The chloroplast pellet was resuspended in the isolation medium without sucrose, recentrifuged and finally resuspended in a small volume of the original medium. Chlorophyll was determined by the method of Arnon (123) and samples were adjusted to a final concentration of 2 or 3 mg Chl/ml for NMR measurements. Other conditions are indicated in the figure legends.

1.2 Measurement of Oxygen Evolving Activity

The steady state O_2 evolution in chloroplasts was measured under continuous illumination using a Clark electrode and Yellow Springs Model 53 Oxygen monitoring system. Choroplasts were suspended in the medium described above containing 0.5 mM FeCy and 1 μM gramicidin D at a chlorophyll concentration of 30 μg/ml. Saturating continuous illumination (250 mW/cm^2) was provided by an incandescent lamp through a Corning CS 3-71 glass filter and a two inch water filter.

O_2 evolution under flashing light conditions was measured on a Joliot type electrode (124) using only one chamber, as no accepter was present. Signals were recorded on a Midwestern Instruments Model 801 oscillographic recorder. Saturating light flashes were obtained from a Phase-R Model DL-2100 A dye laser. 50 μM Rhodamine 6G dissolved in methanol was used to obtain 590 nm light. The laser pulse has a pulse width of 0.6 μs at halfheight and terminates in about 2 μs. In order to maintain the same flash conditions as used

in the NMR experiments, flashes were spaced 4 s apart. To avoid variations in flash intensities in the first few flashes, the light was blocked on the first two flashes before exciting the sample. Alternatively, a General Radio Model 1538-A strobe lamp with a pulse width of 3 μs and extended tail up to 10 μs was used for excitation.

1.3 Manganese Determination

The manganese content of the chloroplast membranes was measured by the atomic absorption method. Preparation of the samples was after Blankenship and Sauer (39). One ml of the sample (3 mg Chl/ml) was digested with 2 ml of 85% concentrated HNO_3 and 15% concentrated $HClO_4$, v/v, under gentle heating. The digested sample was filtered through Whatman #50 filter paper and brought to a final volume of 5 ml with deioninzed water. Measurements were made with a Perkin-Elmer Model 303 Atomic Absorption Spectrometer. Standards at 0.2, 0.4, 0.6, 0.8 and 1.0 ppm Mn were prepared in the buffer medium and carried through the same digestion procedure as the sample. Manganese determinations of the samples were extrapolated from the standard curve which was linear, passing through the origin.

Alternatively, the manganese content was determined on sample aliquots by neutron activation analysis. The samples were heat sealed in precleaned polyethyene. A comparitor standard was prepared by pipetting microliter quantities of

solutions of known manganese concentrations onto a Whatman #42 filter in another precleaned vial. The samples and standard were then irradiated for one hour at a flux of 2×10^{12} neutrons/cm^2-s in the Illinois Advanced TRIGA Reactor facility. After a delay of two to three hours to permit the decay of ^{38}Cl, each sample was counted for 900 s using a 10% efficient Ge(Li) detector (Canberra) having a FWHH resolution of 2.1 keV at 1333 keV. The detector is connected to a charge integrating preamplifier (Canberra Model 2001), an amplifier with baseline restoration and pole zero cancellation (Canberra Model 2101) and a pulse pile-up rejection system (Canberra Model 1468) which permits the use of high count rates without serious peak area losses. The spectra were accumulated in a 4096 channel analyzer (Canberra Model 8100) and transferred to computer compatible magnetic tape for subsequent processing.

The gamma-ray spectral data is reduced to elemental concentrations using the program PIDAQ (developed by J. P. Maney, J. L. Fasching and P. K. Hopke, University of Illinois). The values reported represent the weighted mean values calculated by using two different gamma ray lines emitted by radioactive ^{56}Mn. The uncertainty reported is one standard deviation of the mean value based only on the statistical uncertainty of the counting data.

1.4 Measurement of Proton Relaxation Rates

The proton relaxation rates were measured on either a variable frequency pulsed NMR spectrometer constructed by Dr. Paul Schmidt (used in the frequency studies) or a constant frequency (27 MHz) pulsed NMR spectrometer constructed in Dr. H. S. Gutowsky's laboratory (used in the light experiments). The basic design of a spectrometer is given in Figure 5. The NMR sample probe is positioned between the poles of a magnet which provide a sufficiently strong and stable external field ($\overline{H}_o$). For a frequency dependence study the magnet must be capable of providing a variable field over a suitable frequency range. (We employed a Varian Model V-7400 electromagnet with a field strength up to 24 k gauss. A varian Flux Stabilizer, Model V3508, and Field Homogeneity Unit, Model V-7530, were used to provide adequate field stability and homogeneity.) Rf pulses to the sample are produced by an rf transmitter consisting of an rf synthesizer (Rockland Model 6500, 0.1 to 160 MHz), a gating and phase adjust unit (laboratory built) and an rf amplifier (Arenberg Model PG 650 tunable oscillator operated in the gated mode). The synthesizer generates an rf signal at the resonance frequency (according to Equation 15). The signal is divided into two channels, A and B, by a power divider. The A and B signals are gated and phase adjusted for the appropriate 90° and 180° pulses used in the various pulse sequences. The pulse

Figure 5. Generalized Block Diagram of a Pulsed NMR Spectrometer. The rf transmitter consists of an rf synthesizer, a gating and phase adjust unit and rf power amplifier. The rf receiver consists of appropriate amplifiers and a phase sensitive detecter. PD refers to power divider. The NMR sample probe is positioned in a strong magnetic field. A dye laser is used for light excitation of the sample. A pulse programmer determines the rf and light pulse sequence. Signals are recorded by an oscilloscope and oscillographic recorder. See text for details.

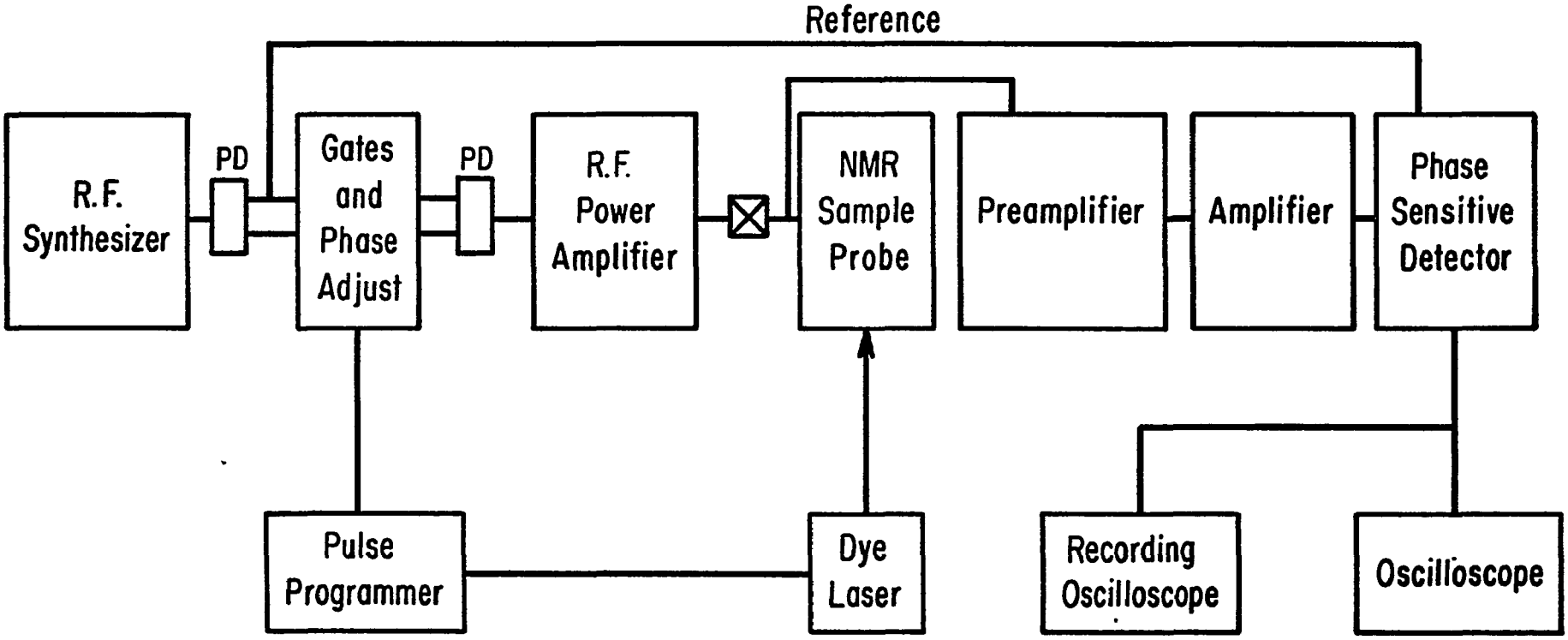
Reference
R.F. Synthesizer
PD
Gates and Phase Adjust
PD
R.F. Power Amplifier
NMR Sample Probe
Preamplifier
Amplifier
Phase Sensitive Detector
Pulse Programmer
Dye Laser
Recording Oscilloscope
Oscilloscope

sequences are determined by a pulse programmer (laboratory built). The rf pulses are then amplified before being applied to the sample.

After the strong rf pulse is applied, the receiver picks up the signal due to the induced magnetization of the sample. Since the probe employs a single coil configuration (i.e., a single coil is used for both transmitting and receiving signals) the transmitter and receiver units are isolated from each other by cross diodes. The rf receiver consists of broadband amplifying units (a Watkins-Johnson preamplifer and Kay Elemetrics amplifier were used) and a phase sensitive detector (Hewlett-Packard double balanced mixer). The detecter selects signals only at the resonant frequency in reference to the phase of the applied rf pulse. The signal can be monitored on oscilloscope and recorder. In the flashing light experiments excitation was provided by a pulsed dye laser (described in Section 1.2, this chapter) triggered by the pulse programmer. $1/T_1$ and $1/T_2$ were measured by the inversion recovery and CPMG methods, respectively, as outlined in Section 3, Chapter II.

With our instrumentation plots of the magnetization according to Equations 19 and 20 show essentially no scatter. Representative data are shown in Figure 6. (In the plot for $1/T_1$ the magnetization is normalized to $2\overline{M}_o$ since the signal is measured from its maximum value along -z' axis, through 0

Figure 6. Magnetization Plots of the Proton $1/T_1$ and $1/T_2$ Relaxation of a Chloroplast Sample. (a) $1/T_1$ relaxation measured using the inversion recovery method (Section 3.1, Chapter II) (b) $1/T_2$ relaxation measured using the CPMG method (Section 3.2, Chapter II) Data were obtained on a pea chloroplast sample, 3 mg Chl/ml, measured at 27 MHz, 25°C. $\bar{M}_0$ is the magnetization of the sample at equilibrium while $\bar{M}_z$ is the component of the magnetization along the z' axis at some τ after the initial 180° pulse for $1/T_1$ or for $\tau \geq 0$ for $1/T_2$. The rates are proportional to the slopes of the plot according to Equations 19 and 20.

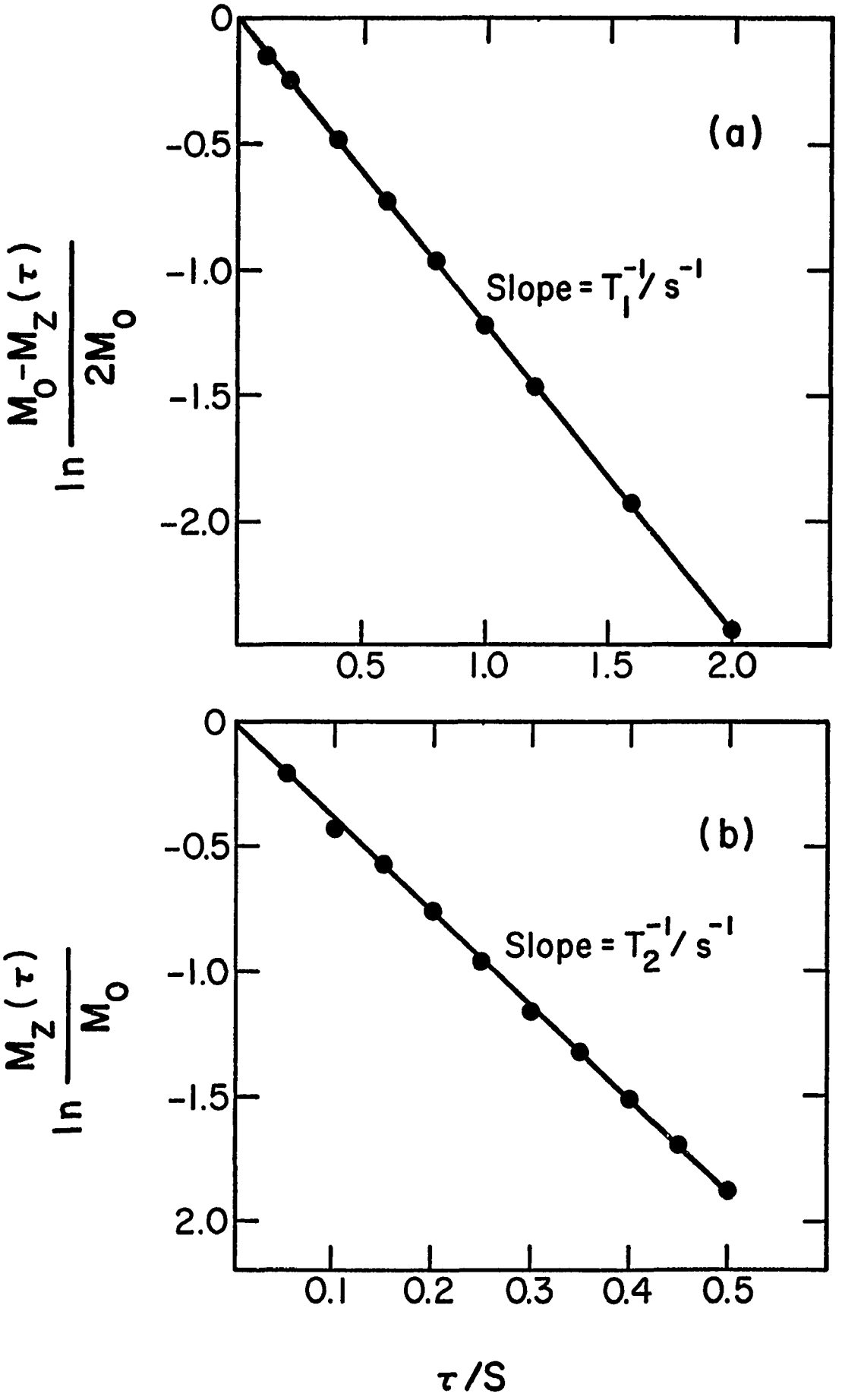
0
-0.5
-1.0
-1.5
-2.0
(a)
Slope = T_1^{-1}/s^{-1}
$\ln \frac{M_0 - M_Z(\tau)}{2M_0}$
0.5
1.0
1.5
2.0
0
-0.5
-1.0
-1.5
2.0
(b)
Slope = T_2^{-1}/s^{-1}
$\ln \frac{M_Z(\tau)}{M_0}$
0.1
0.2
0.3
0.4
0.5
τ/S

to its maximum value along +z' axis.) Reproducibility of the rates is within ±3%. For example, the average of nine measurement of $1/T_2$ on a chloroplast sample was 10.2 ± 0.21.

For relaxation measurements made in the dark at different frequencies and temperatures a NMR probe which holds standard 5 mm NMR tubes was used. Variable capacitors incorporated into the circuit allowed for tuning the probe to various resonant frequencies. The probe was encased in a glass Dewar flask and the temperature was controlled by a thermostatic flow of N_2 gas. Temperatures were measured with a calibrated thermocouple encased in the NMR probe; the temperature did not vary more than 1°C once the probe was equilibrated to a particular temperature.

In order to measure light-induced changes in the relaxation rates the NMR probe was designed to provide the best optical geometry while still maintaining a sufficiently good signal to noise ratio. Figure 7 shows the design of the probe constructed by Dr. Ray Finney. A thin chamber is fitted within the region of the NMR coils by two flat glass lenses (1 mm thick). Sample ports allow access to the chamber via 24 gauge teflon tubing connected to a syringe, essentially setting up a stop-flow system. The chamber has a diameter of 9 mm and is 1/64" thick and holds about 100 µl of sample.

As very thick samples (2-3 mg Chl/ml) are needed to get a sufficiently large effect of the chloroplasts, the exciting

Figure 7. NMR Probe Design Used in Light Experiments. See text for details.

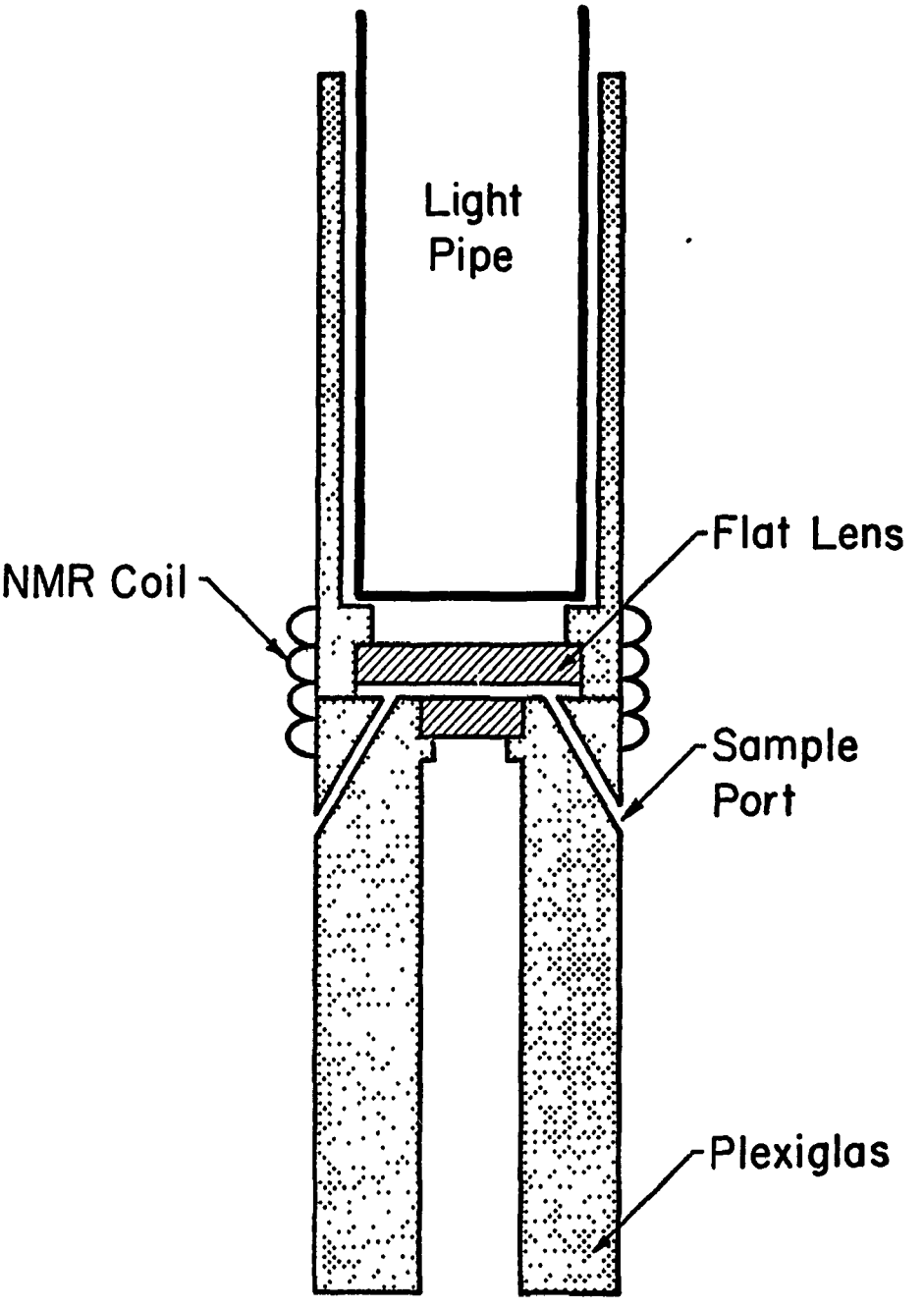
Light
Pipe
NMR Coil
Flat Lens
Sample
Port
Plexiglas

light intensity must be adequate to saturate the sample. For continuous light measurements saturating light was obtained from a 200 watt mercury-iodide incandescent lamp. The light was focussed down the NMR probe onto the sample through a lens (9 mm focal length) and three Corning CS 1-59 heat filters. Temperatures varied no more than 2°C between light and dark periods. Saturating light flashes were obtained from a high power (1 joule maximum output) pulsed dye laser (see Section 1.2, this chapter). The laser pulses were directed to the sample through a 1/4" nonmagnetic light pipe (Corning fiber optics) which fits into the NMR probe to sit just above the sample.

1.5 Computer Analysis

In the analysis of the frequency data, best fit theoretical curves to the experimental points were obtained through an iterative least squares type program employing the Rosenbrock method of minimization (125) (MINROS). The version of MINROS as developed by Duane Steidinger, University of Illinois, was used. The theoretical Solomon-Bloembergen-Morgan equations were entered as a sub-routine to MINROS and the NMR parameters were varied until the squares of the difference between the calculated and experimental relaxation rates at all frequencies were minimized.

In the theoretical fit of the $1/T_2$ flash oscillations, the concentration of the individual S state after each flash

was calculated according to Kok et al. (77) model, for various starting conditions (i.e., using various initial concentrations of S_0, S_1 or S_2, miss and double hit parameters). Various weighting factors were then assigned to each S state and multiplied by the concentration for that S state after a particular flash. These values were summed to give the relative theoretical $1/T_2$ value after a particular flash and normalized to the experimental points. Those weighting factors which give the best fit to the observed $1/T_2$ oscillations are used.

Calculations were made on an IBM 360-75 computer by Dr. Steve Marks.

2 Experimental Results

2.1 Characterization of Chloroplast Proton Relaxation Rates

2.1.1 Contribution of Chloroplast Manganese

The proton relaxation rates (PRR) of aqueous suspensions of chloroplast membranes are considerably faster than the rates for the buffer medium alone. Figure 8 shows that the $1/T_1$ for chloroplast membranes is linear with chloroplyll concentration, extrapolating to the values for the buffer medium at zero chlorophyll concentration. As shown in Figure 6 the magnetization plots are single exponentials, indicating that the rates are proportional to only one water fraction, the bulk or solvent water.

Figure 8. Dependence of $1/T_1$ on Chlorophyll Concentration. $1/T_1$ was measured at 27 MHz, 25°C. Pea chloroplasts were used.

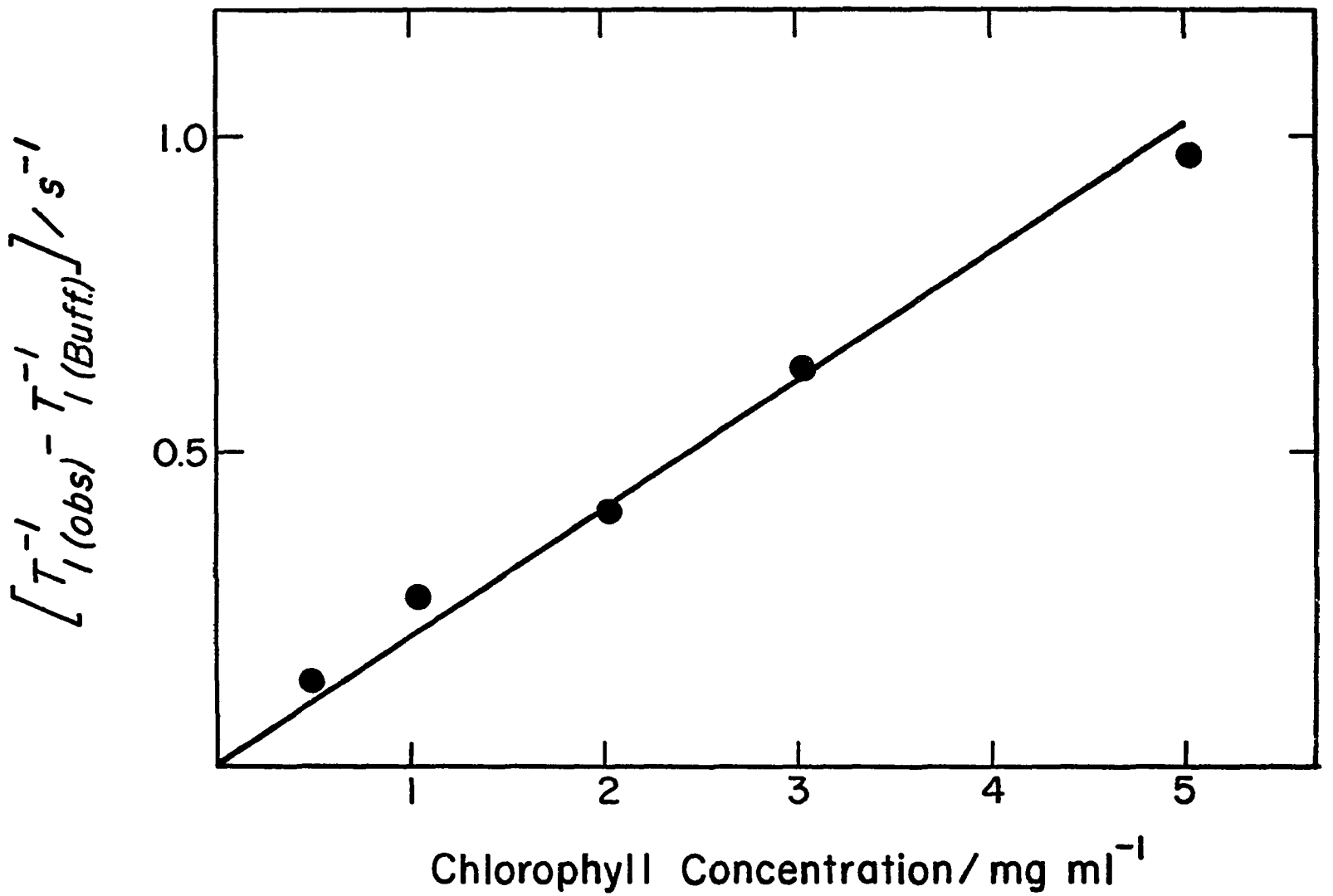
$[T_{1(obs)}^{-1} - T_{1(Buff.)}^{-1}] / s^{-1}$
1.0
0.5
1
2
3
4
5
Chlorophyll Concentration / mg ml^{-1}

For a complex system such as a chloroplast membrane, the observed rates can be considered as the sum of contributions from all sites in the membrane accessible to the solvent water plus the relaxation of free water.

$$1/T_{1,2(obs)} = \sum_i P_i/T_{1,2(i)} + 1/T_{1,2(free)} \qquad (28)$$

where P_i is the fraction of water in site i. Most water is free ($P_{free} \simeq 1$) and $1/T_{1,2(free)}$ is taken as the relaxation rate in the buffer medium without chloroplasts. The quantity $[1/T_{1,2(obs)} - 1/T_{1,2(free)} = 1/T_{1,2}]$ is therefore the relaxation contribution due to the chloroplast membranes. Unless otherwise noted all rates are corrected with the rate of the buffer medium plus any reagents that have been added.

As discussed in Chapter II, bound paramagnetic ions dominate the PRR in macromolecular systems. Since Mn(II) has one of the strongest relaxing effects on protons (113), we expected the bound Mn to make a significant, if not major, contribution to the PRR of chloroplasts.

To pinpoint the effect due to the chloroplast Mn we tried several treatments which are known to specifically alter the environment of the chloroplast Mn (Section 2.3, Chapter I). The results and details are given in Table 1. NH_2OH-EDTA, TRIS and TRIS-acetone washing all lead to decreases in $1/T_1$ and completely inhibit O_2 evolution, consistent with the removal of Mn from the membrane.

Table 1. Effect of Various Treatments Which Alter the Environment of Native Bound Manganese on the $1/T_1$ of Chloroplast Membranes

Condition	T_1^{-1}/s^{-1}
Spinach	
[a]Washed Control	1.04
[b]NH_2OH-EDTA Washed	0.54
[c]TRIS Washed	0.41
+ 10^{-4} M EDTA	0.74
Peas	
[a]Washed Control	0.82
[d]TRIS-Acetone Washed	0.21

[a]Spinach or pea chloroplasts were washed in HEPES buffer medium (50 mM HEPES, pH 7.5, 400 mM sucrose and 10 mM NaCl) and resuspended to a final concentration of 3 mg Chl/ml. $1/T_1$ was measured at 27 MHz, 25°C.

[b]Chloroplasts were incubated in HEPES buffer medium containing 2 mM $MgCl_2$, 1 mM EDTA and 3 mM NH_2OH for 20 min in dark at 25°C, centrifuged and resuspended in HEPES buffer medium, according to Ort and Izawa (127).

[c]Chloroplasts were incubated in 0.8 M TRIS, pH 8.2, for 20 min in dark at 4°C, centrifuged and resuspended in HEPES buffer medium, according to Yamashita and Butler (31).

[d]Chloroplasts were incubated in 0.8 M TRIS, pH 8.2, 20% acetone (v/v) for 20 min at 4°C, centrifuged and resuspended in HEPES buffer medium, according to Yamashita and Tomita (128).

However, we have found variable results with TRIS washed chloroplasts (126), apparently depending on the source of the plant material. In summer spinach, in some cases, $1/T_1$ showed an increase after TRIS washing. In view of the controversy over how much Mn is removed after TRIS washing (39) such a result may not be unreasonable. Since PRR is sensitive to bound Mn, it will not matter whether Mn is non-specifically bound or is at the native site in the membrane. It may be that in these cases after TRIS washing there is a lot of non-sepcifically bound Mn around and that the increases in the rates are due to changes in the environment of the bound Mn (see Chapter IV for further discussion).

Table 1 also shows the effect of EDTA on $1/T_1$. EDTA is known to be permeable to chloroplast membranes (39). It always leads to a decrease in the PRR, but never completely eliminates the effect (or the light induced changes, see later). EDTA readily chelates with metal ions and could have an effect by replacing water ligands on the bound ions.

Another method to extract Mn from the membrane used by Chen and Wang (129) is to incubate chloroplasts in high concentrations of $MgCl_2$ for relatively long times. Under these conditions Chen and Wang found a complex relationship between the Mn content and O_2 evolution in fresh preparations. Their observation is confirmed in our preparations as shown in Figure 9. Here the Mn content and O_2 activity is expressed

Figure 9. Plot of Percent O_2 Activity versus Percent Manganese Content. Mn extraction was achieved by incubating pea chloroplasts for 2 hr in dark at 4°C in HEPES buffer medium (see legend of Table 1) containing $MgCl_2$ at the following [Mg]/[Chl] ratios: 0, 167, 332, 667, 2500 and 10,000. After incubation the chloroplasts were centrifuged and the pellet was resuspended to 3 mg Chl/ml. Mn content was determined by neutron activation analysis. For the control it was 0.62 ± 0.03 µg Mn/mg Chl. Rate of O_2 evolution for the control was 120 µmoles O_2/mg Chl/hr.

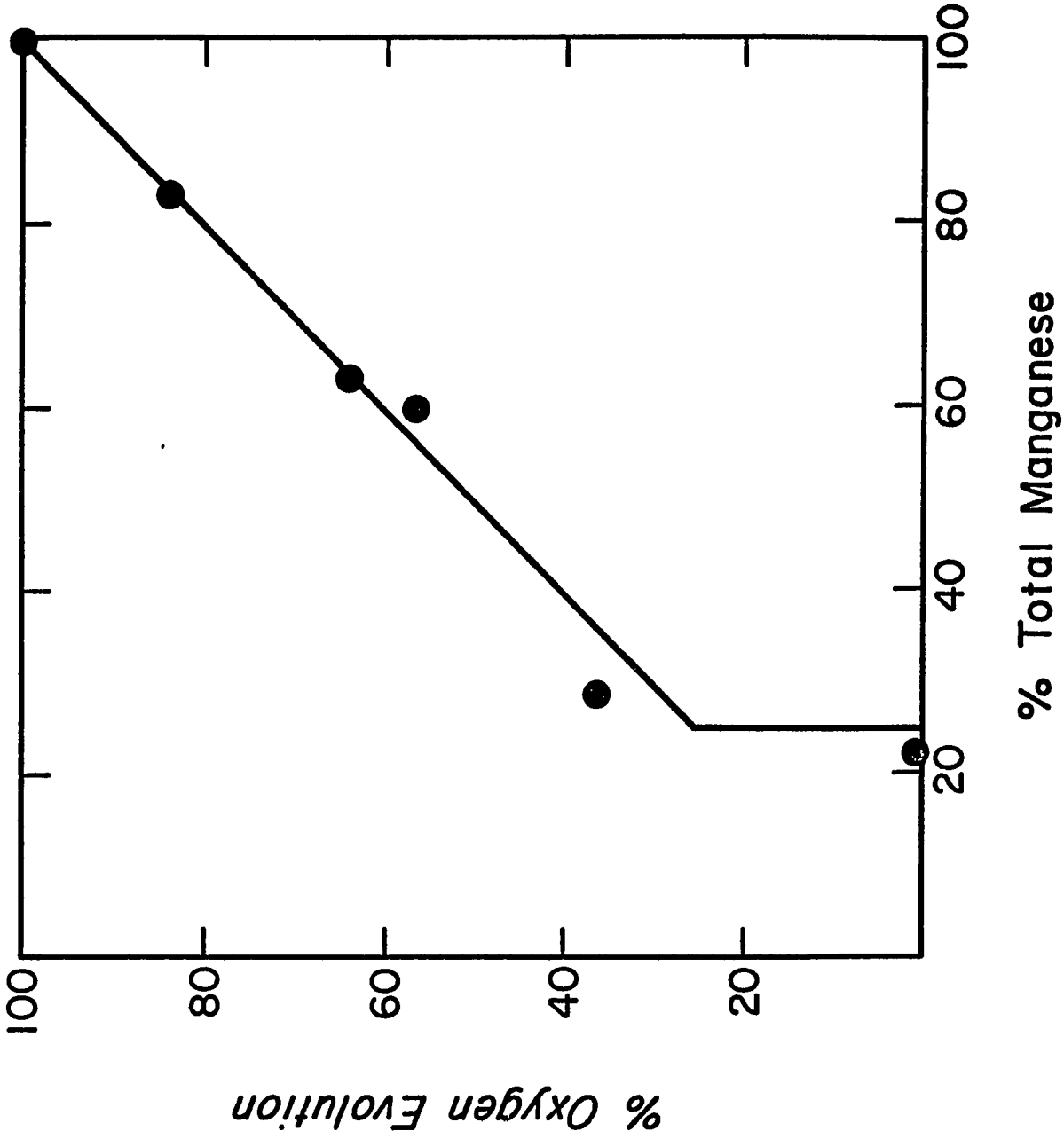
% Oxygen Evolution
100
80
60
40
20
% Total Manganese
20
40
60
80
100

as a percentage of the control value. The control was carried through the same incubation procedure but without $MgCl_2$. The O_2 activity is linear with Mn content until about 2/3 of the Mn is removed. However, when 2/3 of the Mn is removed there is still a significant O_2 evolution activity. According to Cheniae's (75) two pool hypothesis, however, O_2 evolution should have been completely inhibited; this is the case when TRIS washing, NH_2OH or heat extraction procedures are used. Chen and Wang postulated that the further decrease in O_2 evolution with longer incubation times in $MgCl_2$ was due to some conformational change, rather than to the removal of Mn itself. They did find a direct relationship between O_2 activity and the loosely bound Mn when they used aged (frozen) chloroplast preparations.

Figure 10 shows the percent values of $1/T_1$ and $1/T_2$ plotted as a function of percent Mn of the control. The $1/T_1$ shows a complex pattern as does O_2 activity with Mn content. Once the loosely bound Mn is removed, there is no further change in $1/T_1$, representing about 20% contribution to $1/T_1$. The $1/T_2$, on the other hand, appears to be linear with the total Mn content. It extrapolates also to the same background contribution. The different behavior for $1/T_1$ and $1/T_2$ with Mn content is peculiar and may arise from the fact that there is a greater non-site specific or outer sphere contribution to $1/T_2$ (see Section 1.1, Chapter IV).

Figure 10. Plot of Percent Values $1/T_1$ and $1/T_2$ versus Percent Manganest Content. Conditions for Mn extraction are given in the legend of Figure 9.

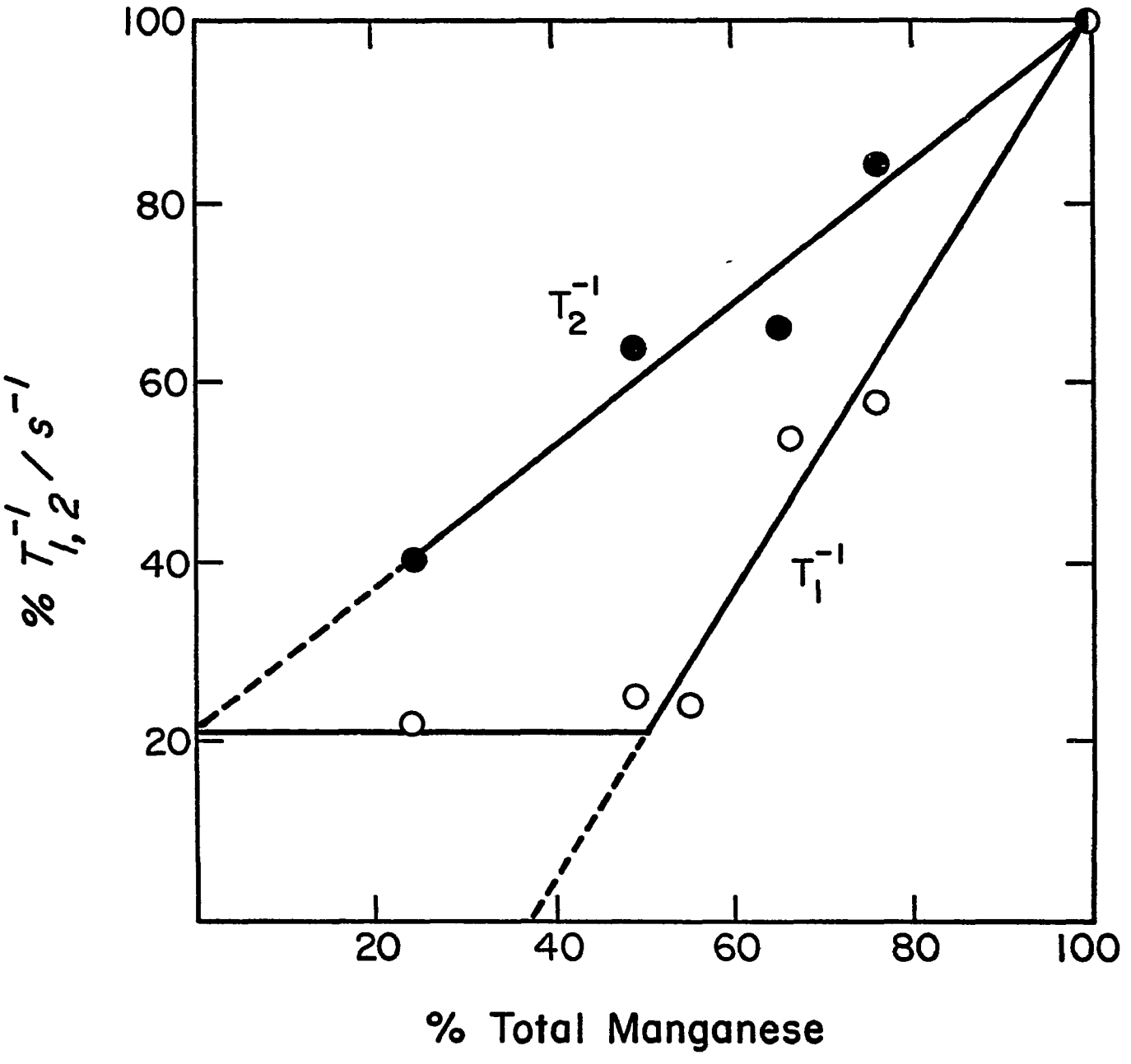
100
80
60
40
20
20
40
60
80
100
% $T_{1,2}^{-1}$ / s^{-1}
T_2^{-1}
T_1^{-1}
% Total Manganese

Figure 11 shows a corresponding plot of the percent values of $1/T_1$ and $1/T_2$ as a function of the percent O_2 activity. It follows the same behavior as with the chloroplast Mn. These results indicate a direct relationship between the PRR, the loosely bound Mn and O_2 evolution in chloroplasts. The significance of the breaks in the curves, however, still remains unclear.

2.1.2 Analysis of Proton Relaxation Rates

In order to gain an insight into the kinds of magnetic relaxation mechanisms involved, the PRR is studied as a function of NMR frequency which may then be analyzed according to the Solomon-Bloembergen-Morgan equations (Section 5, Chapter II). Figure 12a shows the uncorrected $1/T_{1(obs)}$ at various frequencies for dark-adapted pea chloroplasts (open circles). The data points, obtained on several preparations, show a considerable scatter up to 20%. The Mn contents of different preparations also show a variation of up to 20% (Table 2). When the rates are normalized to the same Mn concentration the scatter is significantly reduced as shown in Figure 12b. This result supports our contention that the major effect on the PRR is due to the chloroplast Mn.

The most outstanding feature of Figure 12b (open circles) is the broad peak in the rates in the 10-20 MHz range. This frequency behavior is characteristic of a frequency dependent correlation time which can only arise when the electronic relaxation of paramagnetic ions govern the PRR (115). As has

Figure 11. Plot of Percent Values of $1/T_1$ and $1/T_2$ versus Percent of O_2 Activity. Conditions for Mn extractions are given in the legend of Figure 9.

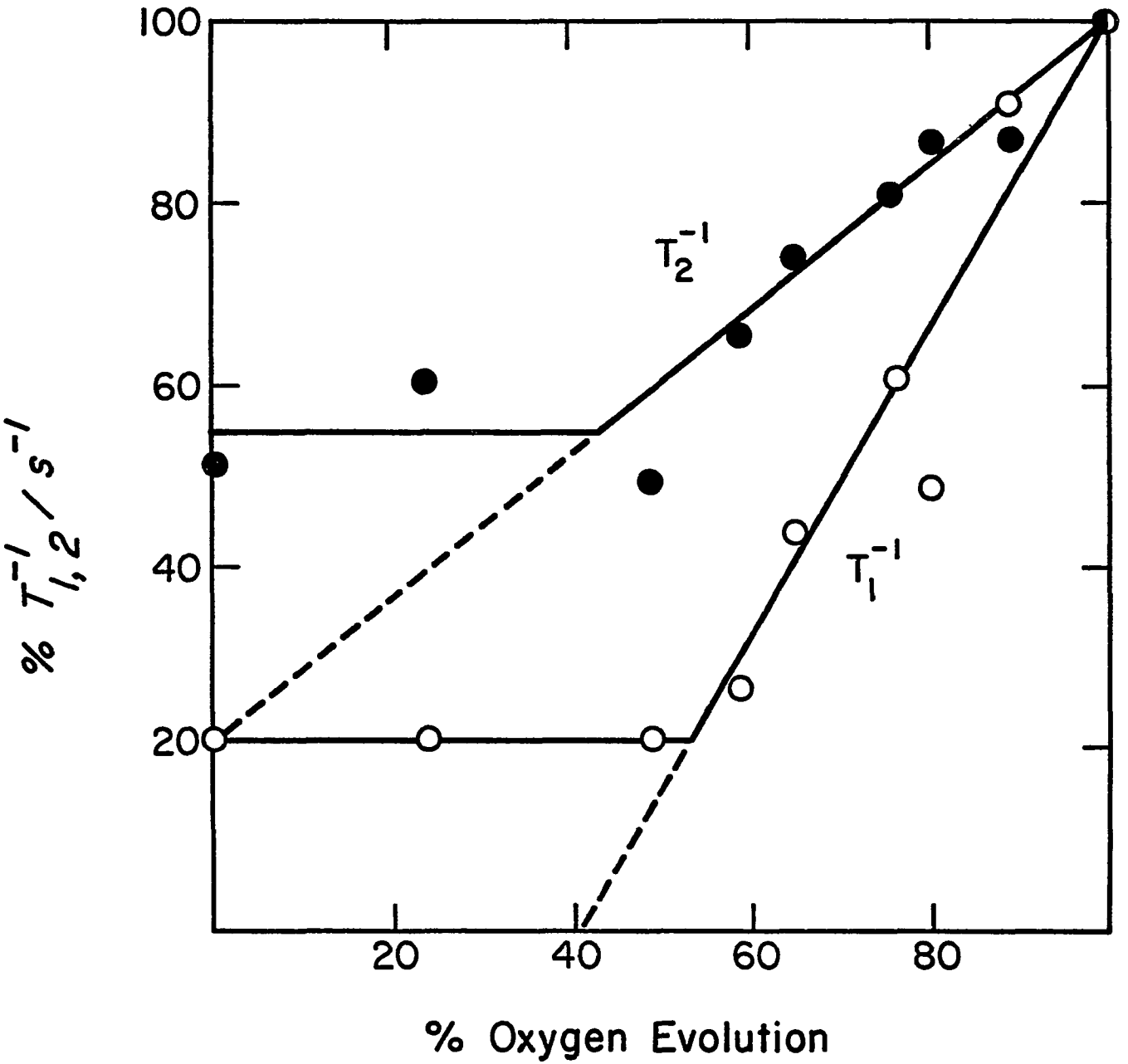
100
80
60
40
20
20
40
60
80
% $T_{1,2}^{-1}$ / s^{-1}
% Oxygen Evolution
T_2^{-1}
T_1^{-1}

Figure 12. Frequency Dependence of $1/T_{1(obs)}$ for Dark-Adapted Chloroplast Membranes. (a) Uncorrected observed rates for several different samples. (b) Observed rates normalized to the same Mn concentration. Samples of pea chloroplasts contained 3 mg Chl/ml. T-A Chlpts refers to TRIS-Acetone washed chloroplasts in which the loosely bound fraction of Mn is removed. $1/T_1$ was measured at room temperature (23-25°C).

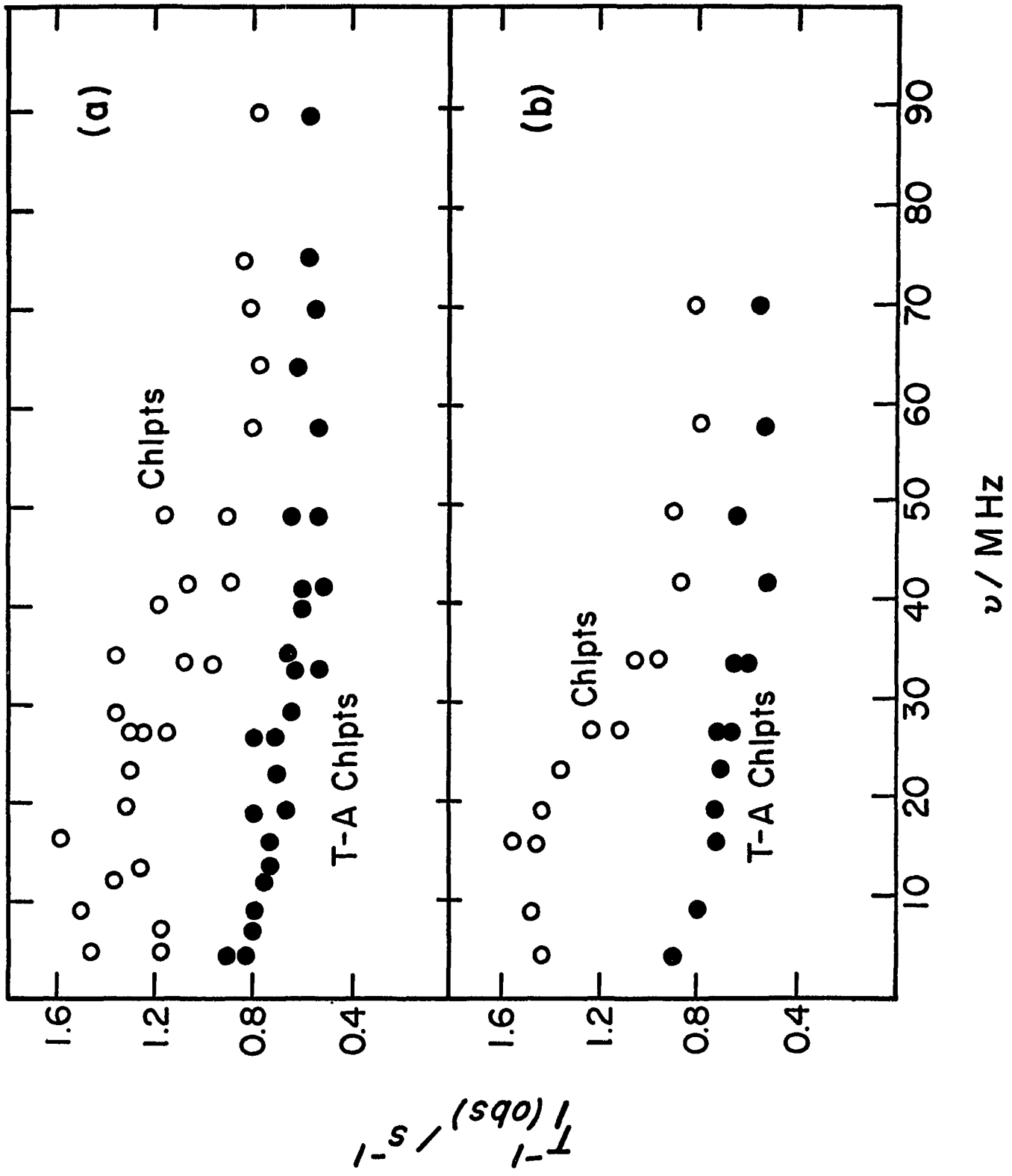
(a)
(b)
Chlpts
T-A Chlpts
1.6
1.2
0.8
0.4
10
20
30
40
50
60
70
80
90
ν / MHz
T1(obs) / s-1

Table 2. Variation in Total Manganese Content in Several Chloroplast Preparations

Sample Number Pea Chloroplasts	Manganese Content µg Mn/mg Chl
1	0.490
2	0.440
3	0.400
4	0.440
5	0.425
[a]6	0.466 ± 0.010
[a]7	0.496 ± 0.010
[a]TRIS-Acetone Washed	0.150 ± 0.020

[a]Manganese contents in these samples were determined by neutron activation analysis. The manganese contents in the other samples were determined by atomic absorption methods.

been pointed out earlier (Section 2.3, Chapter I) it is believed that the loosely bound fraction of Mn is primarily responsible for O_2 evolution. Since there is a significant background contribution to the PRR as shown in Figure 10, it is important to know how much of the frequency behavior can be ascribed to the loosely bound Mn, before a proper analysis can be made. Yamashita and Tomita (128) found that extraction of Mn from the membrane can be facilitated during TRIS washing when 20% acetone is included in the incubation medium. Apparently, the acetone makes the membrane leaky to the released Mn thereby avoiding the problems of simple TRIS washing. They have shown that the procedure completely inhibits O_2 evolution, but keeps the electron transport chain intact to the extent that $NADP^+$ photoreduction can still take place when artificial electron donors are present. TRIS-acetone washing removes about 70% of the Mn in our preparations (Table 2).

Figures 12a and 12b also show the frequency dependence for the observed and normalized rates respectively for TRIS-acetone washed chloroplasts. Here, the $1/T_{1(obs)}$ shows a very little frequency dependence, indicating that the loosely bound Mn is responsible for the peak in $1/T_{1(obs)}$ for the control chloroplasts. We assume, therefore, that the PRR of TRIS-acetone washed chloroplasts (T-A) represents the total background contribution, so that the observed (obs) rates of

the control chloroplasts corrected with the rates of the TRIS-acetone washed chloroplasts give the paramagnetic contribution (corr) due to the loosely bound Mn:

$$1/T_{1,2(corr)} = \left[1/T_{1,2(obs)} - 1/T_{1,2(T-A)}\right] \qquad (29)$$

We thus proceed to analyze the corrected rates according to Equations 23-27. In the analysis we assume $T_{1,2(M)} > \tau_M$ (see later) so that τ_M is neglected in Equation 23. We combine all of the constants in Equations 24 and 25 along with the mole fraction, p, and co-ordination number, q, in Equation 23 and ascribe it the symbol C. Thus, for $1/T_{1(P)}$ we use:

$$C = \frac{2pq\ S(S+1)\ \gamma_I^2\ g^2\ \beta}{15r^6} \qquad (30)$$

where the symbols are as in Section 5, Chapter II, and for $1/T_{2(P)}$ we use C/2. The computer then optimizes the values for C and τ_S to give the best fit to the experimental data.

In our initial attempts to fit the experimental data, we first assumed a pure electronic relaxation mechanism (i.e., $1/\tau_C = 1/\tau_S$). We allowed the computer to vary C and τ_V and B (which from Equation 27 determines the frequency dependence of $1/\tau_S$) to fit the data. However, this analysis failed to give a good fit to the data--it could not account for such a broad peak in the 10-20 MHz range nor could it account for the flattening of the $1/T_2$ at higher frequencies (see Figure 13).

Figure 13. Best Fit Theoretical Curves to the Frequency Dependence of the Relaxation Rates for Dark-Adapted Chloroplast Membranes. (a) $1/T_2$ relaxation. (b) $1/T_1$ relaxation. $1/T_{1,2(corr)} = \left(1/T_{1,2(obs)} - 1/T_{1,2(T-A)}\right)$. Rates were measured at room temperature (23-25°C) and normalized to the same Mn concentration at each frequency. Pea chloroplasts at 3 mg Chl/ml were used. $1/T_{1,2(OS)}$ refers to the theoretical outer sphere contribution based on a translational diffusion model. See text for details.

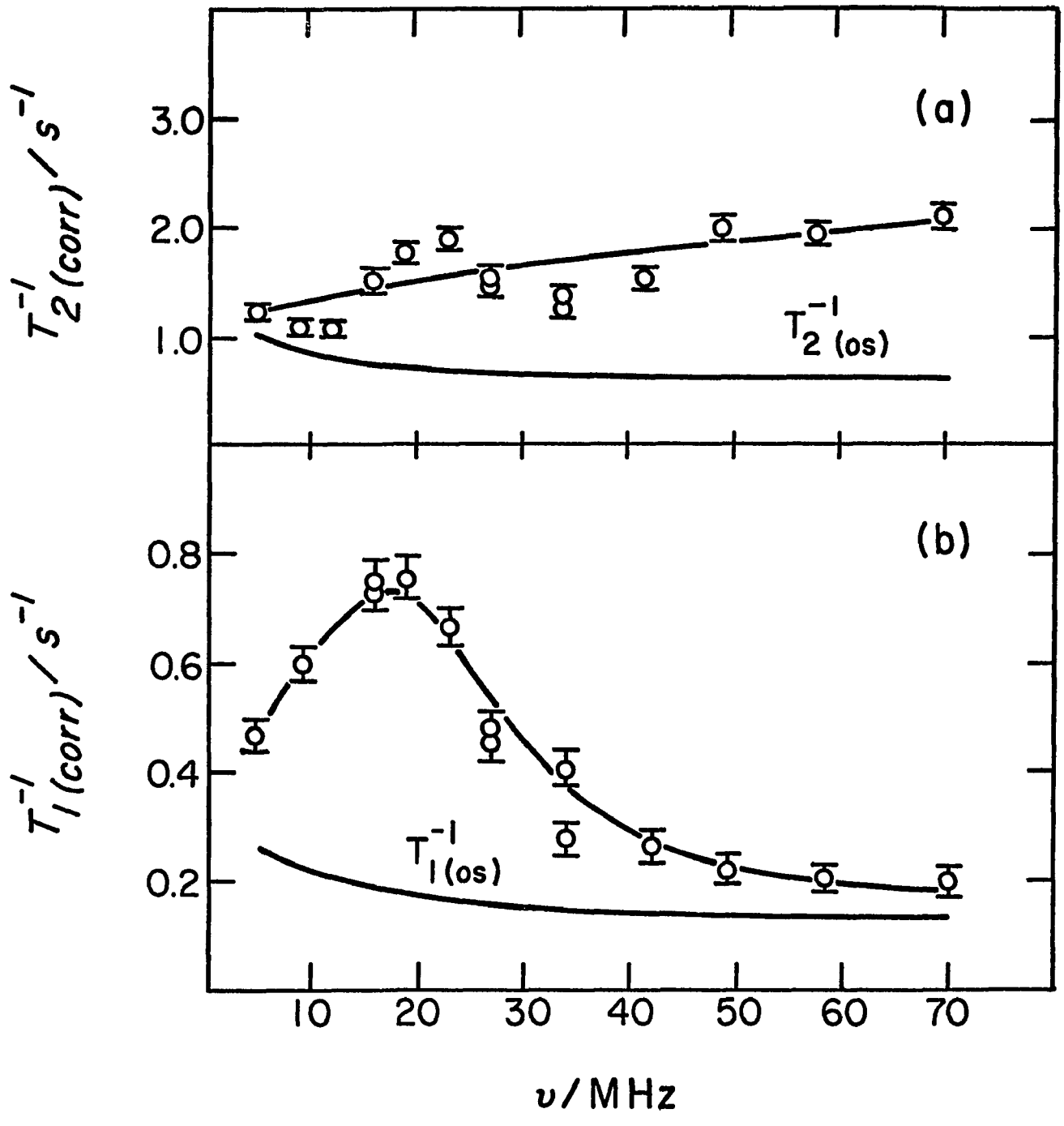
(a)
(b)
3.0
2.0
1.0
0.8
0.6
0.4
0.2
10
20
30
40
50
60
70
$T_{2(corr)}^{-1}$ / s^{-1}
$T_{1(corr)}^{-1}$ / s^{-1}
$T_{2(os)}^{-1}$
$T_{1(os)}^{-1}$
υ / MHz

We next considered that τ_C may have a frequency independent component in addition to a frequency dependent component. Since the tumbling rate ($1/\tau_R$) for macromolecules is relatively slow ($\sim 10^6$ s^{-1}), it will make only a small contribution to $1/\tau_C$. We assume, therefore, that the frequency independent term arises mainly from chemical exchange ($1/\tau_M$); thus, $1/\tau_C = 1/\tau_S + 1/\tau_M$. By varying the values of C, B, τ_V and τ_M a good fit to the peak in $1/T_{1(corr)}$ can be obtained, but the goodness of the fit is lost for $1/T_{1(corr)}$ at high frequencies and $1/T_{2(corr)}$ at low frequencies.

As mentioned in Chapter II non-site specific or outer sphere contributions to the overall paramagnetic relaxation rates may become significant when the rates are small and cannot be neglected, as is usually done in the analysis of other macromolecular systems. We are able to achieve a good fit to both $1/T_{1(corr)}$ and $1/T_{2(corr)}$ when an outer sphere contribution is included according to Equation 23.

The problem was in selecting an appropriate model for $1/T_{(OS)}$. The clue came from the values of $1/T_{1(corr)}$ at high frequencies and $1/T_{2(corr)}$ at low frequencies. In the limit where electronic relaxation governs the outer sphere contribution, the frequency dependence of $1/T_{(OS)}$ follows the same behavior as $1/T_{(M)}$. But in the limit where diffussional processes govern the outer sphere contribution, $1/T_{(OS)}$ for both the longitudinal and tranverse relaxation starts out high at

low frequencies and decreases with increasing frequency. This would tend to flatten the frequency curves at high frequencies for $1/T_{1(P)}$ and at low frequencies for $1/T_{2(P)}$. As shown by the data points in Figure 13 this appears to be the case in chloroplasts.

The translational diffusion model we used to fit the chloroplast data is given by the following equations (pp. 190-191, ref. 115) in which $1/T_{1,2(OS)}$ is a function of ω:

$$1/T_{1(OS)} = K\left[7 f(\omega_S \tau_D) + 3 f(\omega_I \tau_D)\right] \quad (31)$$

and

$$1/T_{2(OS)} = K\left[13/2 f(\omega_S \tau_D) + 3/2 f(\omega_I \tau_D) + 2\right] \quad (32)$$

where τ_D is the diffusional correlation time and K is a constant related to the diffusional coefficients of the paramagnetic ion and the interacting nuclei. Using $\tau_D \sim 10^{-10}$S for pure water (115), then by allowing K to vary, the computer calculates the $1/T_{(OS)}$ contribution which would give the best fit to the $1/T_{(corr)}$ of the chloroplast membranes.

Figures 13a and 13b show the best fit curves for the $1/T_{2(corr)}$ and $1/T_{1(corr)}$, respectively, for dark-adapted pea chloroplasts. The theoretical outer sphere contributions, $1/T_{2(OS)}$ and $1/T_{1(OS)}$, are also given. Thus, from Equation 23 the inner sphere paramagnetic contribution, $1/T_{(M)}$, will be given by the difference between the best fit curves for the

$1/T_{(corr)}$ and the $1/T_{(OS)}$. It is apparent from Figure 13 that the $1/T_{(OS)}$ can make up anywhere from 10-80% of total paramagnetic contributions. It is interesting to point out that $1/T_{2(OS)}$ is about three times larger than $1/T_{1(OS)}$. The optimized parameters obtained from the theoretical fits are $\tau_V = 19.5 \times 10^{-12}$ s, $\tau_M = 2.18 \times 10^{-8}$ s and $B = 0.9 \times 10^{19}$ $(rad/s)^2$, all within the expected range for Mn(II) (see Section 1.1 Chapter IV for further discussion).

One of the important assumptions that we used in the above analysis of the frequency dependence is that the paramagnetic effects are <u>not</u> slow exchange limited, <u>i.e.</u>, $T_{1,2(M)} << \tau_M$. If τ_M would have dominated in Equation 23 then $T_{1,2(M)}$ would have cancelled and $1/T_{1(P)}$ should have equalled $1/T_{2(P)}$. But as clearly demonstrated by the data in Figure 13 this is not the case, $1/T_{2(corr)}$ is greater than $1/T_{1(corr)}$ at all frequencies. This conclusion is further supported by the temperature dependence.

Usually the temperature dependence gives a good indication of the relaxation mechanism that dominates the magnetic interactions. Table 3 gives the theoretical temperature behavior of the relaxation rates for various relaxation mechanisms. For example, when a frequency dependent τ_S mechanism dominates, and when the condition $\omega_I \tau_C > 1$ holds, $d(1/T_{2(M)})/d(1/T)$ is negative while $d(1/T_{1(M)})/d(1/T)$ is positive. For chloroplasts $\omega_I \tau_C > 1$ at 64 MHz (Figure 13). Figure 14

Table 3. Variation of Relaxation Rates with $1/T$ in the Fast Exchange Region

Condition	$\omega_I\tau_C < 1$			$\omega_I\tau_C > 1$		
	τ_R	τ_M	τ_S	τ_R	τ_M	τ_S
$\frac{d(1/T_{1(M)})}{d(1/T)}$	+	+	$b_{\pm}$	-	-	$\mp$
$\frac{d(1/T_{2(M)})}{d(1/T)}$	+	+	$\pm$	+	+	$\pm$

[a]From Dwek (115)

[b]The lower sign is applicable if τ_S is frequency dependent.

Figure 14. Temperature Dependence of the Relaxation Rates for Dark-Adapted Chloroplast Membranes at Several Frequencies. Open circles, $1/T_2$ relaxation; closed circles, $1/T_1$ relaxation. $1/T_{1,2(corr)} = \left(1/T_{1,2(obs)} - 1/T_{1,2(T-A)}\right)$. Pea chloroplasts at 3 mg Chl/ml were used.

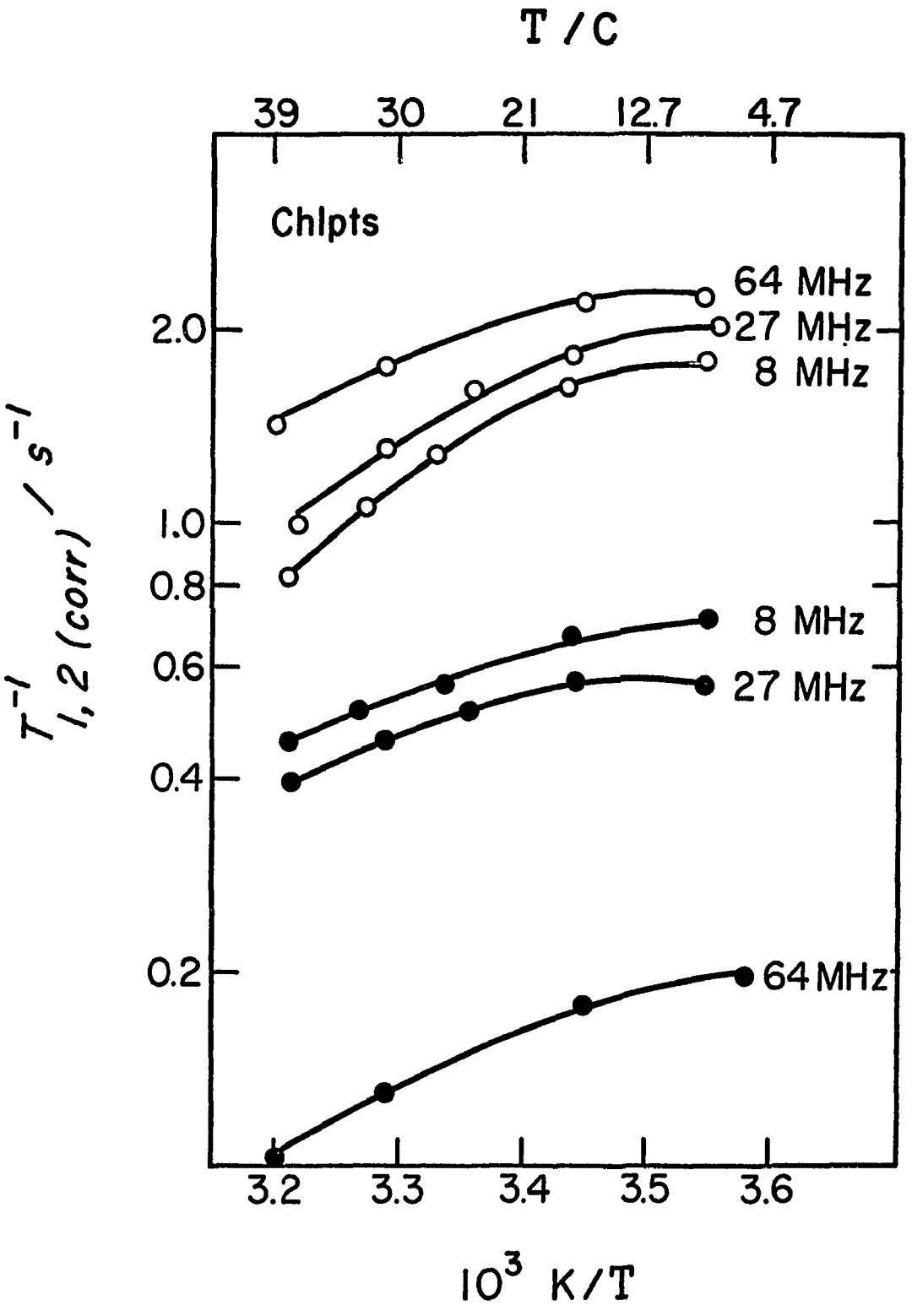
T / C
39
30
21
12.7
4.7
Chlpts
64 MHz
27 MHz
8 MHz
8 MHz
27 MHz
64 MHz
2.0
1.0
0.8
0.6
0.4
0.2
$T^{-1}_{1,2\,(corr)}$ / s^{-1}
3.2
3.3
3.4
3.5
3.6
10^3 K/T

gives the temperature dependence of $1/T_{1,2(corr)}$ for dark-adapted pea chloroplasts in the 5-38°C range at 8, 16 and 64 MHz. At all frequencies the rates increase with decreasing temperature. The temperature dependence at 64 MHz clearly does not fit in with the expected behavior for a frequency dependent τ_S. Upon careful scrutiny of Table 3 it becomes apparent that the chloroplast temperature dependence does not fit in with the expected behavior for any one relaxation mechanism.

The temperature curves in Figure 14 are not linear making it impossible to extract activation energies without knowledge of all the mechanisms involved. But estimates made at the steepest part of the slope yield values in the range of 1-2 kcal/mole. This range is not characteristic for either a pure $1/\tau_S$ or $1/\tau_M$ mechanism (Section 5, Chapter II). In one sense the temperature dependence is consistent with the frequency analysis in that a mixture of relaxation mechanisms is suggested to govern the proton relaxation in chloroplasts.

2.1.3 Effect of Redox Reagents

It is not known what oxidation states of Mn exist in chloroplast membranes. The electronic relaxation, however, is strongly dependent upon the oxidation state. For example, the electronic relaxation rate is two orders of magnitude faster for Mn(III) than it is for Mn(II); consequently, Mn(III) is a much less efficient relaxer of protons than Mn(II).

Oxidation states of bound ions can be shifted by adding redox reagents. Table 4 shows the effect of various redox reagents on the $1/T_1$ of chloroplasts. The addition of oxidants such as FeCy or DCPIP leads to a decrease in the $1/T_1$ while the addition of reductants such as NH_2OH or TPB leads to large increases. That these reagents are affecting only the loosely bound fraction of Mn is shown by the lack of an effect on TRIS-acetone washed chloroplasts. Thus, from these results it may be inferred that there is a mixture of Mn oxidation states in dark-adapted chloroplasts. Upon adding an oxidant a fraction of the Mn is oxidized to a higher oxidation state less efficient in proton relaxation, while upon addition of a reductant a fraction of the Mn is reduced to the highly efficient relaxer Mn(II).

Figure 15 shows the $1/T_1$ for dark-adapted spinach chloroplasts as a function of the reductant tetraphenylboron concentration. Interestingly, the curve shows several distinct plateaus. The curve rises very slowly to the final plateau in the high concentrations range (14-20 mM), perhaps, indicating that this effect may be an artifact of the high concentration of TPB; although such high concentrations of TPB do not affect the buffer medium rates. Nevertheless, results shown in Figure 15 indicate that there are several titratable fractions of the loosely bound Mn.

The effect of FeCy is much less direct than TPB. The decrease in the rates induced by FeCy only occur at relatively

Table 4. Effect of Redox Reagents on the $1/T_1$ of Chloroplast Membranes

Condition	T_1^{-1}/s^{-1}
Spinach	
[a]Control	1.03
FeCy (0.3 mM)	0.57
DCPIP (0.3 mM)	0.61
NH_2OH (0.2 mM)	2.11
TPB (0.5 mM)	1.84
Peas	
[a]Control	0.82
TRIS-Acetone Washed	0.21
TRIS-Acetone Washed + FeCy (50 mM)	0.23
TRIS-Acetone Washed + TPB (5 mM)	0.25

[a]Dark-adapted chloroplasts at 3 mg Chl/ml were used. $1/T_1$ was measured at 27 MHz, 25°C.

Figure 15. Dependence of $1/T_1$ for Dark-Adapted Chloroplast Membranes on Tetraphenylboron Concentration. $1/T_1$ was measured at 27 MHz, 25°C. Spinach chloroplasts at 3 mg Chl/ml were used. After Wydrzynski, et al. (126).

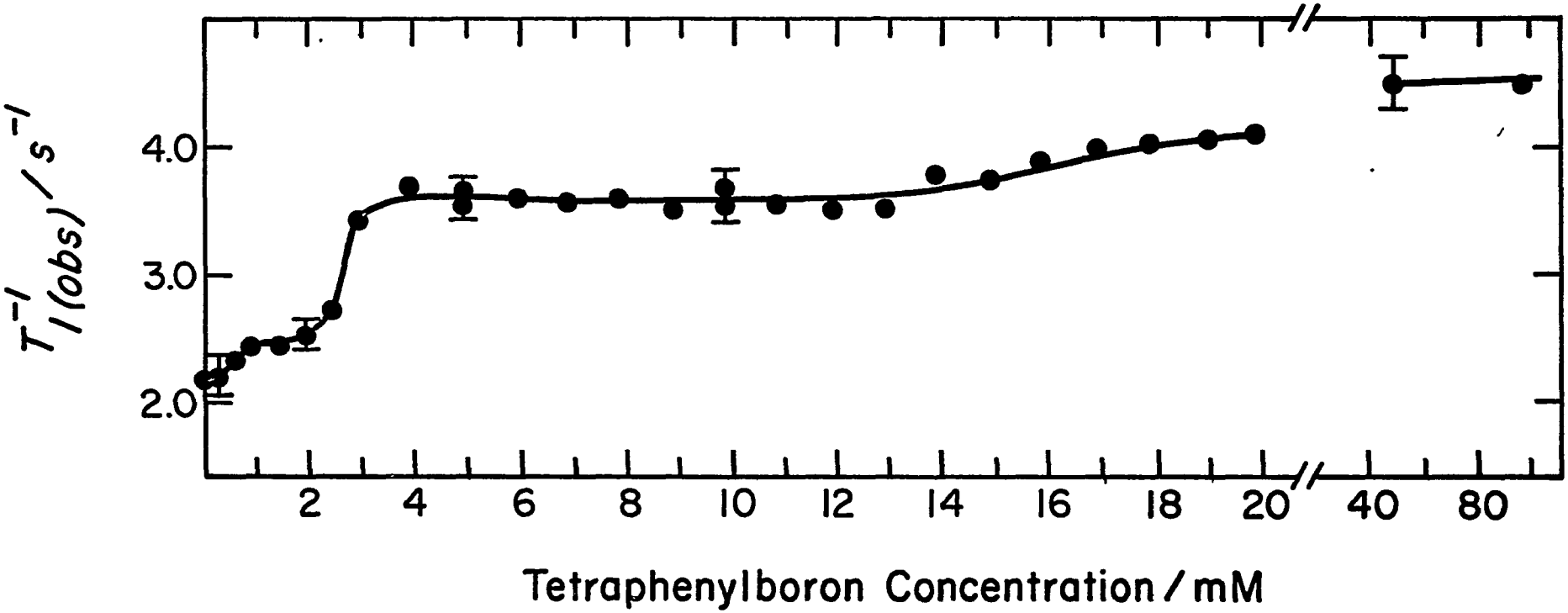
$T_{1(obs)}^{-1} / s^{-1}$
4.0
3.0
2.0
2
4
6
8
10
12
14
16
18
20
40
80
Tetraphenylboron Concentration / mM

high concentrations (i.e., 50 mM) and are sometimes variable. The chloroplast rates must be corrected with those of the buffer medium with FeCy, as there is a small paramagnetic contribution due to the iron. At high concentrations of FeCy the chloroplast suspension becomes thick and sticky. It is perhaps difficult to oxidize bound Mn(II) precisely with repeatable results with reagents like FeCy (explaining some of the variations we encountered).

Since the redox reagents appear to be changing the oxidation state of the loosely bound Mn, we thought that there would be a change in τ_s. Figure 16 shows the frequency dependence of the proton relaxation rates for chloroplasts containing 5 mM TPB or 50 mM FeCy. The rates are corrected with TRIS-acetone washed chloroplasts and normalized to the same Mn concentration at each frequency. The solid lines represent the theoretical best fit to the data points including outer sphere contributions. The optimized parameters were calculated to be $\tau_v = 20 \times 10^{-12}$ s, $\tau_M = 1.0 \times 10^{-8}$ s and $B = 0.9 \times 10^{19}$ $(rad/s)^2$ for TPB treated chloroplasts and $\tau_v = 9.3 \times 10^{-12}$ s, $\tau_M = 0.11 \times 10^{-8}$ s and $B = 1.1 \times 10^{14}$ $(rad/s)^2$ for FeCy treated chloroplasts.

The temperature dependence of $1/T_{1,2(corr)}$ at 8, 24 and 64 MHz for chloroplasts with TPB present is almost identical to the temperature dependence for untreated chloroplasts (Figure 14) except that the magnitude of the rates is much larger.

Figure 16. Best Fit Theoretical Curves to the Frequency Dependence of the Relaxation Rates for Dark-Adapted Chloroplast Membranes in the Presence of Redox Reagents. (a) $1/T_2$ relaxation. (b) $1/T_1$ relaxation. $1/T_{1,2(corr)} = \left(1/T_{1,2(obs)} - 1/T_{1,2(T-A)}\right)$. Rates were measured at room temperatures and normalized to the same Mn concentration at each frequency. Either 5 mM TPB or 50 mM FeCy was used. Pea chloroplasts at 3 mg Chl/ml were used.

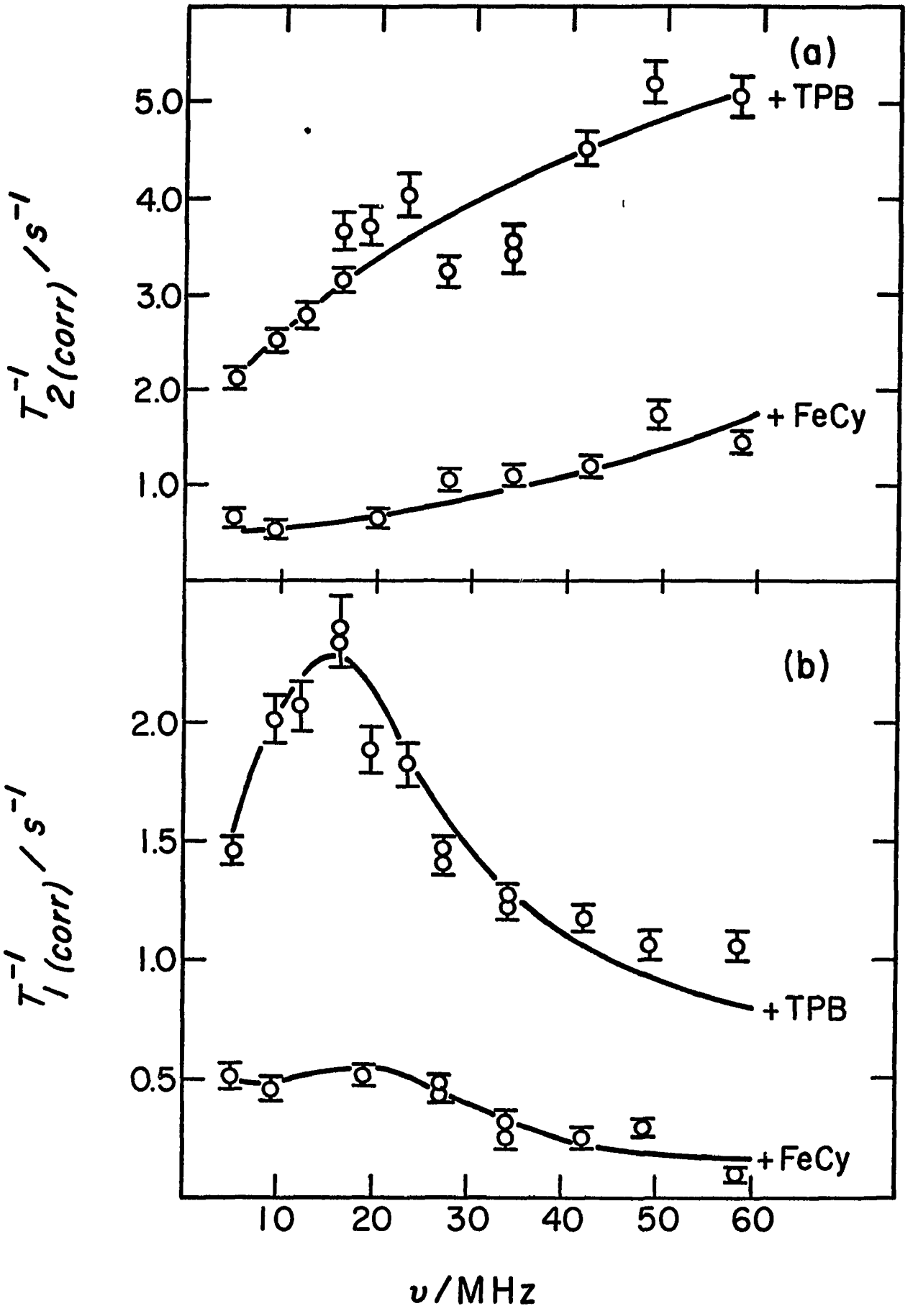
(a)
+TPB
+FeCy
5.0
4.0
3.0
2.0
1.0
$T_{2(corr)}^{-1}/s^{-1}$
(b)
+TPB
+FeCy
2.0
1.5
1.0
0.5
$T_{1(corr)}^{-1}/s^{-1}$
10
20
30
40
50
60
ν/MHz

We thought at first that the presence of FeCy caused a change in τ_V to a much smaller value (as would be the case for Mn(III)). According to Equation 27 a very small τ_V gives $\omega_S\tau_V < 1$ and $1/\tau_S$ becomes frequency independent. But this approach failed to give a fit to the $1/T_{2(corr)}$ data with FeCy. Instead, parameters similar to those obtained for the control chloroplasts fit the data best. This means that the PRR is monitoring mainly one species giving rise to these set of parameters. The changes in the rates induced by the redox reagents are only due to changes in the concentration of this species. As will be discussed in Chapter IV, the values we get for τ_V, τ_M and B are characteristic of Mn(II); thus, the PRR appears to be monitoring the Mn(II) concentrations in the chloroplast membranes.

2.2 The Effect of Light on Chloroplast Proton Relaxation Rates

In the previous section we characterized the chloroplast PRR by a frequency study of the rates and obtained quantitative estimates of the NMR parameters. We ascribe the major effect on PRR to the bound Mn(II) in chloroplasts. Since we now have a way to monitor the native bound Mn, the next question to ask is how is this Mn involved in photosynthesis. Photosynthetic reactions are unique in that they utilize light energy. Thus, in order to relate the bound Mn to photosynthesis we proceeded to determine the effect of light on the PRR.

2.2.1 Continuous Light Effects

In our search for a light effect on the PRR of chloroplasts we first measured the effect of preillumination on $1/T_1$. If dark-adapted spinach chloroplasts are given a 5 min preillumination period the $1/T_1$ in the succeeding dark period increases over the initial dark $1/T_1$. It turns out, however, that in the light there is a net decrease in $1/T_1$. Table 5 shows the $1/T_1$ for a dark-light-dark cycle in spinach and pea chloroplasts. The increase in $1/T_1$ in the dark after the light period is eliminated when the electron acceptor FeCy is present while the light-induced decrease is eliminated when the reductant TPB is present. There is no light effect in TRIS-acetone washed chloroplasts.

These results suggest that the light effect is on the loosely bound Mn and that it involves an oxidation-reduction reaction. In the light Mn is presumably photo-oxidized to an oxidation state less efficient in PRR while in the dark it is reduced back. Peculiarly, after the light the much greater $1/T_1$ in spinach indicates that there is even a greater extent in the reduction of the Mn. However, the light induced dark increase is not apparent in peas. It may reflect some background contribution or result from a conformational change which allows a greater accessibility of water.

The continuous light effects are saturable and are not due to temperature effects; the changes shown in Table 5 are

Tabel 5. Continuous Light Effects on the $1/T_1$ of Chloroplast Membranes

Condition	T_1^{-1}/s^{-1} Dark	Light	Dark
Spinach			
[a]Control	1.75	1.50	2.10
+5 mM FeCy	1.85	1.35	1.85
+5 mM TPB	3.55	3.75	4.50
Peas			
[a]Control	0.81	0.56	0.76
TRIS-Acetone Washed	0.21	0.17	0.19

[a]Dark-adapted chloroplasts at 3 mg Chl/ml were used. $1/T_1$ was measured at 27 MHz, 25°C.

much larger than would be expected for a 1-2°C temperature change (Figure 14).

2.2.2 Flashing Light Effects

2.2.2.1 $1/T_2$ and O_2 Yield Flash Patterns

Most of what is known about the O_2 evolving mechanism has come from studies of O_2 evolved in brief flashes of light. As indicated in Chapter I, most investigators believe that Mn is somehow directly involved in O_2 evolution. Since the PRR monitors bound Mn(II) in chloroplasts and as shown in the previous section there are light induced changes in the PRR, we proceeded to measure the PRR as a function of brief flashes of light to determine whether there is indeed a relationship between bound Mn and O_2 evolution.

In the following experiments, $1/T_2$ not $1/T_1$ was measured for the following reasons. The light flashes must be spaced a few seconds apart. The inversion recovery method for $1/T_1$ takes several minutes to complete, while $1/T_2$ can be easily measured within seconds or less (depending, of course, on how fast the $1/T_2$ is) using the CPMG method, thus making $1/T_2$ the best approach.

Figures 17 and 18 show the $1/T_2$ and O_2 yields as a function of light flashes in chloroplasts isolated from spinach, lettuce or pea leaves. In all the cases the $1/T_2$ follows an oscillatory pattern with several similarities to the O_2 yield.

Figure 17. $1/T_{2(obs)}$ and O_2 Yield Flash Patterns for Spinach Chloroplast Membranes. (top) $1/T_2$ relaxation. (bottom) O_2 yield. $1/T_2$ was measured at 27 MHz, 25°C, on sample aliquots in HEPES buffer medium, pH 7.5, at 3 mg Chl/ml, while O_2 was measured on sample aliquots at 1 mg Chl/ml. Flash procedure: flashes spaced 2 s apart were given in a sequence from 1 to 22 flashes. The CPMG pulse train was initiated at the last flash in the sequence. A 7 min dark period was allowed between each flash sequence. The same flash procedure was used to measure the O_2 yield. Light flashes were obtained from a strobe flash lamp. The results in (top) are from an earlier publication of the author (130).

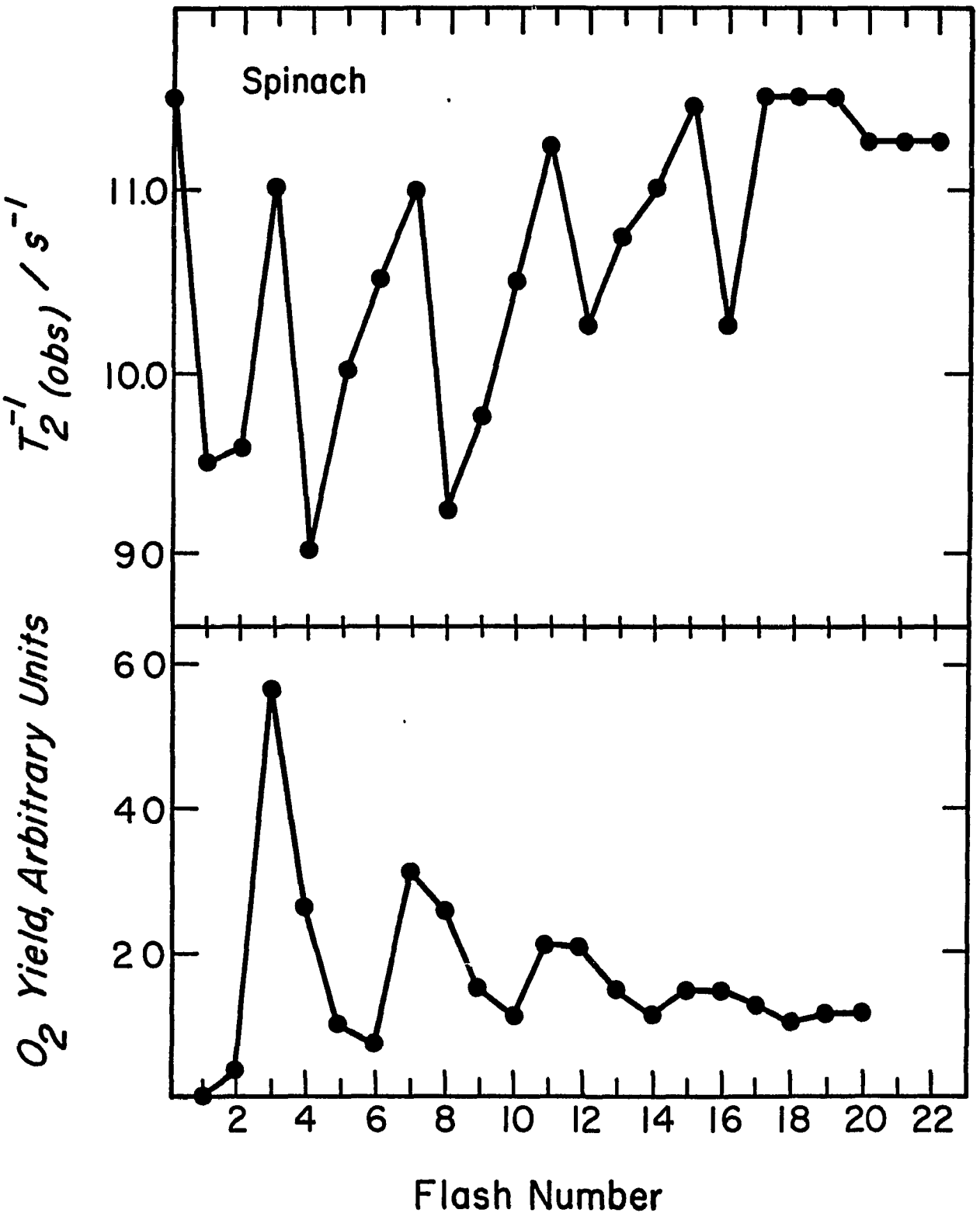
Spinach
11.0
10.0
9.0
T_2^{-1} (obs) / s^{-1}
60
40
20
O_2 Yield, Arbitrary Units
2
4
6
8
10
12
14
16
18
20
22
Flash Number

Figure 18. $1/T_{2(obs)}$ and O_2 Yield Flash Patterns for Lettuce and Pea Chloroplast Membranes. (top) $1/T_2$ relaxation. (bottom) O_2 yield. For lettuce, the flash procedure and conditions given in Figure 17 for spinach was used. For peas, the $1/T_2$ and O_2 were measured after each flash in a pulse sequence. Saturating flashes obtained from a pulsed dye laser (λ, 590 nm) were spaced 4 s apart. Chloroplasts in HEPES buffer medium, pH 7.5, at 2 mg Chl/ml were used in the $1/T_2$ measurements and at 1 mg Chl/ml for the O_2 measurements. $1/T_2$ was measured at 27 MHz, 25°C.

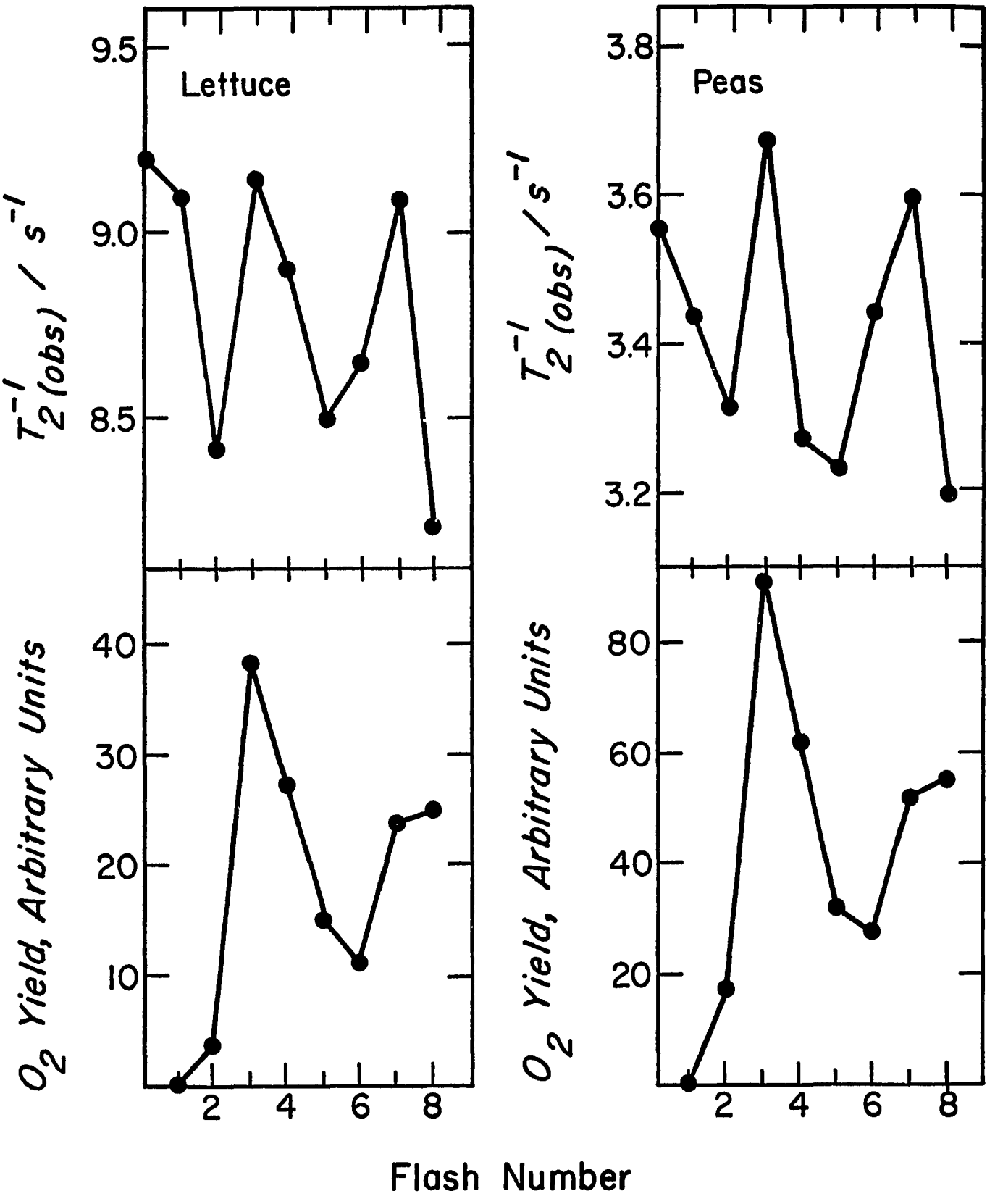
Lettuce
Peas
$T_{2(obs)}^{-1}$ / s^{-1}
O_2 Yield, Arbitrary Units
Flash Number
9.5
9.0
8.5
3.8
3.6
3.4
3.2
40
30
20
10
80
60
40
20
2
4
6
8

Both the $1/T_2$ and O_2 yield peak after the 3rd flash and show a periodicity of four. In the case of spinach, $1/T_2$ damps out at about the same flash number as the O_2 yield oscillations. If O_2 evolution is inhibited with DCMU the $1/T_2$ oscillations are also inhibited as shown in Figure 19a. However, in the dark DCMU causes $1/T_2$ to decrease over the dark control $1/T_2$ value; $1/T_2$ then increases with the first two light flashes and then levels off. This is an interesting result since it implies that the System II reaction center may turn over in the first few flashes in the presence of DCMU. When the loosely bound Mn is extracted by TRIS-acetone washing the rates are low as expected and there are no light effects (Figure 19b). These results strongly suggest that Mn participates in the O_2 evolving mechanism and that the PRR monitor the S states directly.

There are differences between the $1/T_2$ pattern among the different plants used. In spinach the $1/T_2$ minima occur after the peaks (i.e., after the 4th, 8th, etc. flashes, the $1/T_2$ increases from the minima to the peak). In lettuce and peas the $1/T_2$ minima occur after the 5th flash. The first few flashes are different also. In spinach the $1/T_2$ is about the same for the first two flashes while in lettuce and peas $1/T_2$ after the 2nd flash is lower than $1/T_2$ after the 1st flash. We thought at first that these differences may have been due to the flash procedure used. For the spinach

Figure 19. Effect of DCMU and Manganese Extraction on $1/T_{2(obs)}$ Flash Pattern. (a) [DCMU]/[Chl] = 0.089; (b) TRIS-acetone washed chloroplasts. Flash procedure and conditions for pea chloroplasts in Figure 18 were used.

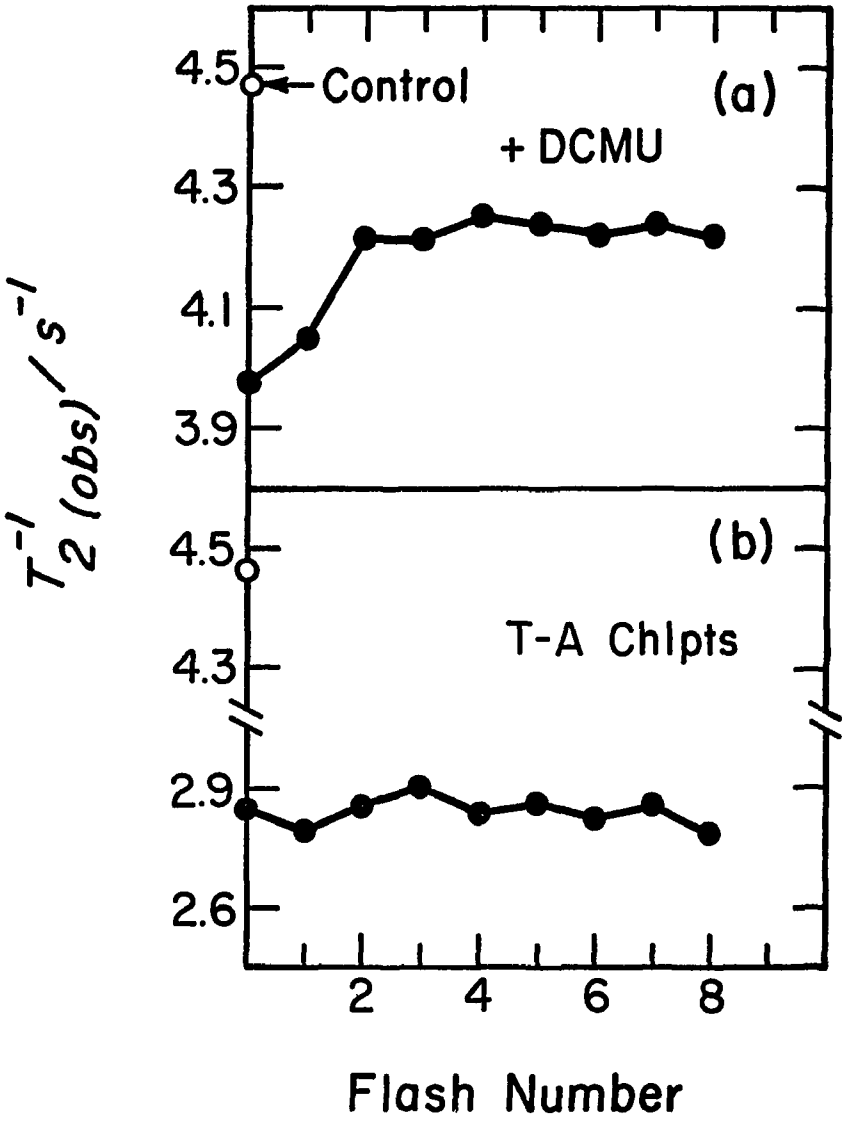
4.5
Control
(a)
+ DCMU
4.3
4.1
3.9
$T_{2\,(obs)}^{-1} / s^{-1}$
4.5
(b)
T-A Chlpts
4.3
2.9
2.6
2
4
6
8
Flash Number

measurements a sequence of flashes (from 1-22) spaced 2 s apart were given and then the $1/T_2$ was measured, the CPMG pulse train being initiated on the last light flash of the sequence. A dark period of 7 min was allowed between each flash sequence. For peas, on the other hand, $1/T_2$ was measured after each light flash in the flash sequence. The light flashes were spaced 4 s apart to allow sufficient time for the magnetization signal to decay completely (the $1/T_2$ pattern did not change if 3, 4 or 5 s were used between light flashes). Light flashes were obtained from a strobe flash lamp in the spinach measurements while a pulsed dye laser was used in the pea measurements. However, the lettuce chloroplasts were measured using the same protocol as for the spinach, yet it gives a flash pattern similar to the one for the peas. Thus, we must conclude that these differences in the flash pattern are inherent to the samples and not an artifact of the flash method.

The O_2 yield measurements were made using the same flash procedure as used for the corresponding $1/T_2$ measurements. For lettuce and peas the 8th flash was almost always higher than the 7th flash, in contrast to the ideal O_2 flash pattern (Figure 2). The spinach O_2 flash pattern follows the ideal pattern but was not obtained in every sample preparation. Several spinach samples gave patterns like those for peas and lettuce. Thus, the differences do not lie in the species

involved but, in all likelihood, in the starting conditions of each preparation.

2.2.2.2 Effect of pH

The actual value of $1/T_2$ and the flash patterns are strongly dependent on pH. The dark value of $1/T_{2(corr)}$ for peas are minimal at neutral pH's (6.5-7.5) increasing sharply at higher and lower pH. Figure 20 shows the $1/T_2$ flash pattern for three different sample preparations of pea chloroplasts at pH 6.7. The peaks in $1/T_2$ occur after the 3rd and 7th flash as usual, but the $1/T_2$ after the 2nd flash is very high with respect to the $1/T_2$ after the 1st flash. The O_2 yield is also shown for these samples. In these experiments short laser pulses were used, essentially eliminating double hits due to long light flashes; hence, no O_2 is observed on the 2nd flash.

Figure 21 shows the $1/T_2$ flash pattern for three samples of pea chloroplasts at pH 7.5. The pattern is the same as for pH 6.7 except the first two flashes; here, the $1/T_2$ after the second flash is lower than the $1/T_2$ after the 1st flash. It is interesting that the O_2 yield pattern also shows a difference--some O_2 is produced after the 2nd flash at pH 7.5. Since the laser pulses used are short, we must conclude that there is no double hit due to flash length, as shown at pH 6.7. However, double hits may have been made possible here due to some physiological reason or else there are some centers

Figure 20. $1/T_{2(obs)}$ and O_2 Yield Flash Patterns at pH 6.7. (a), (c) and (e) are the $1/T_2$ relaxation and (b), (d) and (f) are the O_2 yield for three different samples. Flash procedures and conditions for pea chloroplasts in Figure 18 were used except that the medium was adjusted to pH 6.7.

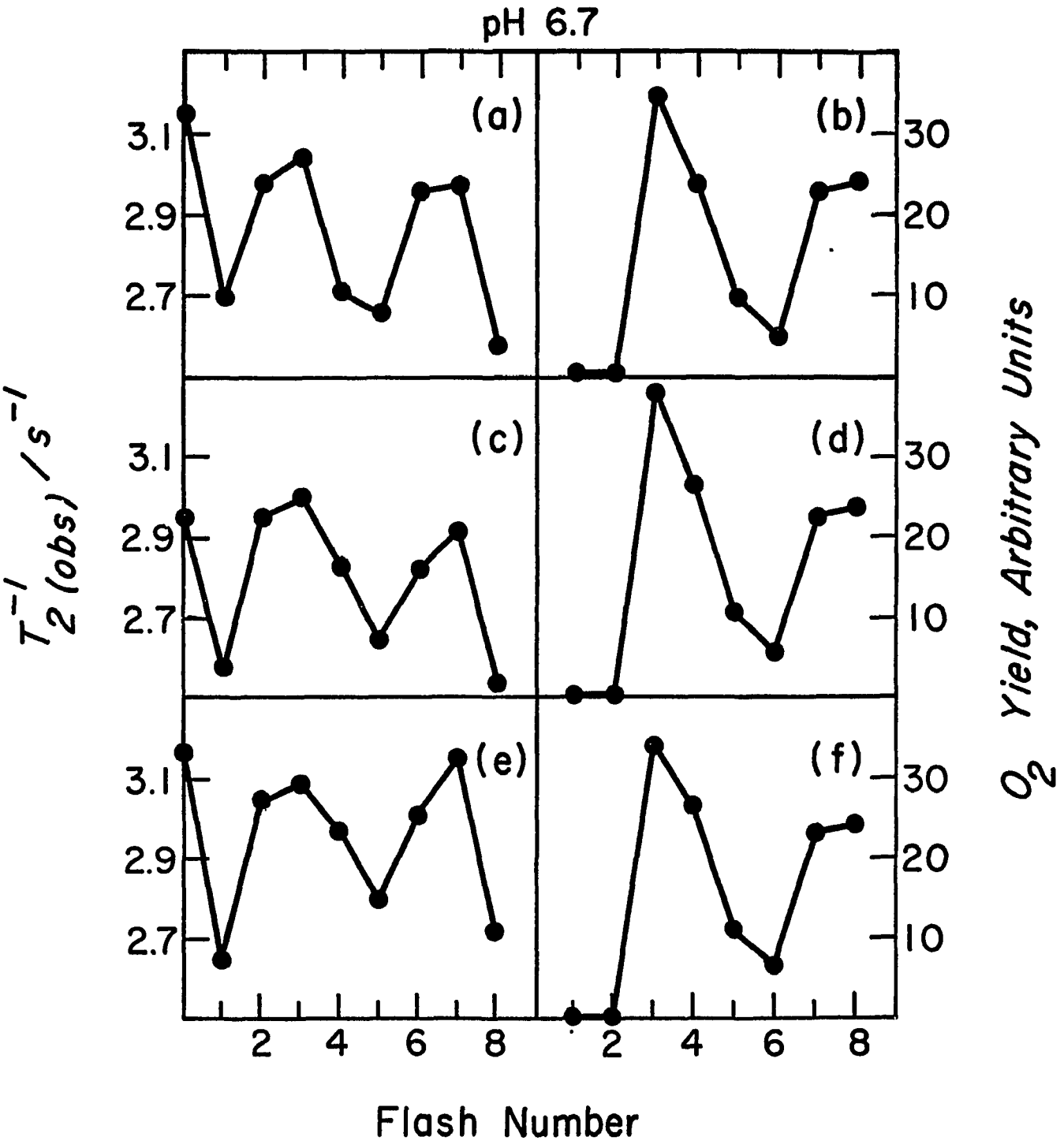
pH 6.7
(a)
(b)
(c)
(d)
(e)
(f)
3.1
2.9
2.7
30
20
10
2
4
6
8
$T_{2(obs)}^{-1}$ / s^{-1}
O_2 Yield, Arbitrary Units
Flash Number

Figure 21. $1/T_{2(obs)}$ and O_2 Yield Flash Patterns at pH 7.5. (a), (c) and (e) are the $1/T_2$ relaxation and (b), (d) and (f) are the O_2 yield for three different samples. Flash procedure and conditions for pea chloroplasts in Figure 18 were used.

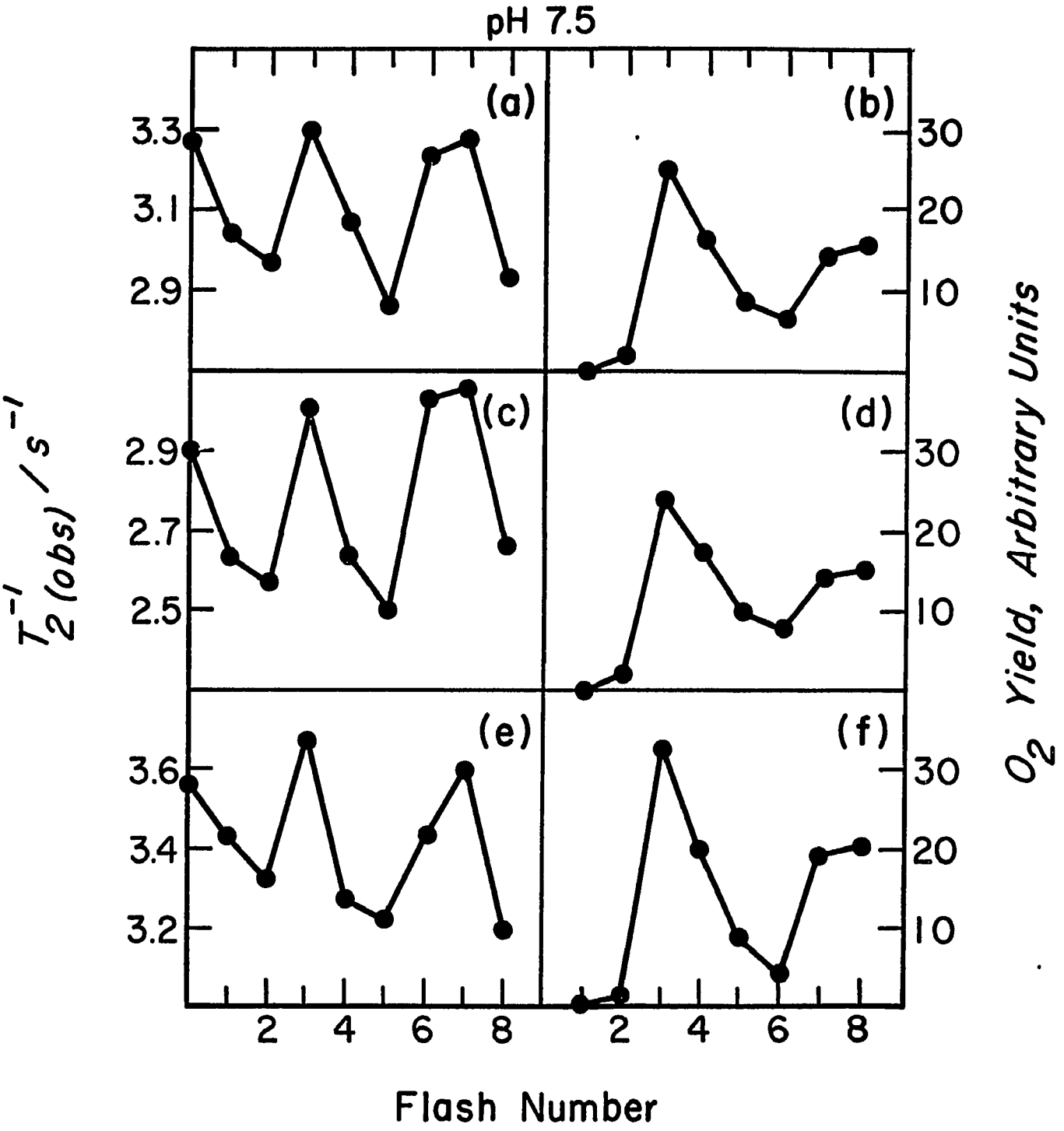
pH 7.5
(a)
(b)
(c)
(d)
(e)
(f)
3.3
3.1
2.9
2.9
2.7
2.5
3.6
3.4
3.2
30
20
10
2
4
6
8
Flash Number
$T_{2(obs)}^{-1}$ / s^{-1}
O_2 Yield, Arbitrary Units

starting out in the S_2 state in dark.

At extreme pH's O_2 evolution is inhibited but the $1/T_2$ can still be measured. Figure 22 shows that $1/T_2$ flash patterns at pH 9 and pH 4. At pH 9 the $1/T_2$ is high in dark and is not affected by the 1st light flash. On the 2nd and 3rd light flashes there are large decreases in $1/T_2$. If the flash sequence is interrupted by a dark period, the $1/T_2$ does not recover, but continues to decrease in a following flash sequence until it approaches the value for TRIS-acetone washed chloroplasts. These results are explained by suggesting that Mn is being released from the membrane at pH 9 with each light flash, or else becomes "hidden" from the bulk water by some "conformational" change. Recently, Briantais et al. (131) have found that there is a Mn release at alkaline pH in the presence of an uncoupler after the 1st light flash and they conclude that the alkaline pH reacts with the higher S states.

If O_2 is measured immediately after the sample is brought to pH 9, O_2 is produced unless an uncoupler is present (132). Apparently, the uncoupler quickly equilibrates the pH across the membrane to cause the inhibition. We observed no O_2 evolution in our preparation at pH 9 without uncouplers; however, these preparations were incubated for 1 hr or more, allowing sufficient time for pH equilibration across the membrane to take place. Inhibition of electron flow after aging

Figure 22. $1/T_{2(obs)}$ Flash Pattern at pH 9 and pH 4. (a) Samples incubated ~1 hr at pH 9. (b) Samples incubated ~1 hr at pH 4. Flash procedure and conditions for pea chloroplasts in Figure 18 were used except the medium was adjusted to pH 9 or pH 4 (with sample present).

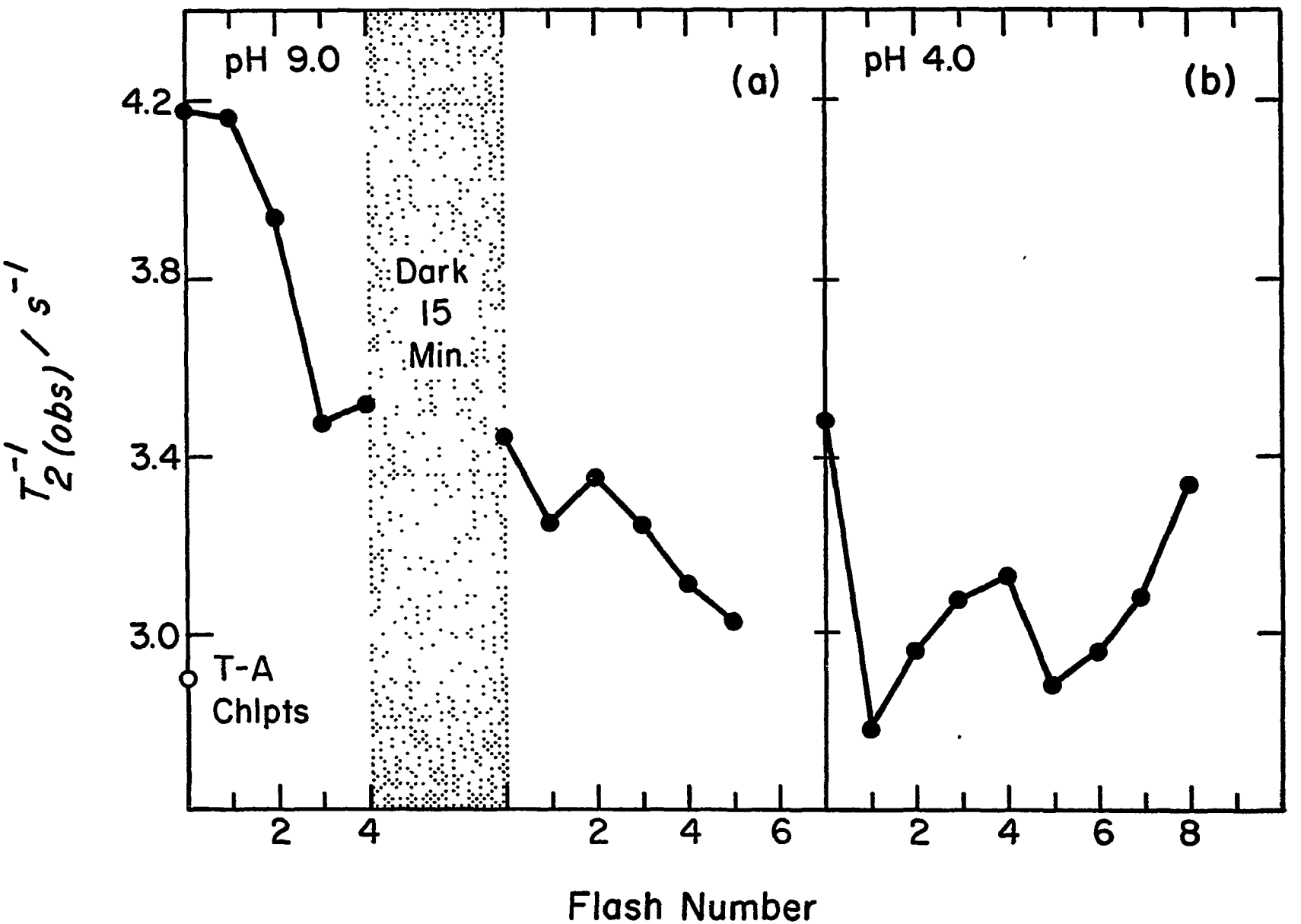
pH 9.0
(a)
pH 4.0
(b)
4.2
3.8
3.4
3.0
Dark
15
Min.
T-A
Chlpts
$T_{2(obs)}^{-1}$ / s^{-1}
2
4
2
4
6
2
4
6
8
Flash Number

in alkaline pH has been observed previously (133).

At pH 4 there also is no O_2 produced. But the $1/T_2$ still oscillates with light flashes--but with peaks after the 4th and 8th flashes (Figure 22b). This result suggests that all of the O_2 evolving centers are shifted to the S_0 state. It also clearly demonstrates that O_2 evolution can be uncoupled from the $1/T_2$ oscillations and hence the cycling of the S states. It has been suggested from luminescence studies that higher S states do form at low pH (134) and that their deactivation is slowed down (135).

2.2.2.3 Effect of Chemical Modifiers

Several reagents are known to inhibit O_2 evolution, but do not destroy the O_2 evolving apparatus. The effect of some of these reagents on the $1/T_2$ flash pattern are shown in Figure 23. Bouges (136) showed that NH_2OH at low concentrations inhibits O_2 evolution in the first few flashes, effectively causing the O_2 yield pattern to shift so that the peak occurs after the 5th or 6th flash. However, the periodicity of four is maintained. This is shown to be the case in our preparation in Figure 24a where the first peak occurs on the 6th flash in the first light cycle. This treatment does not destroy the O_2 evolving apparatus as evidenced by the normal O_2 yield flash pattern on the 2nd light cycle after a 5 min dark adaptation period. Figure 23a shows the effect of the same concentration of NH_2OH on the $1/T_2$ flash pattern (1st

Figure 23. $1/T_{2(obs)}$ Flash Patterns in the Presence of NH_2OH, TPB and CCCP. (a) $[NH_2OH]/[Chl] = 0.044$; (b) $[TPB]/[Chl] = 0.016$; (c) $[CCCP]/[Chl] = 0.089$. The $1/T_2$ for the dark-adapted controls are shown with open circles. Flash procedure and conditions for pea chloroplasts in Figure 18 were used.

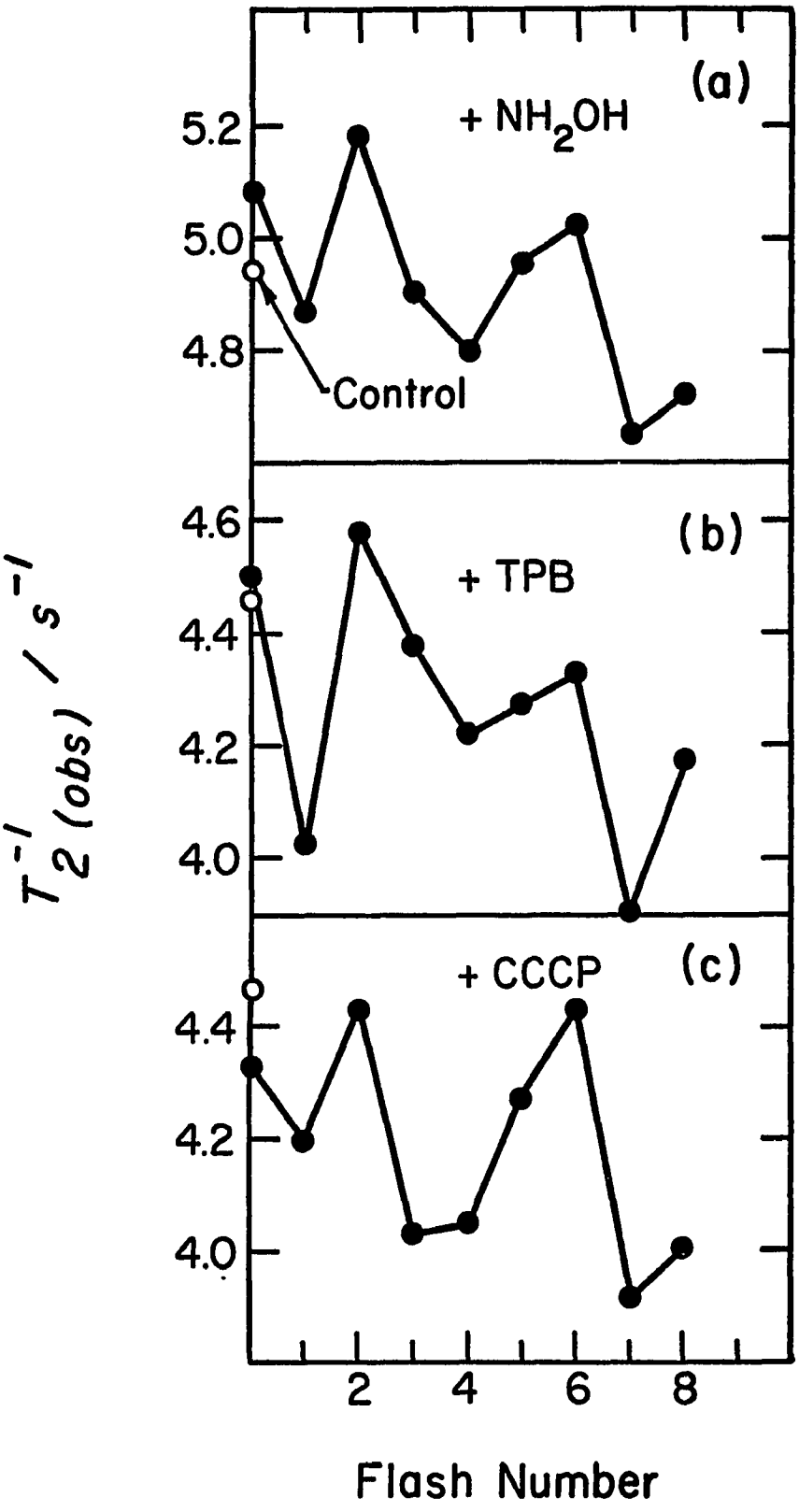
(a)
+ NH_2OH
5.2
5.0
4.8
Control
(b)
+ TPB
4.6
4.4
4.2
4.0
(c)
+ CCCP
4.4
4.2
4.0
2
4
6
8
Flash Number
$T_{2(obs)}^{-1}$ / s^{-1}

Figure 24. O_2 Yield Flash Patterns in the Presence of NH_2OH and TPB. (a) $[NH_2OH]/[Chl] = 0.044$; (b) $[TPB]/[Chl] = 0.016$. 1st cycle refers to first light flash sequence and 2nd cycle to the second light flash sequence after a 5 min dark period. Flash procedures and conditions for pea chloroplasts in Figure 18 were used.

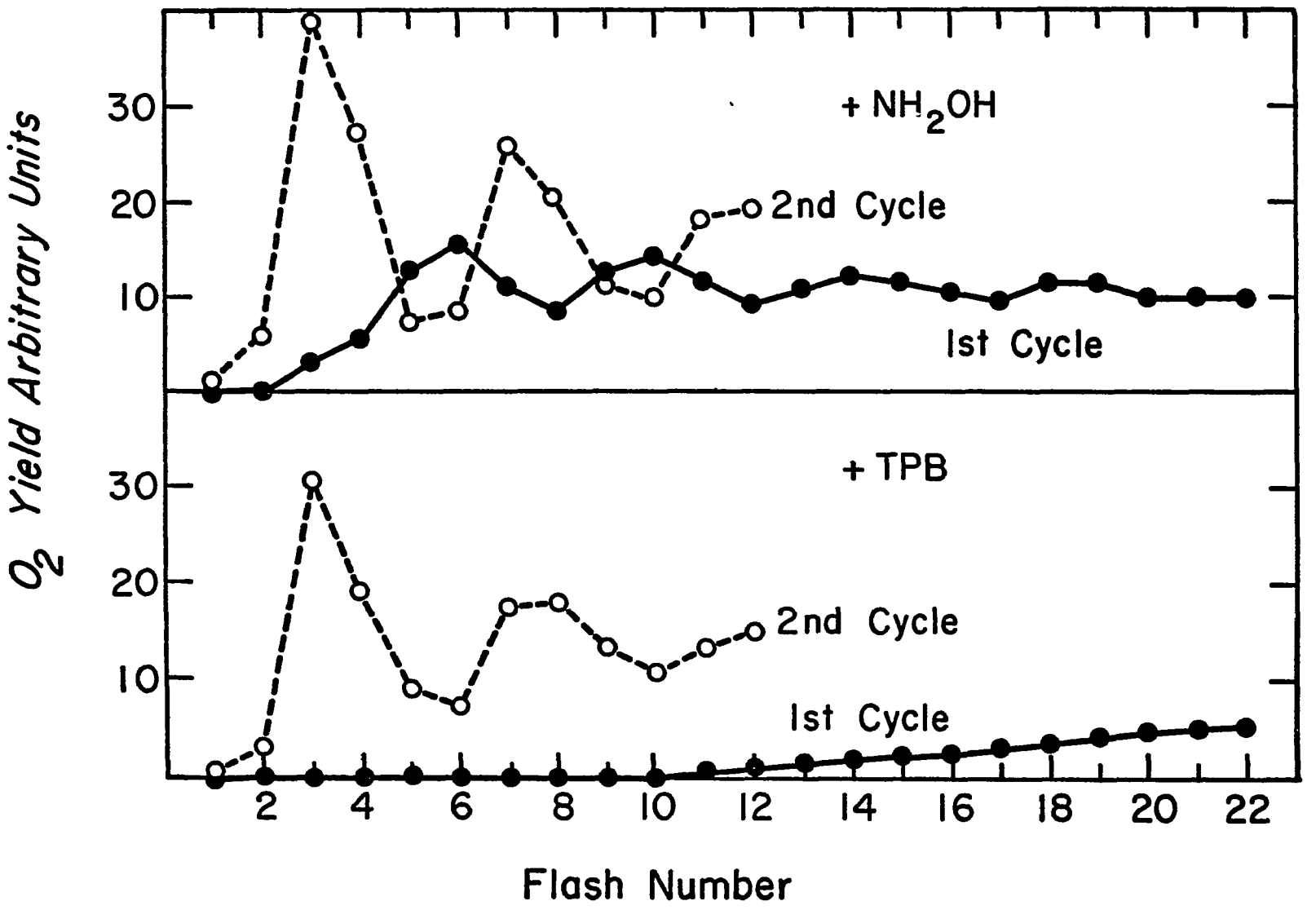
O_2 Yield Arbitrary Units
30
20
10
+ NH_2OH
2nd Cycle
1st Cycle
+ TPB
30
20
10
2nd Cycle
1st Cycle
2
4
6
8
10
12
14
16
18
20
22
Flash Number

cycle). In this case the $1/T_2$ peaks after the 2nd and 6th flash.

Bouges proposed that the NH_2OH causes a shift in the S states by binding to the S intermediate. Two or three molecules bind and are released in the first 2 or 3 flashes after which the normal cycling takes place with H_2O as electron donor. This could be the situation in the $1/T_2$ pattern, since the $1/T_2$ peaks shifted similarly. To account for the peak on the 2nd flash we would have to accept that NH_2OH acts as an electron donor replacing water, hence no O_2 could be evolved, but still allow a cycling of the states in the first few flashes.

Low concentrations of TPB result in the same effect on the $1/T_2$ pattern (Figure 23b). TPB has been suggested to be competitive electron donor to O_2 evolution mechanisms (137, 138). At the concentration of TPB used, O_2 evolution is inhibited in the first 10 flashes and then steadily increases thereafter (1st cycle, Figure 24b). After the TPB is used up (~40 flashes) and a 5 min dark period is given, the normal O_2 flash yields return (2nd cycle, Figure 24b).

CCCP also causes the $1/T_2$ pattern to shift with peaks after the 2nd and 6th flashes. CCCP is one of the reagents which induce a rapid deactivation of the higher S state. According to Renger (Section 3.3.3, Chapter I) these reagents induce a cyclic electron flow between the higher S states and

some endogenous reductant. (Thus, even here higher S states are reduced by some chemical other than H_2O.) At the concentration of CCCP used, O_2 evolution is completely inhibited.

It is obvious from these results that there is an altered cycling of the S states. We thought at first that this was due to the fact that in each case a reductant is involved donating electrons to the S intermediate in place of water. However, to our surprise, a similar change in the $1/T_2$ pattern was obtained under conditions when no reductant is involved. For example, Figure 25b shows that $1/T_2$ peaks after the 2nd and 6th flash at high concentrations of FeCy, when O_2 evolution is essentially inhibited. Obviously, FeCy cannot be acting as a reductant. At low concentrations of FeCy where O_2 evolution is not inhibited and FeCy acts as an electron acceptor, the normal $1/T_2$ pattern is observed with peaks after the 3rd and 7th flash. At both high and low FeCy concentrations the dark level is low with respect to the peak at the 3rd flash, in contrast to the usual situation where the dark levels are always high. (Note that the electron flow inhibitor DCMU had also caused a decrease in the dark level of $1/T_2$. The significance of this will be discussed in Chapter IV.)

In chloroplasts washed free of chloride, O_2 evolution is also inhibited (139). In this case, too, the $1/T_2$ peaks after the 2nd flash (Figure 26a). When NaCl or NaF is added

Figure 25. $1/T_{2(obs)}$ and O_2 Yield Flash Patterns in the Presence of FeCy. (a) and (b) [FeCy]/[Chl] = 0.222. (c) and (d) [FeCy]/[Chl] = 22.2. Flash procedure and conditions for pea chloroplasts in Figure 18 were used.

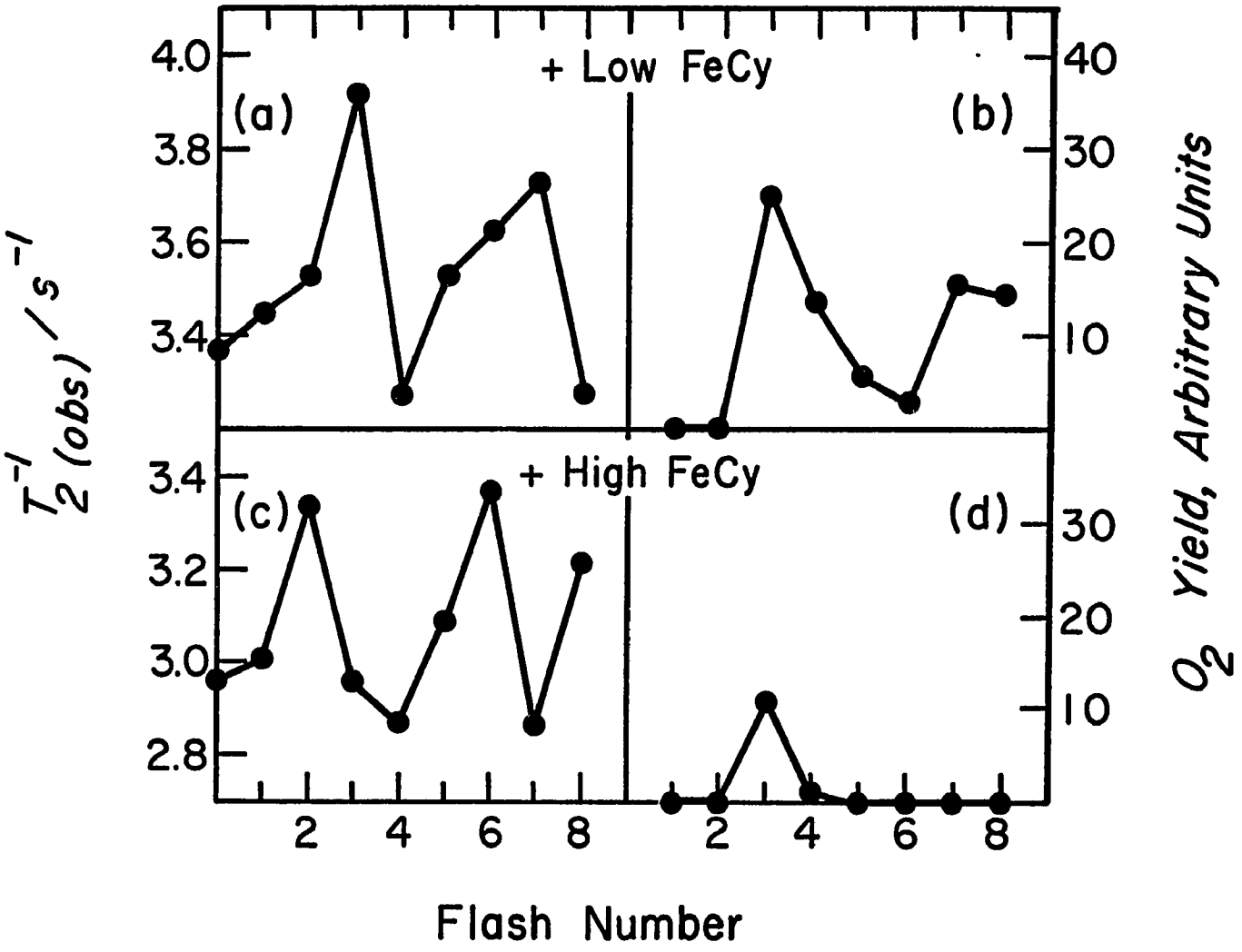
+ Low FeCy
(a)
(b)
+ High FeCy
(c)
(d)
4.0
3.8
3.6
3.4
3.2
3.0
2.8
40
30
20
10
2
4
6
8
$T_{2(obs)}^{-1}$ / s^{-1}
O_2 Yield, Arbitrary Units
Flash Number

Figure 26. $1/T_{2(obs)}$ Flash Patterns in the Presence of NaCl and NaF. (a) Chloroplasts washed free of chloride. (b) [NaCl]/[Chl] = 4.44. (c) [NaF]/[Chl] = 4.44. Flash Procedures and conditions for pea chloroplasts in Figure 18 were used except NaCl was eliminated from the medium.

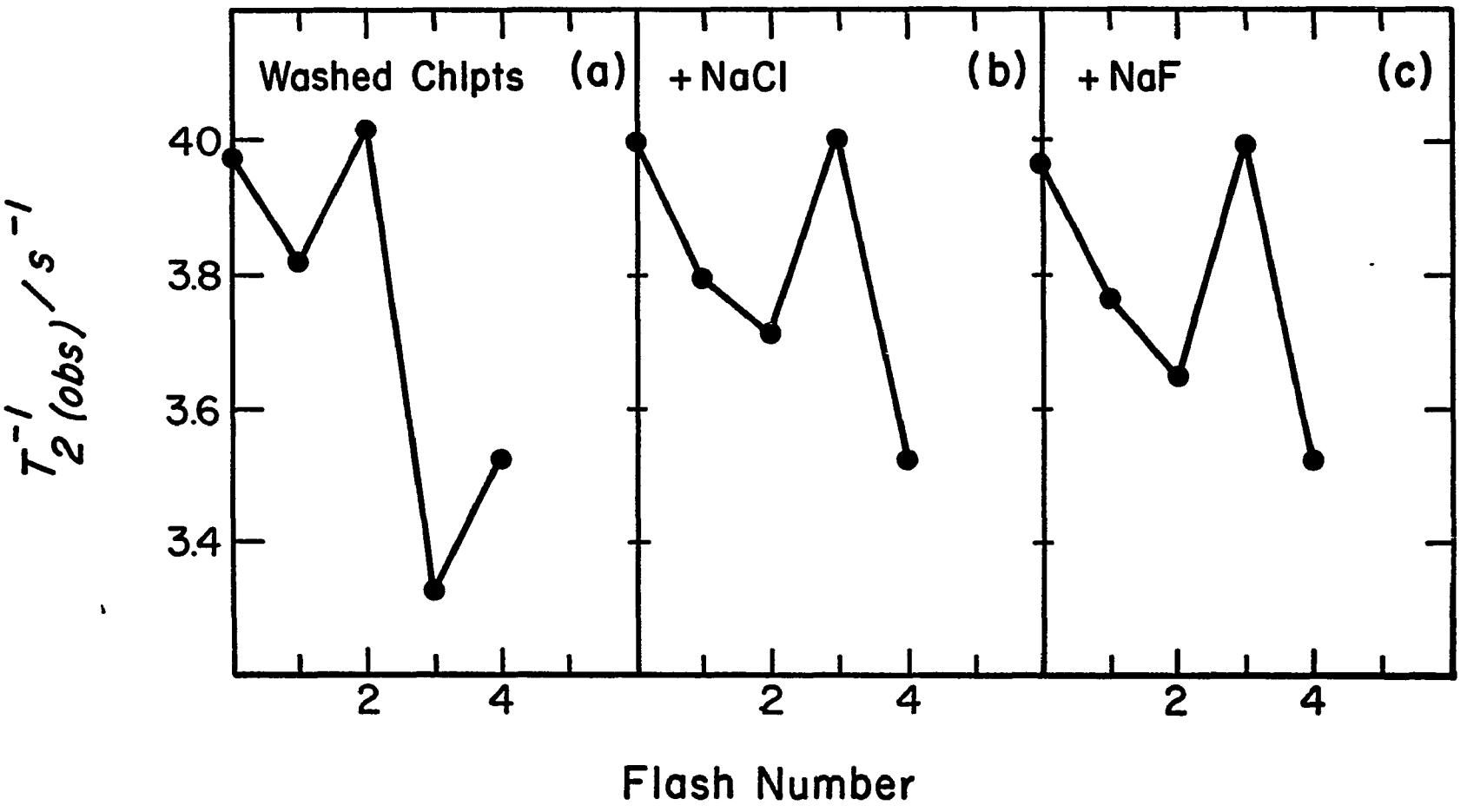
Washed Chlpts
(a)
+ NaCl
(b)
+ NaF
(c)
40
3.8
3.6
3.4
2
4
2
4
2
4
$T_{2(obs)}^{-1}$ / s^{-1}
Flash Number

back to the washed chloroplasts the normal pattern is restored with the $1/T_2$ peak after the 3rd flash (Figure 26b and c).

Thus, these results show that whenever O_2 is inhibited by treatments in which there is an apparent uncoupling of the final O_2 evolving step from the S states and not just when a reductant is present, the $1/T_2$ shows an altered pattern in which the peaks occur after the 2nd and 6th flashes.

Since the amount of paramagnetic ions in the membrane is very small, to measure the paramagnetic effect the bound ions must be accessible to the solvent water protons and the effect averaged over the total water proton population via chemical exchange processes. If the bound ions were not accessible to the solvent water it would be impossible to measure any paramagnetic effect. This is the case for copper in plastocyanin (140)--the copper being buried within the protein molecule and having no effect on water proton relaxation. Thus, a possible mechanism that could contribute to the changes in PRR are conformational changes which either open up or restrict the water accessibility to the bound Mn. We, therefore, measured the $1/T_1$ flash pattern under conditions in which the membrane conformation or configuration is known to be restricted or altered.

Macroconformational changes can be prevented by fixing the membranes in glutaraldehyde. In Figure 27a the $1/T_2$ flash pattern is given for glutaraldehyde fixed chloroplasts

Figure 27. $1/T_{2(obs)}$ and O_2 Yield Flash Patterns After Various Treatments Which Affect Membrane Conformations. (a), (c) and (e) are $1/T_2$ relaxation and (b), (d) and (f) are O_2 yield. (a) and (b) Chloroplasts were fixed in glutaraldehyde (98.5% fixation) according to procedure given in reference 141. (c) and (d) $[MgCl_2]/[Chl] = 2.22$. (e) and (f) Chloroplasts suspended in medium with no sucrose. Flash procedures and conditions for pea chloroplasts in Figure 18 were used.

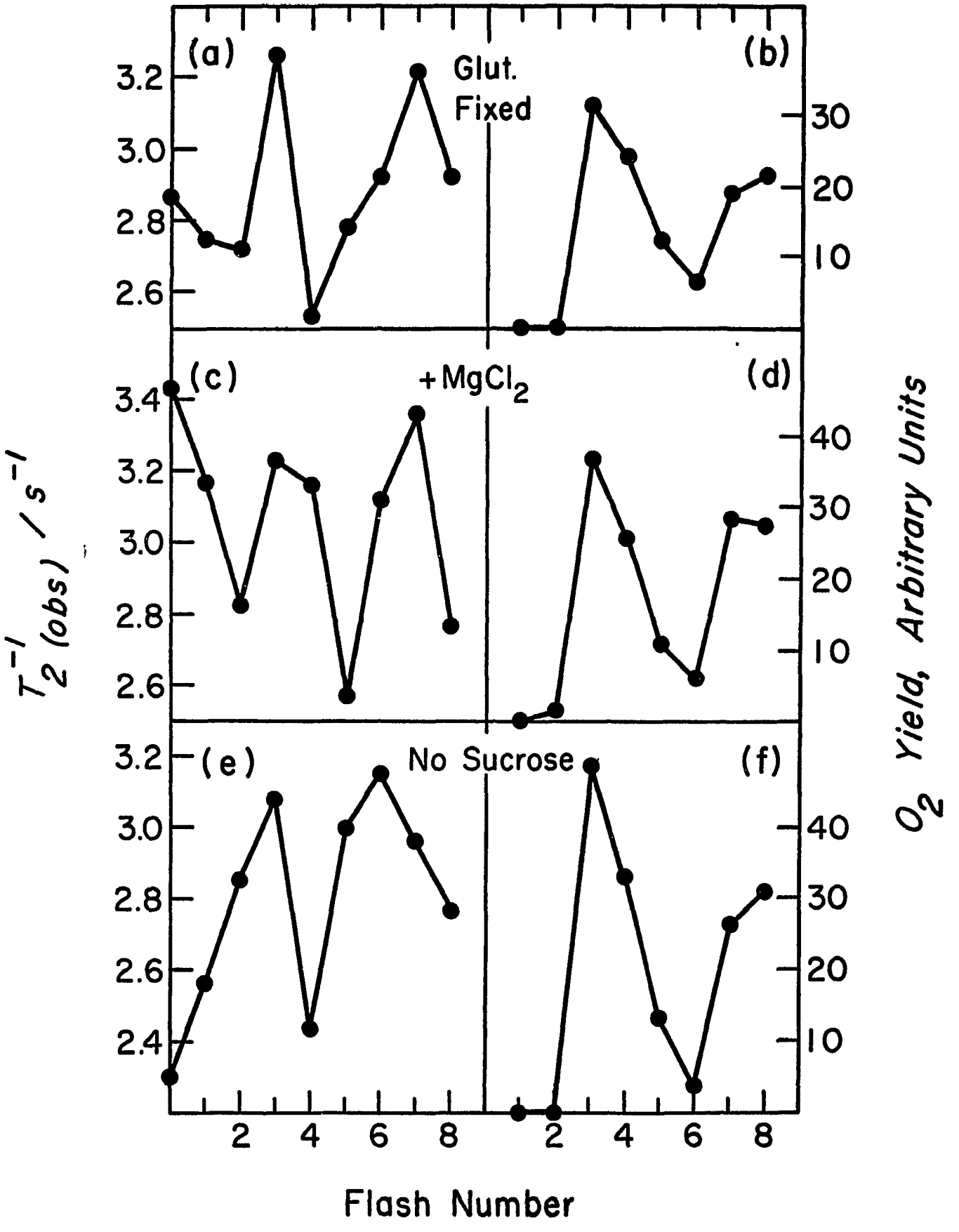
(a)
Glut.
Fixed
(b)
(c)
+MgCl2
(d)
(e)
No Sucrose
(f)
3.2
3.0
2.8
2.6
3.4
2.4
30
20
10
40
2
4
6
8
Flash Number
T2 (obs)-1 / s-1
O2 Yield, Arbitrary Units

according to the procedure of Zilinskas and Govindjee (141). The $1/T_2$ flash pattern is essentially the same as from normal chloroplasts with peaks in $1/T_2$ after the 3rd and 7th flashes. The dark level, however, is somewhat lower. There is no apparent effect on the O_2 flash yield (Figure 27b). This result indicates that macroconformational changes do not contribute to the $1/T_2$ changes in the light.

Low concentrations of $MgCl_2$ are believed to cause membrane conformation changes which affect the energy distribution between the two photosystems and the stacking of chloroplast membranes (142). As shown in Figures 27c and 27d there is no major change in the $1/T_2$ and O_2 yield in this case either.

Under conditions of low osomoticum chloroplast vesicles swell. In contrast to the above procedures, this treatment results in significant changes in the $1/T_2$ pattern as shown in Figure 27e. First, the dark level starts out low, as in the case when FeCy is present (Figure 25), but the $1/T_2$ peaks occur after the 3rd and 6th rather than the 3rd and 7th flashes. The O_2 yield pattern (Figure 27f) seems unaltered. Since in the O_2 electrode set up, the upper chamber contains 200 mM NaCl, it is difficult to say whether the chloroplast are truely at a low osmotic strength when O_2 is being measured. At least the normal O_2 yield pattern indicates there has been no major irreversible change in the O_2 evolving

apparatus due to the low osmotic treatment. Apparently the low osmoticum distorts the membrane in a way that alters the environment of the S intermediate to cause a change in the $1/T_2$ pattern.

These results indicate that the major light-induced changes in the $1/T_2$ do not arise from macroconformational changes of the membrane, but that the state of the membranes can affect the environment of the bound Mn. There, of course, remains the possibility that microconformational changes may still be somehow involved.

CHAPTER IV

THE ROLE OF MANGANESE IN PHOTOSYNTHETIC OXYGEN EVOLUTION

1 Proton Relaxation as a Monitor of Bound Mn(II)

1.1 Contribution of Bound Mn(II)

The evidence presented in Section 2.1, Chapter III strongly suggests that the PRR primarily monitor bound Mn(II) in chloroplast membranes. Although the behavior is a complex one, there is a direct relationship between chloroplast Mn, PRR and O_2 activity as shown in Figures 9-11. Analysis of the frequency dependence yields NMR parameters characteristic of Mn(II). Table 6 compares the best fit parameter values for chloroplast membranes with other Mn(II) systems. The chloroplast values are well within the range expected for Mn(II). Although the precision of the data limits the theoretical fit, differences in the values between bound Mn(II) and aqueous Mn(II) may reflect the local environment of the Mn. Compare, for example, the τ_V for chloroplasts and for Mn(II)-pyruvate kinase with aqueous Mn(II). It is also interesting to point out that chemical exchange contributes in chloroplasts (as well as in the other macromolecular systems), although not in the slow exchange limit (according to Equation 23).

There are, however, several other paramagnetic species in chloroplasts which may contribute to the PRR. But we believe that at the concentrations at which these ions are

Table 6. Best Fit NMR Parameter Values for Chloroplasts Membranes and Other Mn(II) Systems

	τ_V/s x 10^{12}	τ_M/s x 10^8	B/(rad s^{-1})^2 x 10^{19}
Chlpts	20	2.2	0.90
Chlpts + TPB	20	1.0	0.9
Chlpts + FeCy	9.3	0.1	1.1
Aqueous Mn(II)	[a]2.1	2.3	10
Mn(II)-Carboxy-Peptidase A	[b]7 ± 0.6	0.25 ± 0.3	3.1 ± 0.4
Mn(II)-Pyruvate Knase	[c]6	0.5 ± 0.1	1.46
	[b]14 ± 4	0.4 ± 0.04	0.8 ± 0.1

[a]Bloembergen and Morgan (121).

[b]Navon (143).

[c]Reuben and Cohn (144).

present in our preparations, their effects on the PRR remain small. Mn(II) is the most efficient relaxer of the proton magnetic energy states of all ions in the second transition series (113). High spin Fe(II) and Fe(III) have very short electronic relaxation times ($\tau_s \sim 10^{-11}$ s) and are frequency independent in the range of frequencies we employ (115). This, coupled with a smaller magnetic dipole moment, makes the paramagnetic contribution of iron orders of magnitude less than Mn(II). Even though much more iron may be present in the chloroplast membrane than Mn, the Mn(II) effect still dominates. The electronic relaxation of Cu(II) is comparable to Mn(II), but in chloroplasts at least half of the copper is located in plastocyanin, which itself has no effect on PRR (140). The rest of the copper in chloroplasts is located in polyphenoloxidase, an enzyme which is not involved in photosynthesis, and is washed out during the chloroplast preparation. The sum total of the effects of these paramagnetic ions could represent the background contribution.

In the frequency analysis (Section 2.1.2 Chapter III) we had to include a non-site specific or outer sphere contribution in order to fit the data. According to the theoretical fit $1/T_{2(OS)}$ is three times greater than $1/T_{1(OS)}$. This difference may explain the $1/T_1$ and $1/T_2$ behavior to the Mn content of the membranes (Figure 10). The transverse relaxation arises from the loss of phase coherency in the spin system

and as a result $1/T_2$ is sensitive to the local microenvironments of the membrane. On the other hand, $1/T_1$ depends much more on the direct inner sphere contributions of the paramagnetic ions. The tightly bound Mn in the chloroplast is probably buried within the membrane not easily accessible to the solvent water, as evidenced by the lack of frequency dependence of the Tris-acetone washed chloroplasts (Figure 12). (This may explain why this fraction is not easily affected by those treatments which affect the loosely bound Mn.) However, the outer sphere contribution of the tightly bound Mn would still be present. Since $1/T_2$ is more sensitive to the outer sphere mechanism it would be influenced by both the tightly and loosely bound Mn whereas $1/T_1$ would be mostly influenced by the inner sphere contribution of the loosely bound Mn.

1.2 Contribution of free Mn(II)

The effect of Mn(II) becomes largest when it is bound to macromolecules, since under these conditions the electronic relaxation governs the overall correlation time (Equation 26), rather than rapid translational and rotational motions (see theory of enhancement, reference 113). Table 7 compares the $1/T_1$ and $1/T_2$ for the buffer medium with and without 50 μM $MnCl_2$ and a chloroplast sample. Aqueous Mn(II) has a smaller effect on the $1/T_1$ of the buffer than the chloroplast sample. The $1/T_2$ for the buffer is significantly

Table 7. Comparison of the Effects of Free Mn(II) and Chloroplast Membranes on the Relaxation Rates

	Buffer	Buffer +50 μM $MnCl_2$	Chloroplasts
$T_{1(obs)}^{-1}/s^{-1}$	[a]0.51	0.74	1.21
$\left(T_{1(obs)}^{-1} - T_{1(Buff)}^{-1}\right)/s^{-1}$	--	0.23	0.70
$T_{1(norm)}^{-1}/s^{-1}$	--	[b]0.12	0.70
$T_{2(obs)}^{-1}/s^{-1}$	0.69	1.01	4.65
$\left(T_{2(obs)}^{-1} - T_{2(Buff)}^{-1}\right)/s^{-1}$	--	0.32	3.96
$T_{2(norm)}^{-1}/s^{-1}$	--	[b]0.173	3.96

[a]Rates measured at 27 MHz, 25°C

[b]Rates normalized to the Mn concentration in the chloroplast sample, 27 μM.

greater than the $1/T_1$ (in pure water, $1/T_1 = 1/T_2$). This is probably due to viscosity effects of the high sucrose (0.4 M) concentration. However, the aqueous Mn(II) has about the same effect on $1/T_2$ of the buffer in contrast to the chloroplast sample which produces a much larger effect. When the aqueous Mn(II) is normalized to the same Mn concentration present in the sample (27 μM for a chloroplast suspension at 3 mg Chl/ml), the effect of the aqueous Mn(II) becomes even smaller. Thus, free Mn(II) makes only a small contribution to PRR at the concentrations we are dealing with.

In our discussion of Table 1 in Section 2.1.1, Chapter III, we noted that in some cases of TRIS washed chloroplasts the $1/T_1$ increased over the washed control, which would not be expected if it is assumed that this treatment extracts manganese from the membrane. However, according to the model of Blankenship and Sauer (39) TRIS washing causes the release of the native bound Mn to the aqueous phase inside the chloroplast vesicle. Any free Mn in the chloroplast suspension will be in equilibrium with non-specific binding sites on the membrane. Gross (145) has demonstrated the existence of non-specific binding sites for Mn on the membrane. Blankenship and Sauer (39) have estimated the number of these sites to be 1 per 5.5 Chl in normal chloroplasts and 1 per 200 Chl in TRIS washed chloroplasts. They calculate a binding constant (K_D) of 8.3×10^5 M^{-1} in both normal and treated chloroplasts.

Takahashi and Asada (40) estimate the binding constants of the native bound Mn to be $K_L = 1.2 \times 10^4\ M^{-1}$ for the loosely bound fraction and $K_T = 1.9 \times 10^5\ M^{-1}$ for the tightly bound fraction. Interestingly, these binding constants suggest that the non-specific binding sites have an affinity for Mn comparable to the affinity of the tightly bound site. Thus, if much of the native loosely bound fraction of Mn exists in an oxidation state that has a small effect on PRR (see later), when it is released by various treatments it immediately disproportionates to Mn(II) in the aqueous phase, rebinds to the membrane and enhances the PRR.

Recently, Siderer et al. (146) have observed a Mn EPR signal in lettuce chloroplasts which they ascribe to bound Mn. Under the conditions when the zero field splitting is small compared to the Zeeman interaction (i.e., the interaction between the spin and the applied field) and rotational motions are sufficiently fast, a bound Mn EPR signal can arise, but with a much reduced intensity. Siderer et al. have observed this signal in spinach chloroplasts as well, whereas Lozier and Butler (35) and Blankenship and Sauer(39) did not. The discrepancy in the results is not explained; but the point is that even bound Mn can give rise to an EPR signal under certain conditions and in those situations where the EPR signal is assumed to represent only free Mn, some bound Mn may also be present.

The equilibrium between bound and free Mn may also account for the temperature effects on the PRR (Figure 14). The PRR increase with decreasing temperature at all frequencies measured, which is not characteristic for any of the magnetic relaxation mechanisms considered. What may be dominating the temperature effects instead is binding of free Mn(II) at lower temperatures.

1.3 Contribution of Higher Oxidation States of Manganese

The effects of redox reagents on the loosely bound Mn suggest that there is a change in the Mn(II) population. From Table 6 the calculated best fit parameter values for chloroplasts containing either a reductant (TPB) or an oxidant (Fecy) are still in the range for Mn(II). The change produced by the redox reagents is in the magnitude of the PRR. This may be interpreted as changes in the oxidation state of Mn. Thus, in the case of TPB the much increased amplitude of PRR would indicate a reduction of a fraction of the bound Mn to the highly efficient Mn(II). From Figure 15 there appears to be several titratable factions of Mn. These results indicate that a significant proportion of the bound Mn exists in a higher oxidation state which has no or only a small contribution to PRR.

Mn(III) has a negligible effect on PRR at the concentrations we are dealing with. Table 8 compares the $1/T_1$ at several frequencies for Mn(II) in a phospholipid dispersion and

Table 8. Comparison of the Effects of Bound Mn(II) and Bound Mn(III) on $1/T_1$

$MnCl_2$ in Lecithin Dispersion[a]		Mn(III) - Superoxide Dismutase[b]	
ν/MHz	T_1^{-1}/s^{-1}	ν/MHz	$T_{1(P)}^{-1}/s^{-1}$
8	3.16	6	0.083
12	4.15	12	0.071
24	4.38	24	0.062
64	2.53	48	0.055
90	1.68		

[a]Sample was prepared by sonicating dipalmitoyllecithin (80 μM) in 50 μM $MnCl_2$. Phospholipid concentration was determined by spectrophotometric assay. From Zumbulyadis et al. (147).

[b]From Villafranca et al. (148). $1/T_{1(P)}$ was calculated from the molar relaxivities and normalized to 50 μM binding sites.

the $1/T_1$ of Mn(III) (normalized to the same Mn(II) concentration) bound to a superoxide dismutase, taken from the data by Villafranca et al. (148). Note the very small contribution of Mn(III) with respect to Mn(II). Mn(III) also shows an entirely different frequency dependence--there is no peak at the low frequencies (12-24 MHz) as is obvious for Mn(II). Although it is unknown at this time, higher oxidation states of Mn may have only a small contribution as does Mn(III) so that PRR is basically monitoring only the Mn(II) population in the chloroplasts.

1.4 Location of Bound Manganese in the Membrane

Current models of chloroplast thylakoid membranes place the manganese associated with O_2 evolution to the inside of the vesicle (Section 3.3.1 Chapter I). Water exchange across biological membranes has been measured to be relatively slow--the average lifetime of a water molecule inside an erythrocyte ghost is ~5 ms (149)--and, therefore, might be expected to limit internal paramagnetic effects (150). It is important to realize, though, that the inner space of the thylakoid vesicle represents a separate water compartment. Assuming Mn is on the inside of the vesicle, the paramagnetic effect is first experienced by the internal water fraction. This yields an overall PRR for the internal water which then averages with the external water by exchange across the membrane. If the PRR for the internal water is slower than the exchange across

the membrane, then the internal paramagnetic effects will be distributed to the external water.

Although we use very high chlorophyll concentrations (2-3 mg Chl/ml) the internal volume represents only about 3-4% of the total water volume of the sample and the rate could not, therefore, be arising from the internal water only. We observe a single exponential in the magnetization plots (Figure 6) indicating that only one water fraction is being measured. Whether the paramagnetic effect is distributed over the total water population by water exchange or by proton exchange is still unknown; but this does not affect our major conclusion that the PRR monitor the average effect of the internal Mn.

We attempted to measure the relaxation rates of ^{17}O labeled water in chloroplasts. ^{17}O measurements would reflect more directly the bound water since the ligand bond is between the Mn and the oxygen atom of the water molecule. However, preliminary measurements indicate that there is very little paramagnetic effect of chloroplasts on ^{17}O relaxation rates. The relaxation rates of ^{17}O are very fast (in the order of ms) and probably become limited by water exchange across the membrane. When the membranes are solubilized in detergent the ^{17}O rates are slightly enhanced. This result is consistent with the location of the native bound Mn to the inside of the chloroplast vesicle, and that in proton

relaxation the effect is averaged out via water exchange processes across the membrane.

2 Proton Relaxation as a Monitor of the S Intermediate

2.1 Theoretical Fit to the $1/T_2$ Flash Pattern

In order to better understand the implication of the PRR data in terms of the O_2 evolving mechanism, attempts were made to fit the $1/T_2$ flash pattern with a theoretical model. Such a model would be required to fit both the O_2 yield flash pattern and the $1/T_2$ flash pattern. Therefore, we used the Kok et al. (77) model as described in Section 3.2, Chapter I, as our starting point.

To account for the peak yield on the third flash it is assumed that in the dark-adapted condition the O_2 evolving centers exist in a mixture of S_0 and S_1 states. The ideal distribution used in the model is $[S_0] = 0.25$ and $[S_1] = 0.75$ (the sum total of all states at any time being 1.0), but the relative initial distribution may vary depending on the chloroplast preparation. The ratio of the O_2 yield on the 3rd to the 4th flash (i.e., Y_3/Y_4) gives a good estimate of the $[S_1]/[S_0]$ distribution (78). Table 9 gives the calculated Y_3/Y_4 and Y_7/Y_8 ratios for various $[S_1]/[S_0]$ starting distributions. For our pea chloroplast preparations, the experimental Y_3/Y_4 and Y_7/Y_8 fit best with an initial dark distribution of $[S_0] = 0.30$ and $[S_1] = 0.70$.

Table 9. Calculated Y_3/Y_4 and Y_7/Y_8 Ratios for Various $[S_1]/[S_0]$ Starting Distributions

$[S_1]/[S_0]$ Starting Distribution[a]	Y_3/Y_4	Y_7/Y_8
0.25/0.75	1.67	1.01
0.30/0.70	1.46	0.93
0.35/0.65	1.27	0.86
0.40/0.60	1.11	0.78
Pea Chloroplasts, average of 6 Samples	1.44	0.94

[a]Assuming $\alpha = 0.10$, $\beta = 0$.

In the above calculations we assumed a miss parameter (α) of 0.10 at each step. There is no justification at this time to assume the more complicated situation in which α varies for each of the S transitions (see later). Since we are using brief laser flashes and in some conditions (e.g., at pH 6.7) there is no O_2 produced after the 2nd flash, we assume double hits (β) to be nonexistent in our set up. The starting conditions we used, therefore, were $[S_0] = 0.30$, $[S_1] = 0.70$, $\alpha = 0.10$ and $\beta = 0$.

Our approach to fit the $1/T_2$ data is based on the assumption that Mn(II) contributes to the PRR, whereas Mn(III) and other higher oxidation states do not. Theoretical $1/T_2$ patterns can be generated by assigning different weighting factors proportional to the amount of Mn(II) to each of the S states. In the Kok et al. (77) model it is assumed that each S_n state differs from the preceding S_{n-1} state by the accumulation of an additional oxidizing equivalent and that upon reaching the most oxidized S_4 state, the S intermediate then undergoes a concerted reaction with two water molecules to produce O_2 and $4H^+$. Our first attempt to fit the data was to assign decreasing weighting factors for the higher S states, e.g., $S_0 = 4$, $S_1 = 3$, $S_2 = 2$ and $S_3 = 1$, abbreviated as a 4,3,2,1 model (we ignore the S_4 state since it is discharged within a few ms and does not exist in the time of the $1/T_2$ measurement--T_2 being 200-300 ms for pea chloroplasts). The

4,3,2,1 model and other combinations which represent a decreasing Mn(II) contribution all give theoretical peaks after the 4th and 8th flashes. Instead, in order to generate a pattern with peaks after the 3rd and 7th flashes we had to assign large weighting factors to the higher S states.

The model which best fit the data at pH 6.7 (Figure 20) was 2,1,1,3. This is a surprising result in that it indicates that the S_3 state has a greater contribution to the $1/T_2$ than do the S_0, S_1 and S_2 states.

One of the problems we encountered in fitting the $1/T_2$ data was the high dark level before the flash sequence. In most of the untreated control chloroplasts the dark $1/T_2$ has about the same value as the peaks in the flash cycle, whereas all of the models predicted a low dark $1/T_2$, at about the minima in the flash cycle. To fit the high dark $1/T_2$ we had to assume that the S_0 has a larger contribution in the dark than it does during the flash cycle. This assumption implies that there exists a special dark-adapted state of the S intermediate.

The best fit to the $1/T_2$ flash pattern at pH 6.7 is shown in Figure 28a. The closed circles are the experimental data points ($1/T_{2(corr)}$) and the open circles are the theoretical fit generated from a 2,1,1,3 model with $S_0 = 4$ in the dark. The experimental and theoretical points are normalized at the 3rd flash. Figure 28b shows the fit to the O_2 yield pattern.

Figure 28. Theoretical Fit to the $1/T_2$ and O_2 Yield Flash Patterns at pH 6.7. (a) $1/T_2$ relaxation. (b) O_2 yield. Closed circles are experimental data points ($1/T_{2(corr)}$); open circles are theoretical points. For the theoretical fit $[S_0] = 0.30$, $[S_1] = 0.70$, $\alpha = 0.10$, $\beta = 0$ and weighting factors are 2,1,1,3 except that $S_0 = 4$ in the dark.

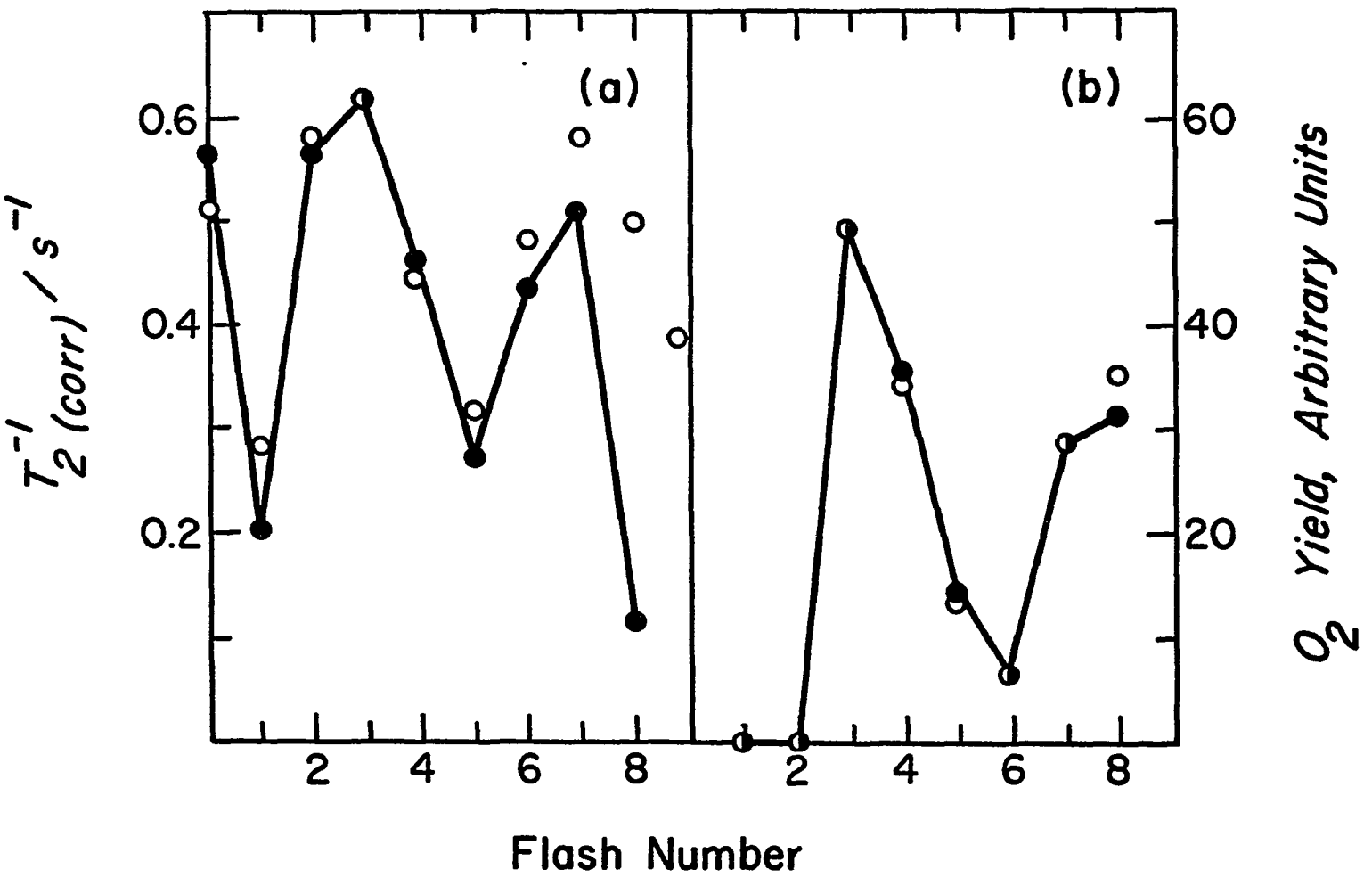
(a)
(b)
0.6
0.4
0.2
60
40
20
2
4
6
8
2
4
6
8
$T_{2\,(corr)}^{-1}$ / s^{-1}
O_2 Yield, Arbitrary Units
Flash Number

If we use $1/T_{2(obs)}$ instead $1/T_{2(corr)}$, the fit is not as good (the oscillation in the observed rates are not as deep as the theoretical oscillations), implying that it is the loosely bound Mn which is undergoing these changes.

The model fits reasonably well with the experimental results except at the 8th flash, where the experimental point shows a large decrease in $1/T_2$. This large decrease is observed in most of our data (occasionally, the 8th flash did not show a large decrease); at this time we have no explanation for it. There seems to be, however, a general downward shift of the experimental points as though some background contribution is decreasing. An additional parameter may have to be introduced to compensate for the downward trend. But the model as it now stands gives a good approximation of the experimental data.

The $1/T_2$ pattern at pH 7.5 is the same as at pH 6.7 except for the first two flashes. Oddly, at this pH there is a small amount of O_2 produced after the 2nd flash although brief laser flashes are used. Assuming there are no double hits due to the laser flash, we must ascribe a physiological significance to the apparent double hits (as does Lavorel (111), see Section 3.3.3, Chapter I) or else assume that the S state distribution in the dark has changed to include some S_2. In fitting the data, we assume the second possibility, setting the S state distribution to be $[S_0] = 0.30$ $[S_1] = 0.67$ and $[S_2] = 0.03$. Then to account for the $1/T_2$ on the first

two flashes, we set the weighting parameters on the first cycle to be 2,1,2,1. On the remaining cycles the weighting parameters are 2,1,1,3 and S_0 = 4 in the dark as before. The theoretical fit to $1/T_{2(corr)}$ at pH 7.5 is shown in Figure 29a and for the O_2 yield in Figure 29b. This result implies that the first cycle of the S intermediate may differ from succeeding cycles depending upon the experimental conditions.

Figure 30 shows several theoretical patterns which qualitatively fit other variations in the experimental data. In spinach (Figure 17), for example, the peaks occur after the 3rd and 7th flashes as usual, but the minima occur on the 4th and 8th flashes, the $1/T_2$ then increasing to the peak. In Figure 30a we have this trend where we have assumed a model of 2,1,2,2 and S_0 = 4 in the dark. If S_0 = 2 in the dark, then the dark $1/T_2$ is low (dotted line in Figure 30a) and we have a pattern similar to the one for pea chloroplasts with low concentration of FeCy (Figure 25a).

In several cases we observed an altered $1/T_2$ pattern with peaks after the 2nd and 6th flashes. This pattern is generated using a model of 0,1,1,3 with S_0 = 4 in the dark. (Compare Figure 30b with Figure 23.) At pH 4 the experimental oscillations can be generated using a model of 0,1,2,3 and S_0 = 4 in the dark. (Compare Figure 30c with Figure 22b.)

These models are rather diverse, but they are specific for the patterns they generate. In Figure 30b S_0 must be

Figure 29. Theoretical Fit to the $1/T_{2(corr)}$ and O_2 Yield Flash Patterns at pH 7.5. (a) $1/T_2$ relaxation. (b) O_2 yield. Closed circles are experimental data points ($1/T_{2(corr)}$); open circles are theoretical points. For the theoretical fit $[S_0] = 0.30$, $[S_1] = 0.67$, $[S_2]$ 0.03, $\alpha = 0.10$, $\beta = 0$ and weighting factors are 2,1,2,1 on the first cycle, 2,1,1,3 on succeeding cycles, except that $S_0 = 4$ in the dark.

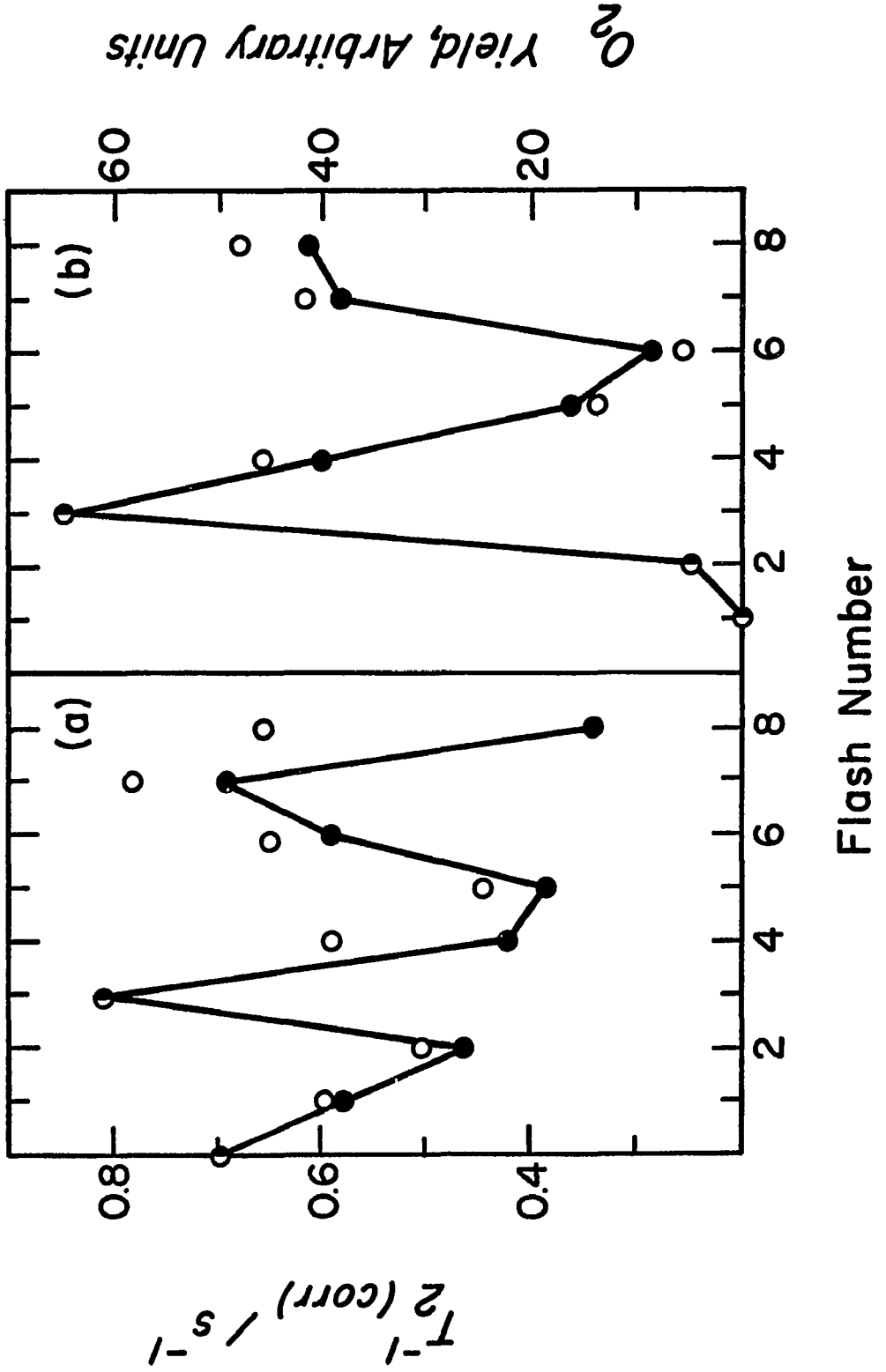
O_2 Yield, Arbitrary Units
60
40
20
(b)
(a)
0.8
0.6
0.4
T_2^{-1} (corr) / s^{-1}
2
4
6
8
Flash Number

Figure 30. Several Theoretical Patterns that Qualitatively Fit Various Experimental $1/T_2$ Flash Patterns. (a) $[S_0] = 0.30$, $[S_1] = 0.70$, $\alpha = 0.10$, $\beta = 0$, weighting factors: 2,1,2,2, except $S_0 = 4$ in dark (solid line) or $S_0 = 2$ in dark (dashed line). (b) $[S_0] = 0.30$, $[S_1] = 0.70$, $\alpha = 0.10$, $\beta = 0$, weighting factors: 0,1,1,3 except $S_0 = 4$ in dark. (c) $[S_0] = 1.00$, $\alpha = 0.10$, $\beta = 0$, weighting factors: 0,1,2,3 except $S_0 = 4$ in dark. The pattern in (a) is similar to the flash pattern for spinach chloroplasts (Figure 17) and glutaraldehyde fixed chloroplasts (Figure 27a). The dashed line in (a) is similar to that for pea chloroplasts with low FeCy (Figure 25a). The pattern in (b) is similar to the flash pattern for pea chloroplasts containing either NH_2OH, TPB or CCCP (Figure 23). The pattern in (c) is similar to the flash pattern for peas at pH 4 (Figure 22b).

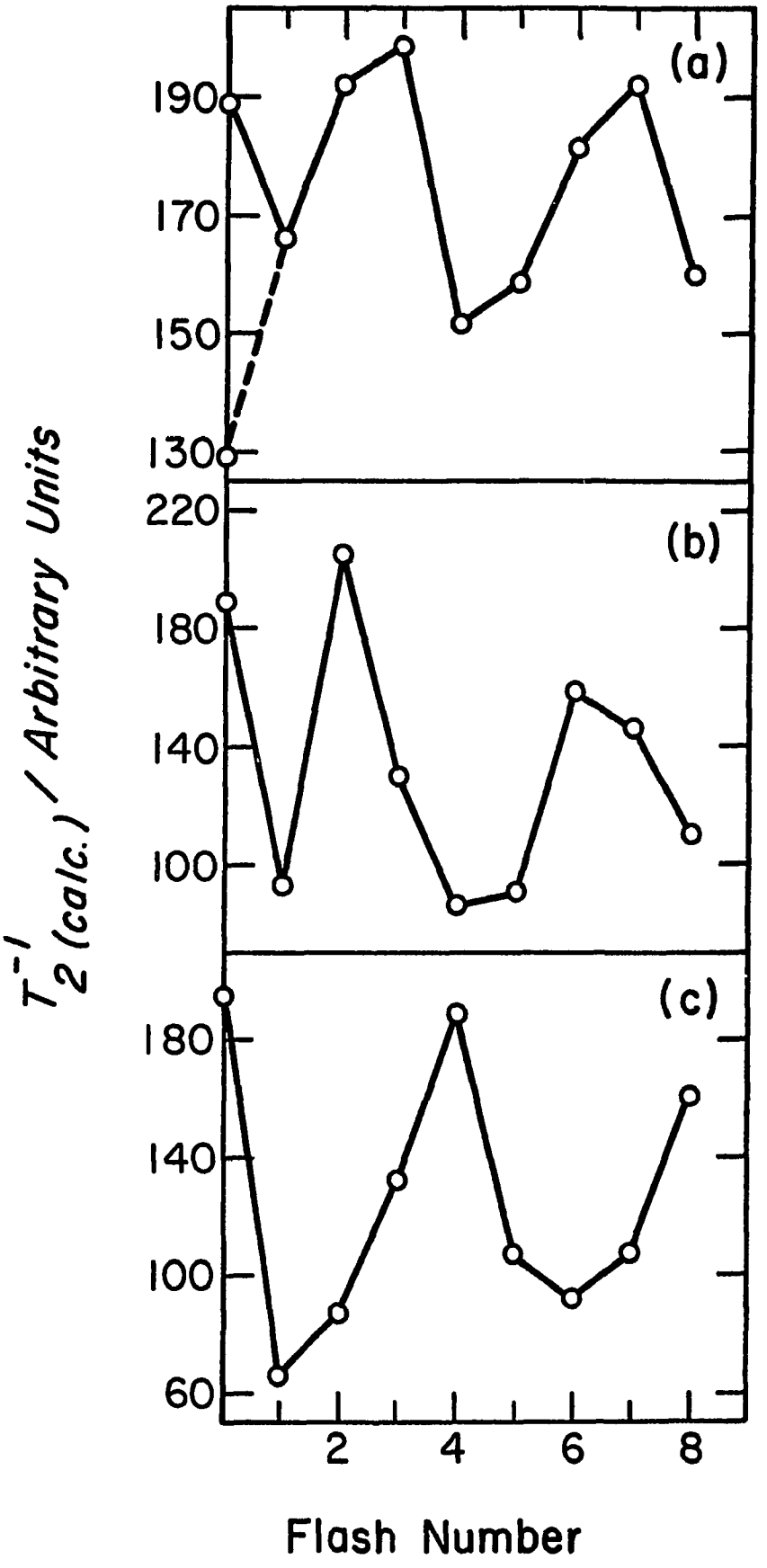
(a)
190
170
150
130
(b)
220
180
140
100
(c)
180
140
100
60
2
4
6
8
Flash Number
$T_{2\,(calc.)}^{-1}$ / Arbitrary Units

zero on the second and succeeding cycles. Any small contributions to S_0 cause the pattern to deviate even more from the experimental data. Likewise, only a 0,1,2,3, $S_0 = 1.00$ in the dark model gives the fit in Figure 30c.

We have tried changing the initial distribution of S states and miss parameters but were unable to achieve better fits to both $1/T_2$ and O_2 data. In some cases we could get a reasonable fit to the $1/T_2$ data, but not to the O_2 yield data and vice versa. For example, a 2,1,2,3 model, S = 4 in the dark, with starting distribution of $S_0 = 0.40$, $S_1 = 0.60$ and $\alpha = 0.10$, $\beta = 0$ can fit the $1/T_2$ pattern at pH 6.7, but does not fit the O_2 yield pattern at that pH. Thus, it appears that several of the proposals discussed in Sections 3.3.2 and 3.3.3, Chapter I, concerning extreme S state starting distributions or abnormally high miss parameters are not supported by our analysis.

2.2 Significance of the Theoretical Fit to the Oxygen Evolving Mechanism

2.2.1 Mn(II) Contribution to the S States

The weighting factors that are needed to fit the $1/T_2$ flash pattern represent the relative contribution of Mn(II) to each of the S states. In our original assumption we interpreted this to mean the amount of Mn(II). However, according to Equation 23 the total paramagnetic effect on proton relaxation depends not only on the concentration of Mn(II), but

also on the number of bound nuclei in the first co-ordination sphere. In Equation 23 q represents the number of water ligands each having two protons. For bound Mn(II) q must be less than 6. The number of water ligands can be calculated when $T_{1(P)}/T_{2(P)} > 1.19$ from the following equation (143):

$$q = 3.26 \times 10^{-14} \frac{[(T_{1(P)}/T_{2(P)}) - 0.5]}{[(T_{1(P)}/T_{2(P)}) - 1.19]^{\frac{1}{2}}} \frac{\omega_I}{NT_{1(P)}} \qquad (33)$$

where N is the molar concentration of the paramagnetic ion, i.e., Mn(II). Using $T_{1(P)}$ and $T_{2(P)}$ calculated from the theoretical curves in Figure 11 corrected with the outer sphere contribution and letting N = 20 μM as the concentration of the loosely bound Mn in samples containing 3 mg Chl/ml, we calculate q to be 0.187, 0.202 and 0.203 at 50, 60 and 70 MHz, respectively. In other words, there is one water ligand per 5 Mn atoms. But this value represents only the lower limit, since in the dark there appears to be a considerable amount of Mn in higher oxidation states and Equation 33 requires the Mn(II) concentration.

A coordination number less than one is still a reasonable situation, however, for it would be consistent with a complex of Mn atoms. Indeed, it has been suggested that a complex of three or four Mn atoms is involved in O_2 evolution (Section 2.3, Chapter I). The several plateaus in the TPB concentration curve (Figure 15) tend to indicate this to be

the case. Since there are five possible titration levels (four in the TPB concentration curve and one level obtained after adding an oxidant FeCy), one could envision the following complex:

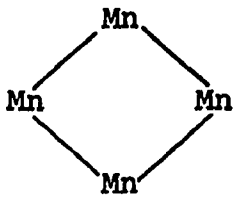

where the titration level at the high TPB concentration represents the condition when all of the Mn is reduced to Mn(II), the titration level in the presence of FeCy when all of the Mn is oxidized to higher state (e.g., Mn(III)), and the three intermediate levels representing the condition when 1,2 or 3 Mn are reduced to Mn(II). The calculated correlation times could be for the complex as a whole. The possibility of cross correlation interactions between the Mn atoms in different oxidation states could very well account for the deviation of the calculated correlation times from that for pure Mn(II) (see Table 6).

If the number of water ligands, and hence the number of bound protons, remains constant during the flash sequence, then the changes in the weighting factors would represent the changes in the Mn(II) concentration. However, in the chloroplast system the water ligands themselves are most likely being oxidized and, therefore, it may not be reasonable to

assume this simple situation. It is now believed that protons are released in steps prior to the release of O_2 (Section 3.3.4, Chapter I). The loss of these protons in intermediate transitions represents the loss of a site which communicates the paramagnetic effect to the bulk water. Thus, the weighting factors must represent a combined effect of the concentration of Mn(II) and the number of exchangeable protons on the PRR. This situation is suggested by preliminary data on the effect of reagents known to influence the proton environment. Addition of 1 μM gramicidin D which breaks down the proton gradient across the membrane results in a binary oscillation in $1/T_2$, peaks occurring after odd numbered flashes. High concentrations of NH_4Cl at which O_2 evolution is inhibited causes the $1/T_2$ flash pattern to shift with peaks after the first and fifth flashes. The strong influence of pH and the complicated flash patterns obtained under some conditions may be indications of a complex effect on $1/T_2$ produced by the number of exchangeable protons as well as the Mn(II) concentration.

Recent unpublished data of Fowler (personal communication to Govindjee) suggest that protons are released in the following proportions: $S_0 \rightarrow S_1$, 0.7; $S_1 \rightarrow S_2$, 0; $S_2 \rightarrow S_3$, 1.3; $S_3 \rightarrow S_0$, 2. If the weighting factors are divided by the number of exchangeable protons, we may assume the resulting ratio to represent the relative concentration of Mn(II) to

each S state. From Fowler's analysis, then, we calculate the relative number of exchangeable protons on each S state to be: $S_0 = 4$, $S_1 = 3.3$, $S_2 = 3.3$, and $S_3 = 2$. Dividing the model of 2,1,1,3 by the relative number of exchangeable protons we get 0.5, 0.3, 0.3 and 1.5 which represents the actual Mn(II) contribution. Basically, the model has not changed, except that the S_3 state has an even greater effect than S_1 and S_2. Both S_1 and S_2 maintain equal contributions. In view of the above, we assume that the major contribution to PRR is by Mn(II) concentration.

The above conclusion has an important bearing on the interpretation of the Kok et al. (77) original model for O_2 evolution. Since the theoretical fit implies no change in the Mn(II) content in the S_1 and S_2 state, then the charge generated in the light during the $S_1 \rightarrow S_2$ transition must react with water by the time the $1/T_2$ is measured (the dead time between the flash and the beginning of the first echo in the CPMG train is about 1 ms). Therefore, the reaction with water must occur rapidly in the $S_1 \rightarrow S_2$ transition, which has a kinetic half time of 400-600 μs. This suggests that there is no charge accumulation in the $S_1 \rightarrow S_2$ transition in the sense that a positive charge remains stable for long periods of time, i.e., within the normal deactivation time of the S_2 state. Likewise, the fit suggests that the S_3 state is highly reduced, even more so than S_1

and S_2, again implying that the charge generated in the light during this reaction is used up by the time of the $1/T_2$ measurement.

Overall, the results imply that water is being oxidized in reactions prior to the final release of O_2 in the $S_4 \rightarrow S_0$ transition. This is entirely consistent with the release of protons in early transitions. A concerted reaction of two water molecules and the S_4 state, as proposed by Kok et al. (78), therefore, seems unlikely.

In terms of energetics, this interpretation is more satisfying, for there is no need to account for the transfer and accumulation of charge on a highly charged intermediate (Section 3.3.1, Chapter I). The oxidizing potential of the reaction center can remain the same at each step, the charge generated immediately reacting with water and being stabilized in the form of a chemical bond. In the 2,1,1,3 model only in the $S_0 \rightarrow S_1$ transition is the accumulation of a charge implied (that is a charge stable for a long period of time). But this charge accumulation is justifiable since one electron can be stabilized on the B(R) intermediate (Section 3.3.2, Chapter I). (For a hypothetical model see Appendix.)

2.2.2 Special Dark-Adapted State of the S Intermediate

To account for the high dark level of the $1/T_2$ we had to assume that the S_0 existed in a special dark-adapted state which makes a greater contribution to the $1/T_2$ than the S_0 state during a light cycle. This special state seems to be

more reduced (rather than a change in the number of exchangeable protons) since it can be eliminated by the addition of an oxidant (Figure 25). It may be affected by the conformation of the membrane, however, since the dark $1/T_2$ is somewhat lower in glutaradehyde fixed chloroplasts and considerable lower in chloroplasts suspended in a low osmoticum. In these cases the highly reduced special state may be oxidized by molecular O_2. If the redox equilibrium of the S states is governed by O_2 and some endogenous reductant as proposed by Kok et al. (Section 3.3.2, Chapter I), the conformational changes could upset this equilibrium.

The existence of a special dark-adapted state (S_{-1}) was proposed by Velthuys based on luminencene measurements (135). If all of the oxidizing charge is used up on the $S_3 \rightarrow S_0$ transition to produce O_2, then the lumunescence (>15 ms) after illumination would be expected to be low when most of the System II centers start out in the S_3 state (assuming luminescence arises from a back reaction at the System II center (25)). But Velthuys found that the luminescence was about the same as when most of the centers start out in the S_2 state, indicating that there must have been the same amount of charge giving rise to luminescence under both conditions (see also Etienne, (110)). He had to postulate that O_2 could be released on the $S_3 \rightarrow S_0$ transition without the transfer of charge from Z^+ to the S intermediate. In his formulation,

this is illustrated as follows:

$$\underset{(S_3)}{S^{4+}ZPQ} \xrightarrow{h\nu} \underset{(S_4)}{S^{4+}ZP^{+}Q^{-}} \longrightarrow SZ^{+}PQ^{-} \longrightarrow \underset{(S_0)}{S^{+}ZPQ^{-}} \qquad (34)$$

$$2H_2O \qquad O_2 + 4H^{+}$$

where the symbols have their usual meanings. Thus, according to Velthuys the S_0 state has one charge and the special dark adapted S_{-1} state has no charge.

According to our model for the $1/T_2$ flash pattern we must assume that in the 1st flash the special dark-adapted state goes to the S_1 state, as though two charges were transferred to the S intermediate. Since one light flash can generate only one charge at a reaction center, we must assume that the extra charge comes from another side charge carrier (C) which does not contribute to the PRR. This may be visualized as follows:

$$\underset{(S_{-1})}{\underset{C^{+}}{SZPQ}} \xrightarrow{h\nu} \underset{C^{+}}{SZP^{+}Q^{-}} \longrightarrow \underset{C^{+}}{SZ^{+}PQ^{-}} \longrightarrow \underset{(S_0)}{\underset{C^{+}}{S^{+}ZPQ^{-}}} \longrightarrow \underset{(S_1)}{\underset{C}{S^{2+}ZPQ}} \qquad (35)$$

$$\text{or} \qquad \underset{C}{S^{+}Z^{+}PQ^{-}}$$

where the symbols have their usual meanings. This reaction sequence would have to occur within the time of the $1/T_2$ measurement (~200-300 ms). The side charge carrier could be the one proposed by Lavorel (151) and perhaps gives rise to the slow EPR Signal II (Section 3.3.2, Chapter I).

Whether the special dark adapted state exists *in vivo* or is an artifact of the chloroplast isolation procedure remains to be determined, but preliminary $1/T_2$ flash measurements on the blue green alga *Phormidium luridum* indicate that the $1/T_2$ dark level is low with respect to the peaks in the flash pattern (R. Khanna, personal communication).

2.2.3 Altered Cycling of the S States

The $1/T_2$ flash pattern may vary considerably depending upon the experimental conditions, indicating that the cycling of the S states are altered. The large number of variations becomes more understandable when one considers that the difference between the S states lies not only in the amount of Mn(II) present but also on the state of the bound water. For example, the S_1 and S_2 states appear to have the same Mn(II) contribution, the difference between these states must, therefore, lie in the bound water. Treatments which could affect the state of the bound water could easily cause a conversion of S_2 to S_1 without a change in the oxidation state of Mn. It becomes easy to visualize, then, that many types of altered cycling can take place which involve changes in either the oxidation state of Mn or the state of the bound water or both.

A diverse group of reagents exhibit the ADRY behavior (Section 3.3.3, Chapter I). For stochiometric reasons Renger (104) suggested that these reagents themselves are not

directly involved in the discharge of the higher S states but instead catalyze a cyclic electron flow between the higher S states and some endogenous reductant. In terms of the theoretical fit to $1/T_2$ the S_3 state is already highly reduced and its discharge cannot involve a reduction reaction. Rather, the discharge of the S_3 state must involve the change in the state of the bound water. This may explain why we observe the same behavior in the $1/T_2$ flash pattern under widely different conditions which lead to inhibition of O_2 evolution, such as high FeCy concentration (Figure 25b), low concentrations of TPB, NH_2OH or CCCP (Figure 23) and Cl^- depletion (Figure 26).

This approach also helps in justifying the distribution of the S states. All of the states may be in equilibrium with each other, the function of the light is to drive the reaction forward to the S_4 state. At high pH we may predict an equilibrium in favor of the higher S states. Thus, some S_2 must be present at pH 7.5 to account for the O_2 yield after the 2nd flash (Figure 21). At pH 4.0 the equilibrium is driven to the lower S states, all centers starting out in S_0 (Figure 22b). With DCMU the equilibrium may be in favor of S_1, hence, the low dark level with respect to the control (Figure 19). The high $1/T_2$ value after the 2nd flash in the presence of DCMU may represent a greater contribution of the highly reduced S_3. Alternatively, there may be some background contribution from System I.

2.2.4 Chemistry

The results indicate that water is oxidized in reactions prior to the release of O_2 and that Mn becomes reduced. Can this be justified chemically? Earley (152) has proposed a model in which a complex of three Mn atoms bridged by oxygen atoms undergo disproportionation reactions. In the process hydroxy ligands are oxidized to peroxide type intermediates. The final release of O_2 then results from a dismutation of the peroxide intermediate. A mechanism by which a peroxide ligand can form from a hydroxy ligand is (153):

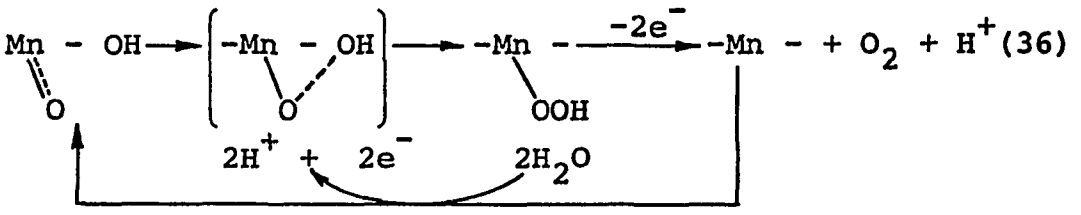

Such a mechanism could be occurring in photosynthetic O_2 evolution. But details are still speculative at this time. More information is needed on the Mn complex and the state of the bound water.

The role of chloride in O_2 evolution is unknown although its site of action has been located on the oxidizing side of System II (139). Figure 23 shows the Cl^- depletion causes an altered $1/T_2$ pattern that can be restored by adding back NaCl or NaF. The normal isotope of fluorine gives rise to an NMR signal. We found that the ^{19}F relaxation parallels the proton relaxation. Chloroplasts show an enhanced ^{19}F relaxation rate which returns to the buffer value after TRIS-acetone

washing (Table 10). Thus, only the loosely bound Mn contributes to the effect on ^{19}F relaxation. Addition of TPB causes a considerable enhancement of this rate. These results may imply that fluoride (and hence chloride) is a ligand to the Mn. The function of a halide ion may be to help stabilize the higher oxidation states of Mn (154) which are used in water oxidation. More data is needed to verify this conclusion.

Table 10. ^{19}Fluorine Relaxation Measurements of Chloroplast Membranes[a]

Condition	T_2^{*-1}/s^{-1}
[b]Buffer	13.7
[c]Chlpts	34.0
Chlpts + 5 mM TPB	60.2
TRIS-Acetone Washed Chlpts	15.6

[a] ^{19}F spectra were measured on a Jeol FX-60 Fourier Transform NMR Spectrometer. Relaxation rates were calculated from the half band width ($\Delta\nu$) of the resonance peak, $1/T_2^* = \pi\Delta\nu$.

[b] HEPES buffer medium containing 20 mM NaF was used.

[c] Dark-adapted pea chloroplasts, 3mg Chl/ml, were washed free of Cl^- and suspended in buffer medium containing NaF.

CHAPTER V

SUMMARY AND CONCLUDING REMARKS

During the course of this study nuclear magnetic relaxation methods were applied to monitor the native bound manganese in chloroplast membranes in order to study the role of manganese in photosynthetic oxygen evolution. It was found that a direct relationship exists between the water proton longitudinal ($1/T_1$) and transverse ($1/T_2$) relaxation rates, the Mn content of the membranes and the O_2 evolving activity (Figures 9-11). The major effect on the proton relaxation rates (PRR) arises from interactions with the large pool of bound Mn (Table 1, Figure 12) which has been associated with the O_2 evolving mechanism (Chapter I). Analysis of the PRR for dark-adapted chloroplasts according to the Solomon-Bloombergen-Morgan equations (Chapter II) shows that bound Mn(II) dominates the relaxation rates (Figure 13, Table 6), free Mn(II) (Table 7) as well as bound Mn(III) (Table 8) having negligible contributions.

The PRR of the chloroplast membranes are strongly affected by the presence of redox reagents. Addition of a reductant causes a large increase while addition of an oxidant causes a decrease in the $1/T_1$ (Table 4), indicating that a mixture of Mn oxidation states exist in dark-adapted chloroplasts. The dependence of $1/T_1$ on the concentration of

reductant reveals several titratable fractions (Figure 15). Analysis of the PRR for chloroplasts in the presence of a reductant or oxidant shows that the NMR parameters are essentially the same as those for the normal chloroplasts (Figure 15, Table 6). The PRR, thus, monitor only relative changes in the contribution of Mn(II) in the membrane.

In continuous light the $1/T_1$ shows a reversible net decrease apparently due to a photooxidation of Mn (Table 5). In a series of brief flashes of light the $1/T_2$ follows a damped oscillatory pattern with peaks after the 3rd, 7th, 11th, etc. flashes similar to the pattern observed for the O_2 flash yield (Figures 17 and 18). When the large pool of bound Mn is extracted or 3-(3,4-dichlorophenyl)-1,1-dimethyl urea is added, O_2 evolution is inhibited and the $1/T_2$ oscillations disappear (Figure 19). These results suggest that the $1/T_2$ also monitors the O_2 evolving mechanism.

The $1/T_2$ flash pattern is strongly dependent on the pH as is O_2 evolution. The $1/T_2$ flash patterns at pH 6.7 and pH 7.5 are essentially the same except after the first two flashes (Figure 20 and 21). At pH 6.7 the $1/T_2$ after the 2nd flash is higher than after the 1st flash while at pH 7.5 it is lower. In the O_2 yield flash patterns no O_2 is produced after the 2nd flash at pH 6.7 but a small O_2 yield is observable at pH 7.5. At extreme pH's where O_2 evolution is completely inhibited the $1/T_2$ shows a considerably altered

flash pattern (Figure 22). At pH 9 the $1/T_2$ starts out at a high value in the dark and then irreversibly decreases with each flash, finally approaching a value which is obtained for chloroplast membranes extracted of the large pool of bound Mn. The decrease in $1/T_2$ with each flash may indicate release of bound Mn(II) from the membrane. At pH 4 the $1/T_2$ shows an altered oscillatory flash pattern, with peaks occurring after the 4th and 8th flashes.

In the presence of the various chemical reagents which suppress or inhibit O_2 evolution (e.g. sodium tetraphenylboron, NH_2OH, carbonyl cyanide m-chlorophenylhydrazone or high concentrations of potassium ferricyanide) the $1/T_2$ flash pattern is also altered, this time with peaks occurring after the 2nd and 6th flashes (Figures 23-25). A similar $1/T_2$ flash pattern is observed when chloroplasts are depleted of chloride (Figure 26). The $1/T_2$ oscillations can apparently be uncoupled from the O_2 evolving step.

According to the current model of O_2 evolution (Chapter I) a chemical intermediate "S" is proposed to cycle through several states in the light before it reacts with water to produce O_2, i.e.,

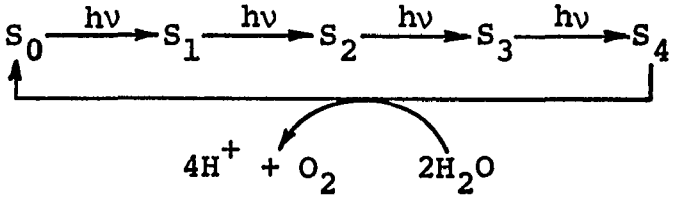

where each S_n state is assumed to differ from the previous

S_{n-1} state by the accumulation of an additional oxidizing equivalent.

Using this model as the starting point, a fit to the $1/T_2$ flash pattern can be made by ascribing to each S state a weighting factor. The weighting factors are assumed to be proportional to the relative Mn(II) contribution. The best fit to the $1/T_2$ pattern for normal chloroplasts at pH 6.7 (Figure 28) is obtained using the following weighting factors: $S_0 = 2$, $S_1 = 1$, $S_2 = 1$, $S_3 = 3$ (S_4 is neglected since its lifetime is much shorter than the time it takes to measure $1/T_2$). To account for a high dark value for $1/T_2$ with respect to the peaks in the flash pattern, S_0 is assigned a weighting factor of 4 starting out in the dark. Variations in the $1/T_2$ pattern observed under different experimental conditions can be generated theoretically by adjusting the weighting parameters (Figures 29 and 30).

The model implies the following: (1) The cycling of the S states involves changes in the oxidation state of bound Mn. (2) The S_3 state is more reduced than the S_1 and S_2 states, rather than being more oxidized as assumed in the current model for O_2 evolution. This indicates that water donates electrons to the S intermediate in reactions prior to the release of O_2. (3) Since S_0 has a larger contribution in the dark, there must exist a special dark-adapted state of the S intermediate in isolated chloroplasts. (4) Since the S_1 and

S_2 states apparently have the same Mn(II) contribution, the difference between these states must lie in the nature of the bound water. Altered cycling of the states could, thus, occur through changes either in the oxidation state of the Mn or the chemistry of the bound water or both.

In conclusion, we have shown that the native bound manganese in the chloroplast membrane acts directly in the intermediate precursor states which lead to photosynthetic O_2 evolution and that NMR relaxation methods provide a unique approach for the study of the O_2 evolving mechanism.

LITERATURE CITED

1. Metzner, H. (1975) J. Theor. Bio. 51, 201-231.

2. Wurmser, R. (1930) "Oxidations et Reductions," Presses Univ. de France, Paris, p. 30.

3. Rabinowitch, E. I. (1945) "Photosynthesis and Related Topics," Vol. I, Wiley (Interscience), New York, pp. 281-299. Also see Vol. II, Part 1 (1951) and Part 2 (1956).

4. Hill, R. and Scarisbrick, R. (1940) Nature (London) 146, 61-62.

5. Ruben, S., Randall, M., Kamen, M. and Hyde, J. L. (1941) J. Am. Chem. Soc. 63, 877-879.

6. Stemler, A. and Radmer, R. (1975) Science 190, 457-458.

7. Warburg, O. and Krippahl, G. (1960) Z. Naturforsch. 15B, 367-369.

8. Warburg, O. (1964) Ann. Rev. Biochem. 33, 1-14.

9. Wydrzynski, T. and Govindjee (1975) Biochim. Biophys. Acta 387, 403-405.

10. Jursinic, P., Warden, J. and Govindjee (1976) Biochim. Biophys. Acta 440, 322-330.

11. Govindjee, Pulles, M. P. J., Govindjee, R., Van Gorkom, H. J. and Duysens, L. N. M. (1976) Biochim. Biophys. Acta 449, 602-605.

12. Stemler, A., Babcock, G. T. and Govindjee (1974) Proc. Natl. Acad. Sci. USA 71, 4679-4683.

13. Metzner, H. (1968) Hoppe-Seyler's Z. Physiol. Chem. 349, 1586-1588.

14. Wang, J. H. (1969) Proc. Natl. Acad. Sci. USA 62, 653-660.

15. Kutyurin, V. M. (1971) 2nd Internatl. Congr. Photosynth. Res., Stressa (G. Forti, M. Avron and A. Melandri, eds.) pp. 93-103.

16. Heidt, L. J. (1966) J. Chem. Ed. 43, 623-636.

17. Emerson, R. (1958) Ann. Rev. Plant Physiol. 9, 1-24.

18. Dorough, G. D. and Calvin, M. (1951) J. Am. Chem. Soc. 73, 2362-2365.

19. Chance, B. and Sager, R. (1957) Plant Physiol. 32, 548-561.

20. Mauzerall, D. and Chivvis, A. (1973) J. Theor. Biol. 42, 387-395.

21. King, T. E., Mason, H. S. and Morisson, M., eds. (1971) "Oxidases and Related Redox Systems," Vol. I and II. University Park Press, Baltimore.

22. Avron, M. (1975) in "Bioenergetics of Photosynthesis" (Govindjee, ed.) Academic Press, New York, p. 374-386.

23. Pirson, A. (1937) Z. Botan. 31, 193-267.

24. Kessler, E., Arthur, W. and Brugger, J. E. (1957) Arch. Biochem. Biophys. 71, 326-335.

25. Lovorel, J. (1975) in "Bioenergetics of Photosynthesis" (Govindjee, ed.) Academic Press, New York, p. 225-319.

26. Spencer, D. and Possingham, J. V. (1961) Biochim. Biophys. Acta 52, 379-381.

27. Hoch, G. and Martin, I. F. (1963) Arch. Biochem. Biophys. 102, 430-438.

28. Cheniae, G. M. and Martin, I. F. (1966) Brookhaven Symp. Biol. 19, 406-417.

29. Kok, B. and Cheniae, G. M. (1966) in "Current Topics in Bioenergetics," Vol. I (R. Sanadi, ed.) Academic Press, New York, pp. 1-47.

30. Cheniae, G. M. and Martin, I. F. (1968) Biochim. Biophys. Acta 153, 819-837.

31. Yamashita, T. and Butler, W. L. (1968) Plant Physiol. 43, 1978-1986.

32. Cheniae, G. M. and Martin, I. F. (1970) Biochim. Biophys. Acta 197, 219-239.

33. Katoh, S. and San Pietro, A. (1967) Arch. Biochem. Biophys. 122, 144-152.

34. Homann, P. (1968) Biochem. Biophys. Res. Comm. 33, 225-234.

35. Lozier, R., Baginsky, M. and Butler, W. L. (1971) Photochem. Photobiol. 14, 323-328.

36. Cheniae, G. M. and Martin, I. F. (1971) Plant Physiol. 47, 568-575.

37. Itoh, M., Yamashita, K., Nishi, T., Konishi, K. and Shibata, K. (1969) Biochim. Biophys. Acta 180, 509-519.

38. Selman, B. R., Bannister, T. T. and Dilley, R. A. (1973) Biochim. Biophys Acta 292, 566-581.

39. Blankenship, R. E. and Sauer, K. (1974) Biochim. Biophys. Acta 357, 252-266.

40. Takahashi, M. and Asada, K. (1976) Eur. J. Biochem. 64, 445-452.

41. Govindjee, Döring, G. and Govindjee, R. (1970) Biochim. Biophys. Acta 205, 303-306.

42. Renger, G. and Wolff, C. (1976) Biochim. Biophys. Acta 423, 610-614.

43. Blankenship, R. E., Babcock, G. T., Warden, J. T. and Sauer, K. (1975) FEBS Lett. 51, 287-293.

44. Warden, J. T., Blankenship, R. E. and Sauer, K. (1976) Biochim. Biophys Acta 423, 462-478.

45. Babcock, G. T., Blankenship, R. E. and Sauer, K. (1976) FEBS Lett. 61, 286-289.

46. Babcock, G. T. and Sauer, K. (1975) Biochim. Biophys. Acta 376, 315-328.

47. Babcock, G. T. and Sauer, K. (1975) Biochim. Biophys. Acta 376, 329-344.

48. Kimimura, M. and Katoh, S. (1972) Plant Cell Physiol. 13, 287-296.

49. Lumsden, J. and Hall, D. O. (1975) Biochem. Biophys. Res. Comm. 64, 595-602.

50. Asada, K., Takahashi, M. and Nagate, M. (1974) Agricul. Biol. Chem 38, 471-473.

51. Elstner, E. F. and Heupel, A. (1975) Planta (Berl.) 123, 145-154.

52. Zilinskas-Braun, B. and Govindjee (1974) Plant Sci. Lett. 3, 219-227.

53. Giaquinta, R. T., Dilley, R. A., Selman, B. R., and Anderson, B. H. (1974) Arch. Biochem. Biophys. 162, 200-209.

54. Selman, B. R., Bannister, T. T. and Dilley, R. A. (1973) Biochim. Biophys. Acta 253, 428-436.

55. Lagoutte, B. and Duraton, J. (1975) FEBS Lett. 51, 21-24.

56. Henriques, F. and Park, R. B. (1976) Biochim. Biophys. Acta 430, 312-320.

57. Tel-Or, E. and Avron, M. (1974) Proc. 3rd Internatl. Photosynth. Congr., Rehovot (M. Avron, ed) 1, 569-578.

58. Junge, W. and Witt, H. T. (1968) Z. Naturforsch. 23b, 244-254.

59. Fowler, F. and Kok, B. (1974) Biochim. Biophys. Acta 357, 308-318.

60. Yamashita, T., Tsuji, J. and Tomita, K. (1971) Plant Cell Physiol. 12, 117-127.

61. Blankenship, R. E., Babcock, G. T. and Sauer, K. (1975) Biochim. Biophys. Acta 387, 165-175.

62. Cheniae, G. M. and Martin, I. F. (1967) Biochem. Biophys. Res. Comm. 28, 89-95.

63. Cheniae, G. M. and Martin, I. F. (1972) Plant Physiol. 50, 87-94.

64. Inoue, Y., Kobayashi, Y., Sakamoto, E. and Shibata, K. (1975) Plant Cell Physiol. 16, 327-336.

65. Cheniae, G. M. and Martin, I. F. (1973) Photochem. Photobiol. 17, 441-459.

66. Inoue, Y. (1975) Biochim. Biophys. Acta 396, 402-413.

67. Emerson, R. and Arnold, W. (1932) J. Gen. Physiol. 16, 191-205.

68. Witt, H. T. (1967) Nobel Symp. 5, 261-316.

69. Kok, B. (1956) Biochim. Biophys. Acta 21, 245-258.

70. Allen, F. and Franck, J. (1955) Arch. Biochem. Biophys. 58, 124-143.

71. Whittingham, C. P. and Brown, A. H. (1958) J. Exptl. Bot. 9, 311-319.

72. Whittingham, C. P. and Bishop, P. M. (1963) Natl. Acad. Sci. - Natl. Res. Counc., Publ. 1145, pp. 371-380.

73. Gingras, G. and Lemasson, C. (1965) Biochim. Biophys. Acta 109, 67-78.

74. Joliot, P. (1965) Biochim. Biophys. Acta 102, 116-134.

75. Cheniae, G. M. (1970) Ann. Rev. Plant Physiol. 21, 467-498.

76. Mar, T. and Govindjee (1972) J. Theor. Biol. 36, 427-446.

77. Kok, B., Forbush, B. and McGloin, M. (1970) Photochem. Photobiol. 11, 457-475.

78. Forbush, B., Kok, B. and McGloin, M. (1971) Photochem. Photobiol. 14, 307-321.

79. Joliot, P. and Kok, B. (1974) in "Bioenergetics of Photosynthesis" (Govindjee, ed.) Academic Press, New York, pp. 387-412.

80. Joliot, P., Barbieri, G. and Chabaud, R. (1969) Photochem. Photobiol. 10, 309-329.

81. Weiss, C. and Sauer, K. (1970) Photochem. Photobiol. 11, 495-501.

82. Joliot, P., Joliot, A., Bouges, B. and Barbieri, G. (1971) Photochem. Photobiol. 14, 287-305.

83. Jursinic, P. T. and Govindjee (1977) Biochim. Biophys. Acta, in press.

84. Bouges-Bocquet, B. (1973) Biochim. Biophys. Acta 292, 772-785.

85. Van Gorkom, H. J. and Donze, M. (1973) Photochem. Photobiol. 17, 333-342.

86. Trebst, A. (1974) Ann. Rev. Plant Physiol. 25, 423-458.

87. Mathis, P., Haveman, J. and Yates, M. (1976) Brookhaven Symp. Biol. 28 267-277.

88. Witt, H. T. (1975) in "Bioenergetics of Photosynthesis" (Govindjee, ed) Academic Press, New York, p. 493-554.

89. Joliot, P. and Delosme, R. (1974) Biochim Biophys. Acta 357, 267-284.

90. Jursinic, P. J., Govindjee and Wraight, C. (1977) Photochem. Photobiol., submitted.

91. Doschek, W. W. and Kok, B. (1972) Biophys. J. 12, 832-838.

92. Kok, B., Radmer, R. and Fowler, C. F. (1974) Proc. 3rd Internatl. Photosynth. Congr., Rehovot (M. Avron, ed.) p. 485-496.

93. Greenbaum, E. and Mauzerall, D. (1976) Photochem. Photobiol. 23, 369-372.

94. Ley, A. C., Babcock, G. T. and Sauer, K. (1975) Biochim. Biophys. Acta 387, 379-387.

95. Kok, B. and Velthuys, B. R. (1976) VII Internatl. Cong. Photobiol, Rome, Book of Abstracts p. S-12.

96. Velthuys, B. R. and Visser, J. W. M. (1975) FEBS Lett. 55, 109-112.

97. Babcock, G. T. and Sauer, K. (1973) Biochim. Biophys. Acta 325, 483-503.

98. Babcock, G. T. and Sauer, K. (1973) Biochim. Biophys. Acta 325, 504-519.

99. Bouges-Bocquet, B. (1973) Biochim. Biophys. Acta 314, 250-256.

100. Velthuys, B. R. and Amesz, J. (1975) Biochim. Biophys. Acta 376, 162-168.

101. Delrieu, M-J. (1974) Photochem. Photobiol. 20 441-454.

102. Lemasson, C. and Barbieri, G. (1971) Biochim. Biophys. Acta 245, 386-397.

103. Radmer, R. and Kok, B. (1975) Ann. Rev. Biochem.44 407-433.

104. Renger, G. (1972) Physiol. Veg. 10, 329-345.

105. Renger, G., Bouges-Bocquet, B. and Delosme, R. (1973) Biochim. Biophys. Acta 292, 796-807.

106. Renger, G. (1973) Biochim. Biophys. Acta 325, 247-254.

107. Bouges-Bocquet, B., Bennoun, P. and Taboury, J. (1973) Biochim. Biophys. Acta 325, 247-254.

108. Duysens, L. N. M. (1972) Biophys. J. 12, 858-876.

109. Rosenberg, J. L., Sahu, S. and Bigat, T. K. (1972) Biophys. J. 12, 839-850.

110. Etienne, A. L. (1974) Biochim. Biophys. Acta 333, 320-330.

111. Lavorel, J. (1976) FEBS Lett. 66, 164-168.

112. Wydrzynski, T., Zumbulyadis, N. Schmidt, P. G. and Govindjee (1975) Biochim. Biophys. Acta 408, 349-354.

113. Mildvan, A. S. and Cohn, M. (1970) Adv. Enzymol. 33, 1-70.

114. O'Sullivan, W. J., Marsden, K. H. and Leigh, J. S. (1973) in "Molecular Biology, Part C: Physical Principles and Techniques of Protein Chemistry" (S. J. Leach, ed.) Academic Press, New York, p. 245-300.

115. Dwek, R. A. (1973) "Nuclear Magnetic Resonance (N.M.R.) in Biochemistry: Application to Enzyme Systems," Claredon Press, Oxford.

116. James, T. L. (1975) "Nuclear Magnetic Resonance in Biochemistry," Academic Press, New York.

117. Farrar, T. C. and Becker, E. D. (1971) "Pulse and Fourier Transform NMR: Introduction to Theory and Methods," Academic Press, New York.

118. Smith, W. B. and Prouix, T. W. (1976) J. Chem. Ed. 53, 700-703.

119. Solomon, I. (1955) Phys. Rev. 99, 559-565.

120. Bloembergen, N. (1957) J. Chem. Phys. 27, 572-573.

121. Bloembergen, N. and Morgan, L. O. (1961) J. Chem. Phys. 34, 842-850.

122. Johri, M. M. and Varner, J. E. (1964) in "Methods in Developmental Biology" (F. H. Wilt and N. K. Wessells, eds.) Thomas Y. Crowell Company, New York, p. 604.

123. Arnon, D. I. (1949) Plant Physiol. 24, 1-15.

124. Joliot, P. and Joliot, A. (1968) Biochim. Biophys. Acta 325, 213-229.

125. Rosenbrock, H. H. (1960) Computer J. 3, 175-184.

126. Wydrzynski, T., Govindjee, Zumbulyadis, N. Schmidt, P. G., and Gutowsky, H. S. (1976) in "Magnetic Resonance in Colloid and Interface Science" (H. A. Resing and C. G. Wade, eds.) Am. Chem. Soc., pp. 471-482.

127. Ort, D. R. and Izawa, S. (1974) Plant Physiol. 53, 370-376.

128. Yamashita, T. and Tomita, G. (1974) Plant Cell Physiol. 15, 252-266.

129. Chen, K-Y. and Wang, J. H. (1974) Bioinorg. Chem. 3, 339-352.

130. Wydrzynski, T., Zumbulyadis, N. Schmidt, P. G., Gutowsky, H. S. and Govindjee (1976) Proc. Natl. Acad. Sci. USA 73, 1196-1198.

131. Briantais, J-M., Vernotte, C., Lavergne, J. and Arntzen, C. J. (1977) submitted to Biochim. Biophys. Acta.

132. Reimer, S. and Trebst, A. (1975) Biochem. Physiol. Pflanzen. 168 S, 225-232.

133. Cohn, D. E., Cohen, W. S. and Bertsch, W. (1975) Biochim. Biophys. Acta 376, 97-104.

134. Wraight, C. A., Kraan, G. P. B. and Gerrils, N. M. (1972) Biochim. Biophys. Acta 283, 259-267.

135. Velthuys, B. R. (1976) Ph.D. Thesis, The State University, Leiden, the Netherlands.

136. Bouges, B. (1971) Biochem. Biophys. Acta 234, 103-112.

137. Homann, P. (1972) Biochim. Biophys. Acta 256, 336-344.

138. Erixon, K. and Renger, G. (1974) Biochim. Biophys. Acta 333, 95-106.

139. Izawa, S., Heath, R. L. and Hind, G. (1969) Biochim. Biophys. Acta 180, 388-398.

140. Blumberg, W. E., and Peisach, J. (1966) Biochim. Biophys. Acta 126, 269-273.

141. Zilinskas, B. A. and Govindjee (1976) Z. Pflanzenphysiol. 77 S, 302-314.

142. Arntzen, C. J., Armond, P. A., Briantais, J-M., Burke, J. J. and Novitzky, W. D. (1976) Brookhaven Symp. Biol. 28, 316-331.

143. Navon, G. (1970) Chem. Phys. Lett. 7, 390-394.

144. Reuben, J. and Cohn, M. (1970) J. Biol. Chem. 245, 6539-6546.

145. Gross, E. (1972) Arch. Biochem. Biophys. 150, 324-329.

146. Siderer, Y., Malkin, S. Poupko, R. and Luz, Z. (1977) Arch. Biochem. Biophys. 179, 174-182.

147. Zumbulyadis, N., Wydrzynski, T. and Schmidt, P. G. (1976) in "Magnetic Resonance in Colloid and Interface Science" (H. A. Resing and C. G. Wade, eds.) Am. Chem. Soc., pp. 467-470.

148. Villafranca, J. J., Yost, F. J. and Fridovich, I. (1974) J. Biol. Chem. 249, 3532-3536.

149. Vieira, F. L., Shaafi, R. I. and Solomon, A. K. (1970) J. Gen. Physiol. 55, 451-466.

150. Case, G. D. (1975) Biochim. Biophys. Acta 375, 69-86.

151. Lavorel, J. and Lemasson, C. (1976) Biochim. Biophys. Acta 430, 501-516.

152. Early, J. E. (1973) Inorg. Nucl. Chem. Lett. 9, 487-490.

153. Wang, J. H. (1970) Acc. Chem. Res. 3, 90-97.

154. Cotton, F. A. and Wilkinson, C. (1966) "Advanced Inorganic Chemistry, A Comprehensive Text," 2nd Ed. Wiley (Interscience), New York, p. 834-847.

APPENDIX: A HYPOTHETICAL MODEL FOR OXYGEN EVOLUTION

In order to better visualize the cycling of the S states in terms of dynamic changes in the Mn(II) contribution to the S intermediate we may propose the following hypothetical model. Assuming a complex of four Mn atoms (Section 2.2.1, Chapter IV) and using the model for pea chloroplasts at pH 6.7 where the weighting factors are: $S_0 = 2$, $S_1 = 1$, $S_2 = 1$ and $S_3 = 3$ (Section 2.1, Chapter IV), the S states may be represented as shown in Figure 31. For simplicity in this model each weighting factor unit is ascribed to one Mn^{2+}, although the weighting factor may be a function of the co-ordination number as pointed out earlier. Manganese in a higher oxidation state is simply designated as Mn^{3+}. Thus, for S_0 which has a weighting factor of 2, there are two Mn^{2+} and two Mn^{3+} atoms in the complex. The positive charge generated in the light reaction is shown to first appear in the Mn complex by the $S_n \rightarrow S_n'$ transition; but by the time of the T_2 measurement the charges on the Mn complex are adjusted to account for the weighting factors, i.e., the $S_n' \rightarrow S_{n+1}$ transition.

Included in the model is the release of protons (H^+) according to the analysis of Fowler and of Crofts (Section 3.3.4, Chapter I). To be consistent with the $1/T_2$ weighting factors and the proton release data include the possibility of charges stabilized outside of the Mn complex. The water molecules on the outside of the complex are merely symbolic

Figure 31. A Hypothetical Manganese Model for Oxygen Evolution. See test for details.

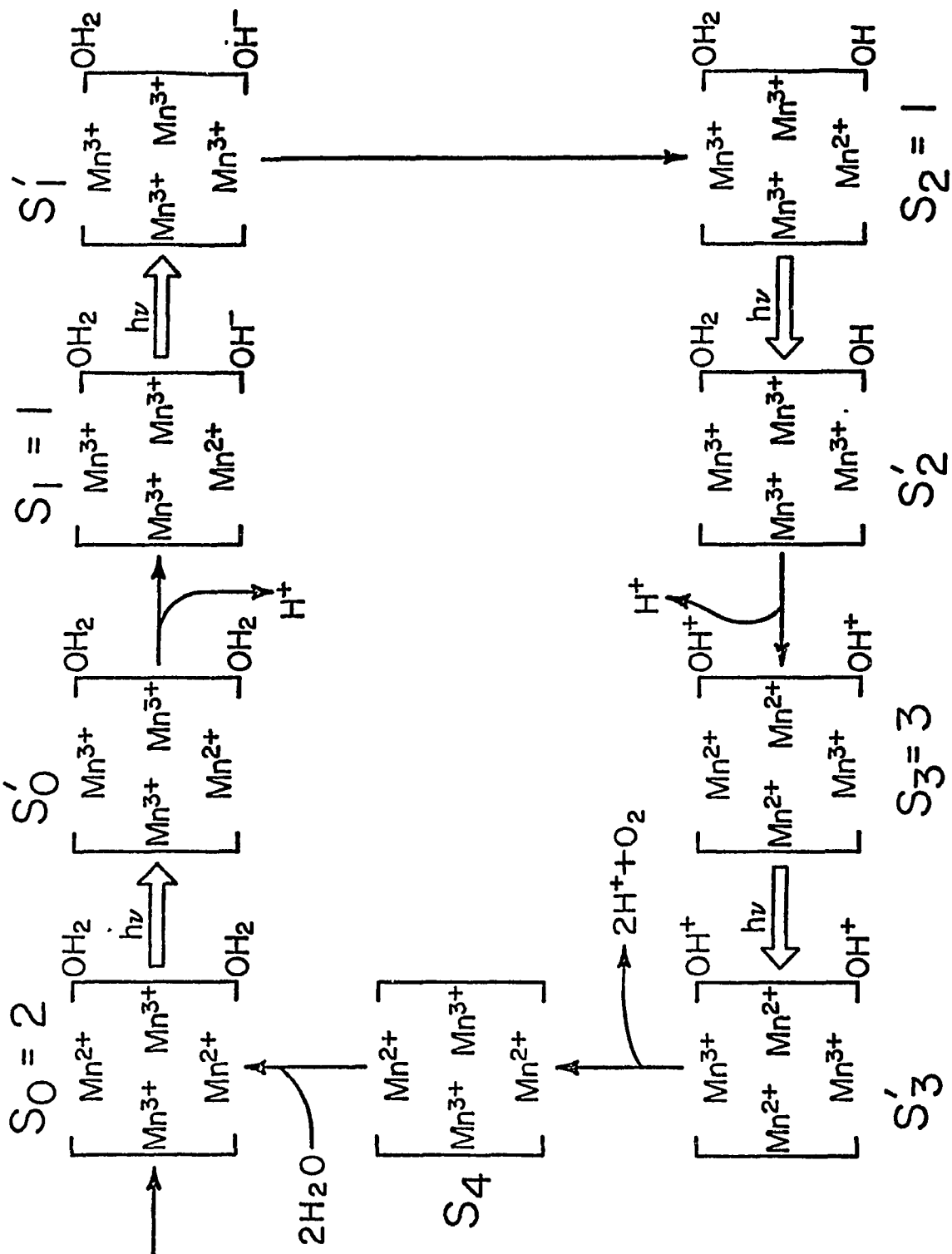
Dark Adapted State
$S_0 = 2$
S_0'
$S_1 = 1$
S_1'
$S_2 = 1$
S_2'
$S_3 = 3$
S_3'
S_4
$2H_2O$
$2H^+ + O_2$
$h\nu$
H^+
OH_2
OH^-
OH
OH^+
Mn^{2+}
Mn^{3+}

of changes in the state of the bound water upon the release at H^+.

The model illustrates the complexity of the system. It must be kept in mind that the $1/T_2$ changes may reflect changes in both the state of the bound water as well as the oxidation state of the manganese. This could account for the diverse $1/T_2$ patterns observed under various experimental conditions. For example, at pH 4 (Figure 2b) water could still be acting as an electron donor, but the chemistry of the bound water is affected in a way so that no O_2 is released. Alternatively, the cycling of the S intermediate could be mediated by oxidation at neighboring protein residues, resulting in a photodestruction of the system. More details of the chemistry of manganese reactions must be known before a more realistic mechanism can be proposed.

VITA

Thomas John Wydrzynski was born on July 8, 1947 in St. Louis, Missouri, where he received his primary and secondary education. In 1969 he obtained an A.B. degree in Biology from the University of Missouri at St. Louis and from 1969-1970 he attended Queen's University, Kingston, Ontario. He joined the Photosynthesis Laboratory at the University of Illinois in 1972. During his graduate studies he held teaching and research assistantships in the Department of Botany (1972-1975) and received a National Research Service Award (HEW PHS GM 7283-02 604) (1975-1977). In March, 1976 he was awarded a Postdoctoral Energy-Related Fellowship (SMI 76-17909) from the National Science Foundation to continue his research at the Lawrence Berkeley Laboratory. In March, 1977 he received a first place rating in the Sigma Xi Student Paper Competition on work presented in this thesis.

He is a member of the American Society of Plant Physiologists, the Biophysical Society, the American Chemical Society and Sigma Xi Scientific Research Society of North America. He is coauthor of the following publications:

(1) Salt-Induced Alterations of the Fluorescence Yield and of Emission Spectra in Chlorella pyrenoidosa, Plant & Cell Physiol. 15 (1974) 213-224.

(2) Monovalent and Divalent Cation-Induced Changes in Chlorophyll a Fluorescence and Chloroplast Structure, Proc. 3rd Internatl. Congr. on Photosynthesis (M. Avron, ed) Rehovot (1974) pp. 345-361.

(3) Effects of Sodium and Magnesium Cations on the "Dark" and Light-Induced Chlorophyll a Fluorescence Yields in Sucrose-Washed Spinach Chloroplasts, Biochim. Biophys. Acta 376 (1975) 151-161.

(4) A New Site of Bicarbonate Effect in Photosystem II of Photosynthesis: Evidence from Chlorophyll a Fluorescence Transients in Spinach Chloroplasts, Biochim. Biophys. Acta 387 (1975) 403-408.

(5) Water Proton Relaxation as a Monitor of Membrane Bound Manganese in Spinach Chloroplasts, Biochim. Biophys. Acta 408 (1975) 349-354.

(6) Proton Relaxation and Charge Accumulation During Oxygen Evolution in Photosynthesis, Proc. Natl. Acad. Sci., USA 73 (1976) 1196-1198.

(7) NMR Studies on Chloroplast Membranes, in Magnetic Resonance in Colloid and Interface Science (H. A. Resing and C. G. Wade, eds.) Am. Chem. Soc., Washington (1976) pp. 471-482.

(8) Site of Bicarbonate Effect in the Hill Reaction: Evidence from the Use of Artificial Electron Acceptors and Donors, Biochim. Biophys. Acta (1977) in press.

(9) An NMR Study of Manganese in Chloroplast Membranes, presented at Cellular Function and Molecular Structure: A Symposium on Biophysical Approaches to Biological Problems, Columbia, Missouri (1977).